

**PHOTORESPONSIVE DRUG DELIVERY FROM
ANTHRACENE – MODIFIED HYDROGELS**

PHOTORESPONSIVE DRUG DELIVERY FROM
ANTHRACENE-MODIFIED HYDROGELS

By

LAURA ANNE WELLS B.Sc, M.A.Sc

A Thesis
Submitted to the School of Graduate Studies
in Partial Fulfilment of the Requirements
for the Degree
Doctor of Philosophy

DOCTOR OF PHILOSOPHY (2010)
(Chemical Engineering)

McMaster University
Hamilton, Ontario

TITLE: PHOTORESPONSIVE DRUG DELIVERY FROM ANTHRACENE-
MODIFIED HYDROGELS

AUTHOR: Laura Anne Wells, B.Sc, M.A.Sc
(Queen's University, McMaster University)

SUPERVISOR: Professor Heather Sheardown

NUMBER OF PAGES: xi, 227

Abstract

Photoresponsive polymers can act as controllable drug delivery systems that may revolutionize ophthalmic drug delivery for disease treatment in the posterior segment of the eye. Localized, controlled drug delivery devices have significant therapeutic advantages for treating diseases of back of the eye by increasing patient compliance and maintaining therapeutic levels of drug in the tissue. Sustained-release delivery systems that respond to light/laser stimuli are under development to control the rate of delivery resulting in a tuneable treatment profile ideal for retinal diseases. The use of light as a crosslinking mechanism has the potential to create unique materials with controllable swelling, degradation and diffusion properties.

This thesis investigates the synthesis and development of universal, graftable PEG-anthracene molecules and their applications in photosensitive alginate and hyaluronate (HA) “photogels”. Anthracene undergoes reversible dimerization with wavelengths above 300 nm and de-dimerization/dissociation below 300 nm; due to its well-understood chemistry and symmetry, it was used as a starting point and proof-of-concept for the synthesis of reversible dimerizing crosslinkers that may be generically grafted to different polymers to cause crosslinking/decrosslinking. After synthesis, water-soluble PEG-anthracene macromolecules were grafted via carbodiimide chemistry to the carboxyl groups along the polymer backbone of alginate and HA at various densities to create viscous liquids or gels with good handling properties.

Light irradiation can be used to control the swelling and effective crosslinking density of the photogels which in turn can control drug delivery from photocrosslinked

hydrogels as illustrated through the decrease or increase in the delivery of a variety of low molecular weight (<1000 Da) and high molecular weight (>10,000 Da) model drug compounds from both alginate and HA photogels with various light treatments. Novel loading mechanisms were developed through the loading of compounds into uncrosslinked gels followed by crosslinking 365 nm exposures to “lock” in the model drug compounds. Diffusion coefficients effectively compared the different systems showing increase exposures of 365 nm resulted in greater decrease in release of compounds demonstrating the ability to fine-tune release rates. Different formulations and control gels demonstrate a variety of different release profiles. The photogels were valuable long-term controlled release systems (>80 days) that also demonstrate high cytocompatibility when grown with ophthalmic cell lines.

Novel photoresponsive biomaterials for smart delivery of therapeutics which use light-controlled crosslinking and decrosslinking mechanisms have been developed. The PEG-anthracene graftable photocrosslinkers show the ability to introduce photo-controlled crosslinking into hydrogel systems. While anthracene as the photodimerizer and alginate and HA as the bulk materials are used as a proof-of-concept in this work, this grafting system can be further manipulated to include new photosensitive dimerizers and other applicable polymers. The ability to use light stimuli to control release rates in a continual fashion, rather than having delivery that is strictly on or off, is a valuable finding that may lead to the development of drug delivery systems that can be catered towards individuals and the progression of their disease.

Acknowledgments

When I started my doctoral thesis, I never anticipated the large role the support of my advisors, friends and family would play in helping me with its completion. This thesis would not have been possible without all the advice, support and encouragement I received from many people!

Most importantly, I would like to thank my supervisor Heather Sheardown. When I started at McMaster several years ago, I never realized how supportive a supervisor she would make for both my Master's and Doctorate degrees! In addition her expertise guidance, she gave me independence to grow as a researcher while supporting and supervising my academic endeavours. She is a great mentor and friend. If I become half the academic/researcher/role-model/supervisor that she is, I will be proud.

I would also like to show my gratitude to my thesis committee members, Dr. Mike Brook and Dr. Shiping Zhu, for their helpful advice that shifted the focus of my research throughout my Ph.D. thesis to help build the project. I would also like to thank Dr. Alison Holloway and Dr. Helen Burt for serving as examiners and giving me feedback on the thesis, Dr. John Preston use of his excimer laser and Gabriel Devenyi for help with exposing gels with the laser. I would like to express my gratitude to past summer students Brandon Shiplo, Keith Oxby and Stephanie Furukawa for their help in the lab.

I would like to thank my colleagues in the department of Chemical Engineering. They have opened many doors in my life and the collaborative nature of the department made my thesis an enjoyable experience. I would also like to thank colleagues in the Sheardown lab group for their research advice and for supportively allowing me to turn

off all the lights in the lab every day for a few years – a side-effect of performing light-responsive research! More specifically, Lina, Marta, Scott and Fran have been around since I started several years ago and our numerous discussions helped improve my thesis research. Over the years I have had amazing opportunities to become involved in the McMaster University community and would like to thank all the students and Faculty who supported my outreach initiatives to give me a well-rounded academic experience with the flexibility to continue my thesis research.

Over the years there have been many cheerleaders that helped me start, continue and finish my thesis. I would like to thank my Ottawa friends for being patient with me and encouraging me as the “forever-student”. I would also like to thank Marta Princz for chatting through problems and keeping me sane over the last several years both inside and outside of school. Also a big thanks to Brendan Warren – he has helped me out more than he realizes in the last year. Thanks to the many other friends inside and outside of McMaster for their advice and support.

This thesis would not have been possible without the unconditional love and support from my parents, Geri and George, my brothers and their wives, Jamie, Karen, Matthew and Emily, and my nephew Andrew. Thanks for being there for me loudly or silently and always cheering me on!

I would also like to thank NSERC, OGS and the 20/20 NSERC Ophthalmic Materials Network for funding without which my research could not have taken place.

Thank you to everyone who provided me with care, support, advice and encouragement!

TABLE OF CONTENTS

| | |
|---|-----|
| Title Page | i |
| Descriptive Note | ii |
| Abstract | iii |
| Acknowledgements | v |
| Table of Contents | vii |
| List of Figures | ix |
| | |
| 1.0 Literature Review and Scope | 1 |
| 1.1 Retinal Drug Delivery | 1 |
| 1.2 Controlled Drug Delivery | 4 |
| 1.2.1 <i>The Concept</i> | 4 |
| 1.2.2 <i>Ophthalmic Drug Delivery Systems</i> | 7 |
| 1.3 Responsive Drug Delivery | 12 |
| 1.4 Photoresponsive Drug Delivery for the Posterior Segment | 14 |
| 1.5 Photoresponsive Molecules | 15 |
| 1.5.1 <i>Photoreversible Dimerization</i> | 16 |
| 1.5.2 <i>Anthracene</i> | 21 |
| 1.6 Hydrogel Polymers for Posterior Segment Drug Delivery | 22 |
| 1.6.1 <i>Alginate</i> | 23 |
| 1.6.2 <i>Hyaluronate</i> | 25 |
| 1.7 Scope of Work | 26 |
| 1.7.1 <i>Photocrosslinkers</i> | 28 |
| 1.7.2 <i>Anthracene Photogels</i> | 29 |
| 1.7.3 <i>HA Photogels</i> | 30 |
| 1.7.4 <i>Overview</i> | 31 |
| 1.8 References | 32 |
| | |
| 2.0 Methods | 43 |
| 2.1 Photocrosslinker Synthesis | 43 |
| 2.1.1 <i>Carbodiimide Chemistry</i> | 43 |
| 2.1.2 <i>Protecting Groups</i> | 44 |
| 2.1.3 <i>PEG-anthracene</i> | 45 |
| 2.2 Hydrogel Synthesis | 46 |
| 2.3 Light Sources for PEG-anthracene and Photogels Stimuli | 47 |
| 2.3.1 <i>UV Source</i> | 47 |
| 2.3.2 <i>UV Treatment Procedure Specifics</i> | 51 |
| 2.4 Analysis Techniques | 52 |
| 2.4.1 <i>NMR and FTIR</i> | 52 |
| 2.4.2 <i>Spectrophotometry</i> | 52 |
| 2.4.3 <i>PEG Grafting</i> | 53 |
| 2.4.4 <i>Swelling and Effective Crosslinking Density</i> | 54 |

| | |
|--|------------|
| 2.5 Enzymatic Degradation | 56 |
| 2.6 Release Studies | 57 |
| 2.6.1 <i>Model Drug Compounds</i> | 57 |
| 2.6.2 <i>Release Study Protocol</i> | 58 |
| 2.7 Cytocompatibility Studies | 60 |
| 2.7.1 <i>MTT Assay</i> | 60 |
| 2.7.2 <i>Cell Tests</i> | 61 |
| 2.8 References | 62 |
| | |
| 3.0 Paper One: Graftable PEG-Anthracene to Generate Photoresponsive Hydrogels for Drug Delivery | 64 |
| | |
| 4.0 Paper Two: Synthesis and Optimization of Graftable Polyethylene Glycol – Anthracene Macromolecules | 97 |
| | |
| 5.0 Paper Three: Controlled Release with Polyethylene Glycol – Anthracene Modified Alginate | 122 |
| | |
| 6.0 Paper Four: Photoresponsive PEG-Anthracene Grafted Hyaluronate as a Smart Controlled-Delivery Biomaterial | 163 |
| | |
| 7.0 Conclusions and Future Work | 205 |
| | |
| Appendices | 216 |
| 1. PEG-Anthracene Synthesis | 216 |
| 2. Grafting of PEG-Anthracene onto Hyaluronic Acid | 218 |
| 3. Model Drug Assays | 219 |
| 3.1 Small Molecule Detection | 219 |
| 3.2 Protein Detection | 219 |
| 4. Release Study Protocol | 221 |
| 5. Cell Culture Methods | 223 |
| 6. MTT Assay | 225 |
| 7. Cytocompatibility Tests | 226 |

LIST OF FIGURES

| | |
|---|----|
| Figure 1-1. A cross section of an eye illustrates the location of the posterior segment in relation to the macula and retina. _____ | 1 |
| Figure 1-2. Normal (left) versus wet-AMD vision. Courtesy: National Eye Institute, National Institutes of Health. _____ | 2 |
| Figure 1-3. An illustration of side-effects noted with 2000 injections from the ANCHOR trial [1-21]. _____ | 4 |
| Figure 1-4. Drug concentrations over time with repeat administration results in peaks over the maximum safe concentration and lengthy periods in under the minimum effective concentration [1-23]. _____ | 6 |
| Figure 1-5. Drug concentrations with sustained delivery devices after 1 dose are aimed to have drug concentrations that are maintained within the therapeutic range over lengthy periods of time. _____ | 7 |
| Figure 1-6. The multiple optional locations for long term ocular drug delivery devices. Reprinted from [1-27], Copyright (2010) with permission from Elsevier. _____ | 8 |
| Figure 1-7. An overview of the shape and implantation location of Vitrasert, Retisert, I-ivation, NT-501, Posurdex, Iluvien/Medidur and other similar devices. Permission requested from [1-28]. _____ | 9 |
| Figure 1-8. Dimerization and dissociation of anthracene (a), cinnamylidene acetate (b), nitrocinnamate (c) and coumarin (d). _____ | 18 |
| Figure 1-9. Dimerization of anthracene occurs at wavelengths over 300nm and de-dimerization under 300nm. Note that in the presence of oxygen endoperoxide is a competing reaction that may occur [1-74]. _____ | 22 |
| Figure 1-10. The factors that can affect protein and drug release from hydrogel matrices. Reprinted from [1-91], Copyright (2010) with permission from Elsevier. _____ | 23 |
| Figure 1-11. An illustration of the components of alginate. M= β -D-mannuronic acid, G= α -L-guluronic acid. _____ | 24 |
| Figure 1-12. The components of HA. _____ | 26 |
| Figure 2-1. The reaction between carboxyl terminated R ₁ with amine terminate R ₂ using EDC. A: Without NHS. B: With NHS. Adapted from [2-1]. _____ | 44 |

| | |
|---|-----|
| Figure 2-2. Carbodiimide chemistry to create anthracene-terminated PEG from either boc-PEG-amine or trt-PEG-amine. _____ | 46 |
| Figure 2-3. 11 unit amine-terminate PEG-anthracene was the photocrosslinker used in the majority of the studies. _____ | 46 |
| Figure 2-4. The difference between exposure and fluence. _____ | 49 |
| Figure 2-5. Peak wavelengths of some common excimer lasers. _____ | 50 |
| Figure 2-6. Scan of un-dimerized anthracene-9-carboxylic acid. _____ | 53 |
| Figure 2-7. Ninhydrin reacts to produce Ruhemann's purple with the presence of primary amines. _____ | 54 |
| Figure 2-8. The structures of (A) Coomassie Blue, (B) Fast Green and (C) dextran. _____ | 58 |
| Figure 2-9. MTT is converted to formazan by mitochondrial reductase. _____ | 61 |
| Figure 3-1. Photogels based on anthracene dimerization. _____ | 89 |
| Figure 3-2. Synthesis of HA photogels. _____ | 89 |
| Figure 3-3. Photogel crosslinking. _____ | 90 |
| Figure 3-4. Release of Coomassie blue from photogels with UV treatments _____ | 91 |
| Figure 3-5. Release of proteins from photogels with UV treatments. _____ | 91 |
| Figure 3-6. Cytocompatibility testing of cells grown with photogels. _____ | 92 |
| Figure 4-1. Anthracene dimerization with a generic substitution on the ninth carbon. _____ | 116 |
| Figure 4-2. PEG-anthracene synthesis. _____ | 116 |
| Figure 4-3. Spectrophotometer scans of PEG-anthracene before and after irradiation of 365nm (0.5mW/cm ²). _____ | 117 |
| Figure 4-4. Release of Coomassie blue from alginate grafted with PEG ₁₁ -anthracene (photogels) made with a 1 : 1.3 molar ratio and control PEG hydrogels crosslinked with PEG ₁₁ diamine. _____ | 117 |
| Figure 4-5. Release of lysozyme from (A) control PEG hydrogels crosslinked with PEG ₁₁ diamine and (B) PEG ₁₁ -anthracene crosslinked alginate photogels. _____ | 118 |

Figure 5-1. PEG-anthracene photoreversible dimerization and alginate. _____ 151

Figure 5-2. Effective crosslinking density of gels before and after loading. _____ 152

Figure 5-3. Coomassie Blue release from photogels and control PEG hydrogels. ____ 153

Figure 5-4. Fast Green release versus Coomassie Blue release from photogels _____ 154

Figure 5-5. Coomassie Blue release from high alginate concentration photogels ____ 154

Figure 5-6. Coomassie Blue release from calcium alginate gels and calcium-reinforced photogels _____ 155

Figure 5-7. Coomassie Blue release from star-PEG-anthracene containing photogels. 156

Figure 6-1. PEG-anthracene grafted onto HA. _____ 197

Figure 6-2. The effective crosslinking of unloaded versus loaded photogels and control PEG hydrogels. _____ 197

Figure 6-3. Cumulative release of Coomassie Blue, Fast Green and dextran from HA photogels into PBS at 37°C. _____ 198

Figure 6-4. Cumulative release of Coomassie Blue from star-PEG-anthracene containing HA photogels into PBS at 37°C. _____ 198

Figure 6-5. Lysozyme and BSA release from photogels. _____ 199

Figure 6-6. MTT assay results of RPE cells growth with varying PEG-anthracene concentrations over 3 and 7 days. _____ 199

Figure 6-7. Gels added to a confluent layer of RPE cells after 24 hours of growth. _ 200

Figure 6-8. Confluent layers of RPE cells grown with degradation products. _____ 200

1.0 Literature Review and Scope

1.1 Retinal Drug Delivery

A major challenge in ophthalmology is the effective delivery of therapeutic doses of drugs to the posterior segment of the eye targeting the retinal and macular regions as illustrated in Figure 1-1. There are significant ocular barriers that prevent the free movement of drugs from the blood stream and through the layers of the eye presenting a unique drug delivery challenge.

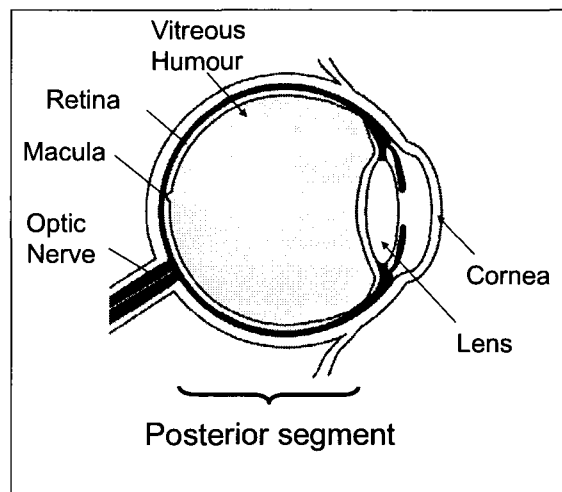


Figure 1-1. A cross section of an eye illustrates the location of the posterior segment in relation to the macula and retina.

Diseases of the posterior segment of the eye, including age-related macular degeneration (AMD) and diabetic retinopathy are the most common causes of visual impairment in Canada, particularly among the aging Canadian population. Age-related macular degeneration is the leading cause of blindness in the population over 50, affecting over 2 million Canadians [1], a number expected to triple in the next 25 years [2]. Exudative AMD (wet AMD) accounts for less than 20% of all AMD cases but is an

aggressive form responsible for the majority of AMD associated vision loss. Vascularization and edema at the macular region causes disruption of the retina and the condition progresses rapidly, leading to legal blindness in as little as 2 years [3]. Figure 1-2 illustrates central vision loss that occurs with wet AMD to negatively impact quality of life and lead to adverse effects on the economy due to loss-of-work and health care costs [4,5].



Figure 1-2. Normal (left) versus wet-AMD vision. Courtesy: National Eye Institute, National Institutes of Health.

Therapies that aim to block the AMD pathogenic protein, vascular endothelial growth factor (VEGF), have shown the great promise for both preventing and possibly reversing choroidal neovascularization (CNV) associated with exudative AMD [6]. As summarized in Table 1-1, these anti-VEGF drugs bind and disable VEGF to slow the progression of neovascularization. Up to 40 other compounds are under development for the treatment of various CNV retinal diseases [7].

Table 1-1. The current approved, used and phase 3 anti-VEGF therapies available for wet AMD.

| Name | Name | Size | Constituents | Approval |
|------------------------------|-------------|-----------------|---|------------------|
| Lucentis (Genentech) | Ranivizumab | 48 kDa [8] | Fab fragment [8] | Approved 2006 |
| Macugen (Eyetechn/Pfizer) | Pegaptanib | 50 kDa [9] | Pegylated aptamer [10] | Approved 2004 |
| Avastin (Genentech) | Ranibizumab | 148kDa [11] | Monoclonal antibody (humanized) [12] | Off-label use |
| VEGF Trap-eye (Regeneron) | VEGF trap | 115 kDa [13] | Soluble receptor [14] | Phase 3 |

The administration methods for these VEGF-blocking treatments are extremely limited and delivery will be a critical determinant of their therapeutic effectiveness. Topical drug delivery, including eye-drops, typically delivers insufficient drug to the posterior segment with only 5 % drug penetration into the front of the eye [15,16]. Systemic drug delivery can result in side effects to non-target organs and most drugs have limited capability for diffusion through the blood-retinal barrier to the target site [17]. Intravitreal injections directly into the posterior eye are currently the most efficient and effective method for delivering therapeutics to the retina. However, typically multiple injections at regular monthly intervals are required in order to continually suppress wet AMD progression and reoccurrence with anti-VEGF drugs [18]. This is associated with low patient compliance due to the invasiveness of the procedure and is expensive as professional administration is necessary [19]. Each injection poses significant risks of cataract formation, retinal detachment, vitreous hemorrhage and endophthalmitis [20]; the frequent injections required for these drugs statistically increase the risk. Figure 1-3 summarizes the results of a study focused on 2000 injections on 450 patients for AMD treatments with Avastin and Lucentis. It is clear that while in 22.3% of the cases patients

reported no adverse side effects, the majority had issues ranging from irritation to potentially blinding diseases [21]. Other studies such as the ANCHOR trial have reported 1.4% cases of endophthalmitis and 0.7% cases of serious uveitis, critical conditions that could lead to blindness. There is clearly a need for new drug delivery systems for these pharmacologic agents as well as for the others that are under development to allow long-term treatment without the added risks and costs associated with multiple repeat injections.

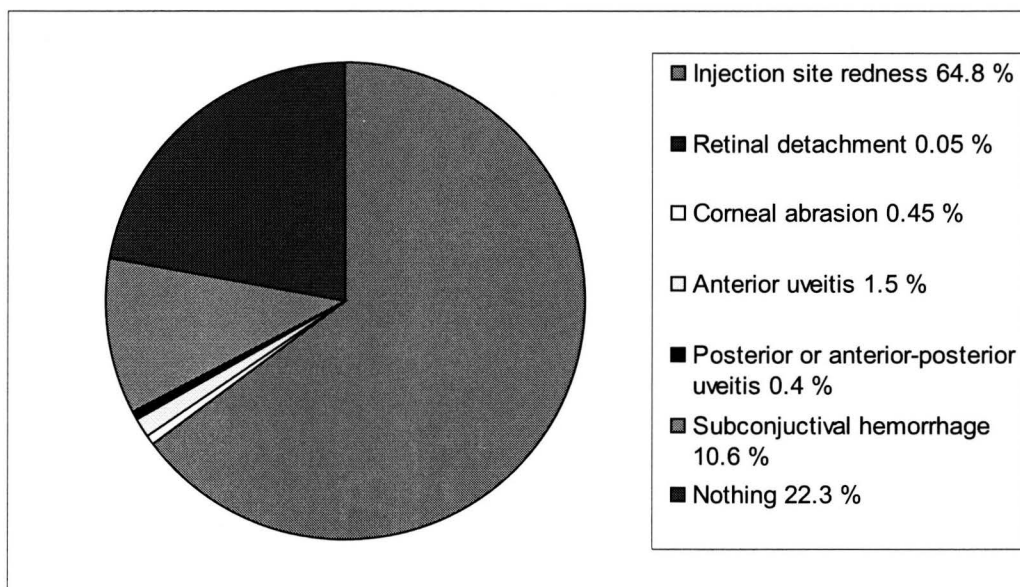


Figure 1-3. An illustration of side-effects noted with 2000 injections from the ANCHOR trial [21].

1.2 Controlled Drug Delivery

1.2.1 The Concept

The goal of drug delivery is to transport drug to the target site and maintain its concentration at therapeutic levels. Delivery methods can include intramuscular,

intravenous, subcutaneous and oral routes in the forms of pills, injections, creams, patches, drops, and aerosols [22]. However many of these methods lead to the systemic delivery of the drug, and necessitate elevated concentrations in the blood stream in order for therapeutic doses to be maintained at the target site. This results in unwanted side-effects in non-target tissues and organs. Shown in Figure 1-4 is an example of a drug concentration profile with repeat dosing. Drug concentrations in the therapeutic range are at effective concentrations. Note that the drug level repeatedly increases above the maximum safe concentration putting a patient at risk of potential toxic side effects and that the drug level also decreases below the minimum effective concentration for prolonged periods of time resulting in ineffective drug levels [23]. These issues are compounded when a patient is non-compliant and misses these doses due to timing, dose invasiveness or forgetfulness. Localized delivery to specific target tissues and organs in a controlled fashion would not only increase effectiveness but also reduce side effects seen in systemic delivery.

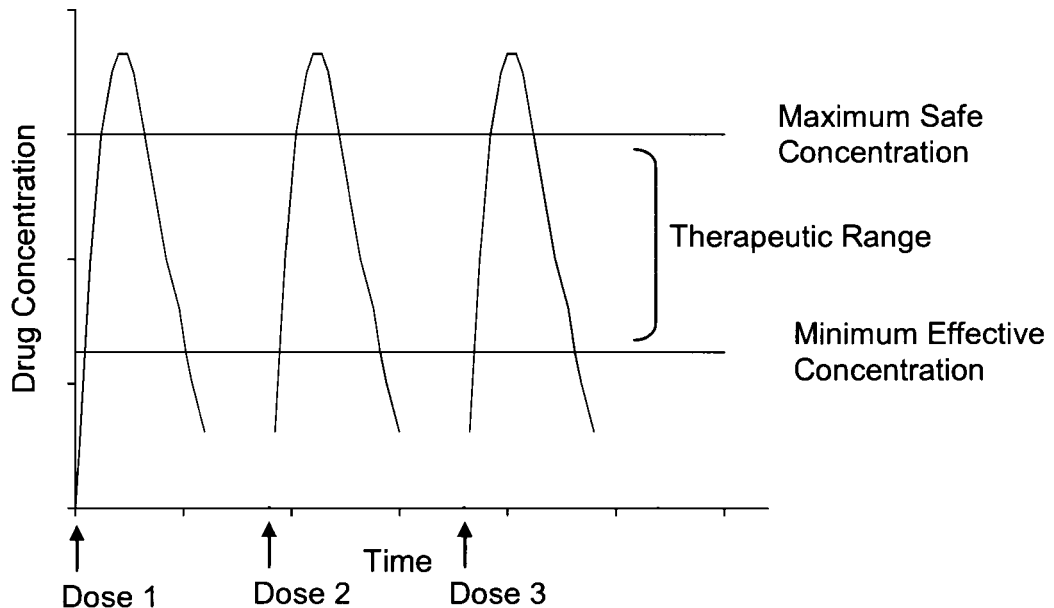


Figure 1-4. Drug concentrations over time with repeat administration results in peaks over the maximum safe concentration and lengthy periods in under the minimum effective concentration [23].

Controlled release devices have a significant therapeutic advantage for treating diseases of the relatively inaccessible back of the eye. By loading drugs into a matrix and allowing for extended release by diffusion, long term delivery from a single device can be obtained [22]. As illustrated in Figure 1-5, the goal in controlled release is to maintain the drug concentrations in the therapeutic concentration range for extended periods of time to maintain the effectiveness of the drug and eliminate possible side effects from the high concentrations that are observed with repeat administrations. For wet AMD anti-VEGF treatments, this would also eliminate the need for repeat injections to increase patient compliance and decrease risks associated with repeat injections.

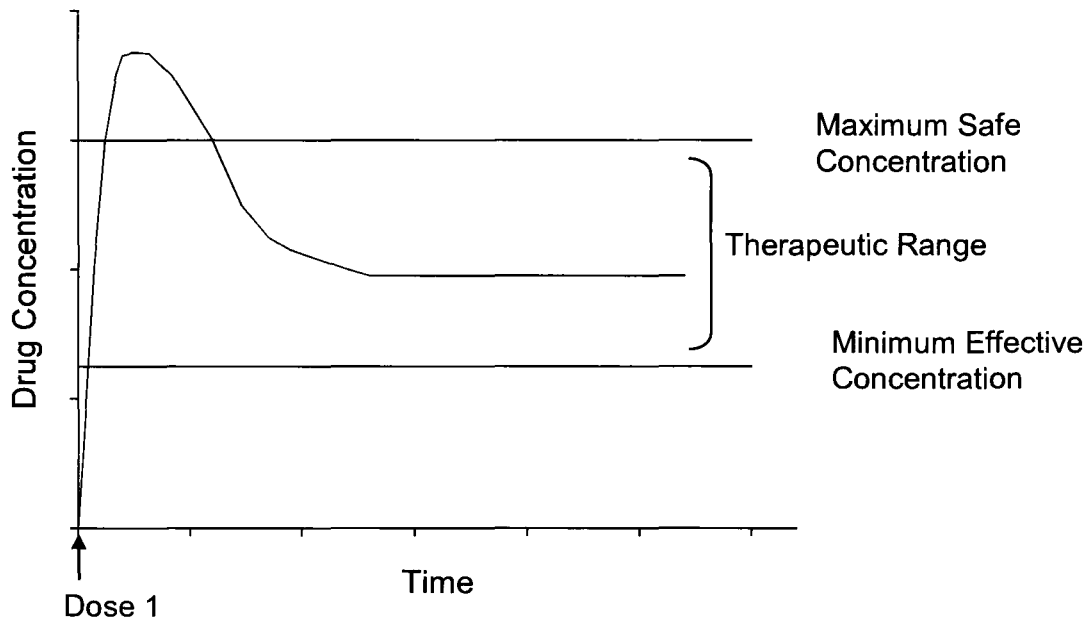


Figure 1-5. Drug concentrations with sustained delivery devices after 1 dose are aimed to have drug concentrations that are maintained within the therapeutic range over lengthy periods of time.

Polymers provide platforms to slow the diffusion of drugs by acting as barriers to allow for their storage and long-term release. For example, monolithic devices consisting of hydrophilic polymer matrices have a mesh size that can restrict drug movement and diffusion to inhibit release [24,25]. Alternatively, reservoir devices consisting of membranes surrounding drug loaded cores have rate-limiting membranes that act as barriers to control drug release [25,26].

1.2.2 Ophthalmic Drug Delivery Systems

For sustained delivery in the eye, it is critical that release devices are maintained outside the visual pathway. Figure 1-6 illustrates the numerous potential locations for long-term ocular delivery devices.

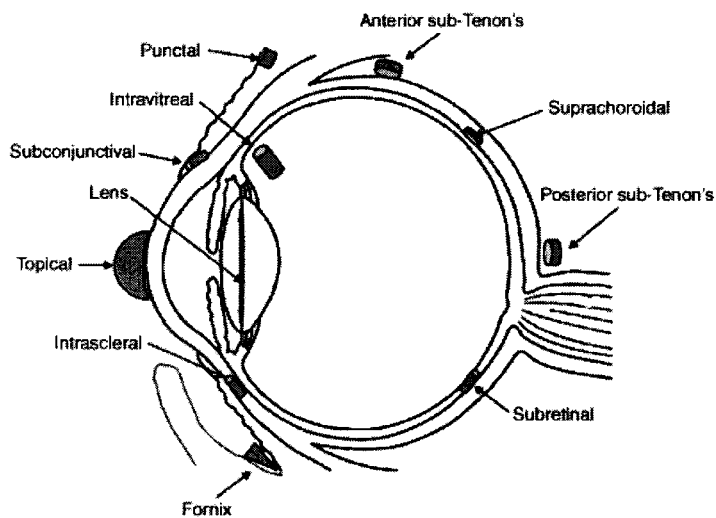


Figure 1-6. The multiple optional locations for long term ocular drug delivery devices. Reprinted from [27], Copyright (2010) with permission from Elsevier.

Several non-degradable and degradable polymeric ophthalmic devices have been commercialized for the treatment of retinal diseases. As listed in Table 1-2, eight devices have shown promise in clinical trials and clinical practice. The implantation location of these devices is outlined in Figure 1-7.

Table 1-2. A summary of current ophthalmic posterior segment sustained drug delivery systems. PVA= poly vinylalcohol, EVA= ethylene vinyl acetate, PLGA= poly(lactic-co-glycolic acid), HPMC= hydroxypropyl methylcellulose

| Name | Company | Therapeutic | Degradable | Material |
|-------------------------|---------------------------------|------------------------------|------------|----------------------------------|
| Vitrasert [28] | Bausch & Lomb | Ganciclovir | No | PVA & EVA |
| Retisert [28,29] | Bausch & Lomb | Fluocinolone acetonide | No | PVA & Silicone |
| I-vation | SurModics | Triamcinolone acetonide | No | polybutyl methacrylate & polyEVA |
| Iluvien/Medidur [30,31] | Alimera Sciences Inc | Fluocinolone acetonide | No | PVA |
| Posurdex [28,32] | Allergan | Dexamethasone | Yes | PLGA |
| Surodex [28,33] | Oculex Pharmaceuticals/Allergan | Dexamethasone | Yes | PLGA HPMC |
| Ozurdex [32] | Allergan | Dexamethasone | Yes | PLGA |
| NT-501 [28] | Neurotech Pharmaceuticals | Encapsulated cell technology | No | Fiber membrane |

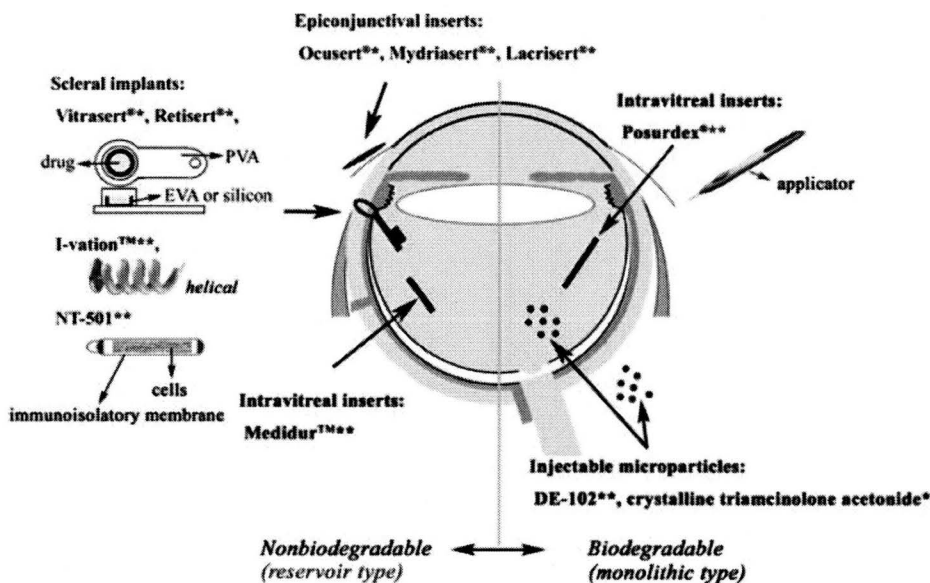


Figure 1-7. An overview of the shape and implantation location of Vitrasert, Retisert, I-vation, NT-501, Posurdex, Iluvien/Medidur and other similar devices. Reproduced from [28] with kind permission of Springer Science+Business Media.

Vitrasert delivers ganciclovir to treat cytomegalovirus retinitis. Composed of a drug-containing tablet coated with poly vinylalcohol (PVA) and ethylene vinyl acetate (EVA), Vitrasert can control release over 5-8 months. It is surgically implanted by placing it in a surgically-cut cavity followed by fixation with anchoring sutures. Visual impairment can occur 2-4 weeks after implantation likely from the surgical implantation, since the complication improves afterwards [28].

Retisert delivers fluocinolone acetonide for chronic non-infectious uveitis. Composed of a drug-containing core coated with PVA and silicone laminate, drug release can be controlled at a steady rate up to a period of 30 months. Steroid-induced ocular complications can occur within 34 weeks of implantation with 60% of patients requiring glaucoma treatment and, within 2 years, 32% of patients requiring glaucoma surgery [29]. However, these complications are also associated with uveitis inflammation so overall, Retisert is still highly effective. Using the same procedure as Vitrasert, Retisert is also implanted surgically [28].

I-vation delivers triamcinolone acetonide to treat diabetic macular edema. It is a corkscrew-shaped device which minimizes the invasiveness of its implantation and maximizes surface area for drug delivery. Its small diameter allows for a sclerotomy-based implantation. Consisting of a drug-containing polymer coating on a metal based, release profiles can be adjusted by altering the thickness of the polymer coating. The coating is composed of a blend of polybutyl methacrylate and polyEVA [28]. Ongoing clinical trials show that at 24 months of delivery devices containing 925 μg of

triamcinolone in both slow and fast release formulations show 64% and 72% improvement in visual acuity and in macular thickness [34].

Iluvien and Medidur are different names for the same device that delivers fluocinolone acetonide for the treatment of diabetic macular edema. This insert is a small 3.5 mm long cylinder with a radius of 0.37 mm that may be injected into the posterior segment with a 25 gauge needle to deliver over 18-24 or 24-30 months [28,30]. Recent studies comparing 0.2 $\mu\text{g}/\text{day}$ versus 0.5 $\mu\text{g}/\text{day}$ fluocinolone acetonide delivery from Iluvien inserts into diabetic macular edema patient eyes showed both groups had mean improvements at 3 months with reduced foveal thickness maintained at 1 year [31]. Intraocular pressure was less than those seen with other inserts. However, the groups were small so phase III trials will give more substantiated evidence once completed in 2010 [31].

Posurdex delivers dexamethasone for the treatment of persistent macular edema which is a complication of diseases such as diabetic retinopathy, uveitis, retinal vein occlusions and cataract surgery. Composed of poly (lactic-co-glycolic acid) (PLGA), this insert can be implanted through small incisions or a new prototype can be inserted via a disposable applicator [28]. Ozurdex also delivers dexamethasone for the treatment of macula edema up to 6 months. It is a rod-shaped implant made of PLGA [32].

NT-501 is an encapsulated cell technology device to produce sustained delivery of cell-derived molecules such as ciliary neurotrophic factor for the treatment of retinitis pigmentosa. The cells are modified to synthesize and release therapeutics through a semi-

permeable membrane with demonstrated protein delivery up to 18 months. There is potential to release a variety of proteins, antibodies and cytokines [28,35].

Despite all the advances of posterior segment drug delivery devices, none have publicly demonstrated the ability to deliver active anti-VEGF agents described in Table 1-1. However some research is ongoing; for example, Avastin has shown controlled delivery from ring capsular devices [7] and a collaborative effort between Genentech and SurModics is investigating controlled delivery of Lucentis from microparticles [14]. These efforts will continue since long-term controlled drug delivery devices for anti-VEGF agents have been well recognized to potentially alleviate injection issues [36-38].

While these devices show promise in long-term controlled delivery of drug to the posterior segment of the eye, they have fixed rates which may not be representative of chronic diseases that require life-long treatment. Studies have suggested there are potential benefits from altered Lucentis drug dose regimens that are monitored effectively with Optical Coherence Tomography [39,40]. The controlled release of drugs from smart materials that can have alterations in released doses with stimuli could optimize AMD treatments with anti-VEGF agents.

1.3 Responsive Drug Delivery

Responsive drug delivery devices whose delivery rates can be adjusted with internal or external stimuli may better suit disease progression by having decreases in release rates during disease regression and increases in release rates during disease progression. Possible stimuli are outlined in Table 1-3; internal stimuli occur naturally *in*

vivo while external stimuli may be applied at determined time points. By adjusting the polymer properties, pulsatile (on/off) or incremental (increase/decrease) changes in release of drugs out of polymer matrices can be adjusted throughout the life time of the delivery device.

Table 1-3. Internal and external stimuli responses that may be introduced into polymer biomaterials systems.

| Mechanism | Stimulus |
|-----------|--|
| External | Temperature Light Magnetic Ultrasound Electrical |
| Internal | Temperature pH Enzymes Ions |

Internal stimuli are changes that occur naturally *in vivo*. The pH of various tissues and intracellular compartments can vary, for example, from 5 in intracellular lysosomes to 7.45 in blood; in a cancerous tumour, the pH can decrease down to 6.5 [41]. Enzymes present in certain tissues and pathologies may cleave polymer bonds to act as stimuli for delivery [42]. Injectable materials can be designed to gel *in situ* due to temperature changes from room temperature to physiologic [43]. Internal stimuli from disease and natural biological rhythms could also be applied to create responsive materials [44].

External stimuli provide an opportunity to control biomaterial properties and drug delivery at chosen time points. Lasers and light are suited to transparent systems such as the eye where they may penetrate to reach the posterior segment [45]. Electrical, magnetic and ultrasound stimuli can target tissue with minimal side-effects [46]. Controlled changes in temperature may also be applied to cause pulsatile changes and has been investigated with hypothermic cycling in patients [42].

1.4 Photoresponsive Drug Delivery for Posterior Segment Drug Delivery

Ophthalmic drug delivery to the posterior segment of the eye could highly benefit from a responsive controlled drug delivery mechanism. Light or laser induced changes are exceedingly feasible due to the transparency of the eye and the advanced technology in ophthalmic lasers that allow for strict control of wavelengths, intensities and focal points [45,47,48]. Visible, ultraviolet (UV) and infrared (IR) light/lasers can be used as stimuli whose wavelength can be highly controlled to fine-tune outcomes. Light and laser outcomes are instantaneous providing fast response times, unlike those observed in pH and thermoresponsive materials which have lagged response times since they require the diffusion of ions and transfer of heat [49].

Light therapies have demonstrated the feasibility of the application of photoresponsive materials in the eye. Photodynamic therapy with verteporfin is an approved treatment for a variety of choroidal vascular disorders that now rarely includes wet-AMD since the emergence of anti-VEGF agents onto the market [50]. Prodrugs are intravenously injected into patients then subsequently photochemically activated through

the application of 692 nm light at 100 J/cm^2 in the back of the eye. Since systemically delivered, verteporfin therapy and other similar prodrugs/photodynamic therapies have potential risks to non-targeted tissue. For example patients that have undergone verteporfin photodynamic therapy must wait 5 days before exposure of eyes or skin to external light sources [51].

Lessons learned with photodynamic therapy implementation, including the development of high power diode lasers, suggest that UV light can easily be directed at photoresponsive drug delivery devices located in the vitreous humour. Lasers allow for high intensity monochromatic light to be directed at precise spots of $8000 \mu\text{m}$ [3]. In addition to ophthalmology, systems in gynaecology, dermatology, otolaryngology, gastroenterology and physiotherapy are also amenable to light and laser responsive devices and are medical areas that are already well-versed in the application of lasers [48].

1.5 Photoresponsive Molecules

Molecules that undergo isomerization or dimerization with specific UV and visible light can be exploited to introduce reversible qualities in biomaterials through their covalent incorporation into polymer systems. There is extensive literature exploring biomaterials that incorporate molecules that undergo either photoisomerization or photodimerization.

Azobenzene [52] and spirobenzopyran [53] undergo photoisomerization with UV and visible light which can introduce photoinitiated structural and solubility alterations

when bound within polymers [54]. Polymer-bound photoisomerizing groups can modify rheological and crosslinking properties of polymer gels. For example, azobenzene bound to polymer networks can create photoinduced hydrophobic domains that bridge polymer networks to cause crosslinking [55]. When bound to 2 chains, the length decrease associated with azobenzene trans to cis isomerization (9.0 to 5.5 angstroms)[56]) can alter mesh sizes and therefore crosslinking density of polymer networks [55,57]. While photoisomerizing molecules clearly introduce reversible changes into bulk polymer systems, they have shown minimal influence on changing diffusion and delivery rates of molecules [55,58]. In addition, the ability for visible light to act as stimuli is undesirable; unintentional changes may occur in ophthalmic applications since visible light is constantly exposed to the eye. Molecules that undergo reversible photodimerization with strictly UV light/lasers will be the focus since large quantities of UV light should not naturally penetrate to the posterior segment [59] so the dimerization and materials responses can be strictly controlled.

1.5.1 Photoreversible Dimerization

Molecules that have the ability to dimerize with a second molecule could be used to form reversible crosslinking systems to create photoresponsive systems with minimum side-product formation, fast curing and high spatial control [60]. Anthracene [60], cinnamylidene acetate [61], nitrocinnamate [62] and coumarin [63] are popular dimerizing molecules in the investigation of photosensitive polymerization and crosslinking of both synthetic and natural hydrogels. As illustrated in Figure 1-8,

nitrocinnamate, cinnamylidene acetate, and coumarin undergo isomerisation followed by reversible $[2\pi+2\pi]$ photoaddition to form cyclobutane rings [54,64-66] and anthracene undergoes reversible $[4\pi+4\pi]$ photocycloaddition with dimerization at wavelengths over 300nm and dissociation at wavelengths less than 300nm [67-69]. Table 1-4 briefly summarizes some examples of polymer systems modified with photodimerizing molecules.

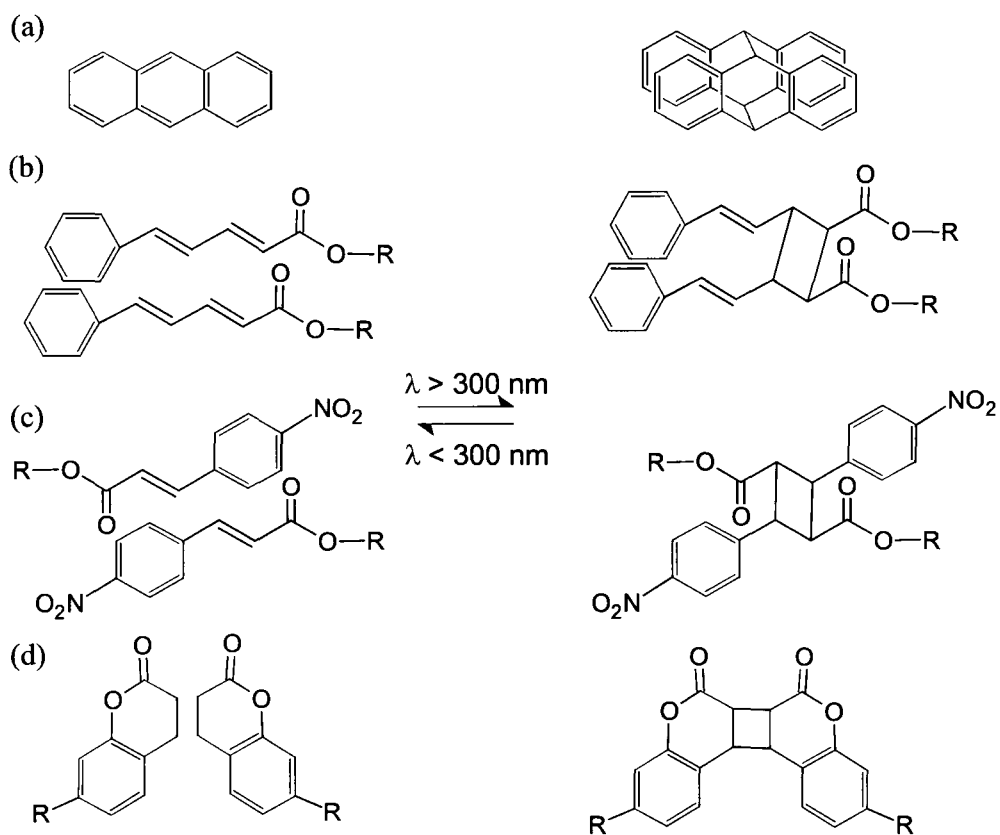


Figure 1-8. Dimerization and dissociation of anthracene (a), cinnamylidene acetate (b), nitrocinamate (c) and coumarin (d).

Table 1-4. Overview of investigated photoreversible-polymer hydrogel systems. PEG=polyethylene glycol. PMAA=polymethacrylic acid. PMMA=polymethyl methacrylate MA=methacrylate PS=polystyrene

| Photoreversible group | Polymer | Results | References |
|------------------------------|----------------|---|-------------------|
| Cinnamylidene acetate | PEG 4-armed | <ul style="list-style-type: none"> • Photoswitching behaviour • Physical properties controlled by wavelength exposure • Long exposure times required | [61,70-73] |
| | MA copolymer | <ul style="list-style-type: none"> • Photosensitive • Effects swelling and gelation | [74] |
| Nitrocinnamate | PEG 8-armed | <ul style="list-style-type: none"> • Photocissable in the absence of photoinitiators or catalysts • Rapid reversible crosslinking • FGF-2 drug release over short term | [62,75,76] |
| | Gelatin | <ul style="list-style-type: none"> • Control swelling with UV light exposure • Low cytotoxicity | [77] |
| Anthracene | PMAA | <ul style="list-style-type: none"> • For reversible molecular imprinting | [78] |
| | PEG 8-armed | <ul style="list-style-type: none"> • Photoreversible up to 20% • No sol-gel-sol physical transition | [60] |
| | Dextran | <ul style="list-style-type: none"> • Hydrophilic with hydrophobic microdomains | [79] |
| | PMMA | <ul style="list-style-type: none"> • Examined critical number of crosslinks and photocission-Not a water based system • Indicated more investigations required | [80] |
| | MA copolymer | <ul style="list-style-type: none"> • Small spacer between backbone • Examined side reactions | [81] |
| | PS | <ul style="list-style-type: none"> • Complete photoreversibility • Used as chain builder, not crosslinker | [82] |
| | PS/PMMA | <ul style="list-style-type: none"> • End capped polymer • Used to form diblock copolymers | [83] |
| Coumarin | PEG | <ul style="list-style-type: none"> • For photoreversible chain extension | [63] |

Incorporation of photodimerizing groups with polymers can potentially create materials that can support cell growth and protein attachment and potentially alter the diffusion of molecules. Due to its high compatibility, PEG based hydrogels with photodimerizing groups have been investigated [84], for example, cinnamylidene acetate terminated four arm PEG can form gels with UV light exposure [72], coumarin-bound organophosphorus hydrolase could be photoimmobilized [71] and protein flux could be lowered through these materials with UV light treatments [61]. Incomplete sol/gel transitions were noted due to a small amount of crosslinking from dimerization that also occurs at low UV wavelengths of 254 nm [70]. Anthracene terminated 8 arm PEG that undergoes photocrosslinking has also been synthesized demonstrating light responsive reversible surface roughness [60]. Investigations into drug delivery applications of photoreversibly crosslinked hydrogels have been initiated by Andreopoulos *et al.* (2006). Nitrocinnamate capped 8-armed PEG polymers have been used to deliver fibroblast growth factor 2 at rates dependent on UV light exposure [75]. Release of growth factors from these materials showed UV-induced decreased release with 50-70% delivery at 120 hours (5 days) [75]. A drug delivery system with increased photosensitivity and better control of the sustained release of macromolecules would be beneficial for long-term drug delivery applications.

High wavelength light is known to better penetrate the eye. Despite possible interactions low wavelength light faces when penetrating the eye, losses are likely negligible when irradiation is on the order of 600mW/cm^2 [3]. Two-photon absorption (TPA) offers an opportunity to cause dimerization and de-dimerization at the back of the

eye. Ocular tissues at the front of the eye may absorb UV leading to deleterious effects [59]. TPA however uses wavelengths in the visible range to allow penetration through the cornea and lens with high three dimensional spatial selectivity [85] and has been demonstrated to effectively cause the dissociation of coumarin [86].

1.5.2 Anthracene

Anthracene is a well-known photodimerizing molecule useful for proof-of-concept studies for photoreversible drug delivery systems. Anthracene can dimerize at wavelengths over 300 nm and dissociate with exposure to UV light at wavelengths less than 300 nm or at temperatures approaching 130°C [67,81] as shown in Figure 1-9. The $[4\pi+4\pi]$ photocycloaddition of anthracene is a reductive process forming an ortho-substituted benzene molecule [67]. Side reactions may occur during UV light exposure in the presence of high amounts of oxygen as shown in Figure 1-9. Photodimerization is in competition with endoperoxide formation which can be monitored spectrophotometrically with increased absorption at 200 nm [81,87]. In addition, once dimerized, the photodimers will not absorb any light at 300 nm making it easy to track photodimerization spectrophotometrically [67]. Carbon 9-substituted anthracene dimers tend to form a “head to tail” conformation in solution, therefore if substituted at carbon 9, bound substituents will likely exist on opposite ends [68,69,88].

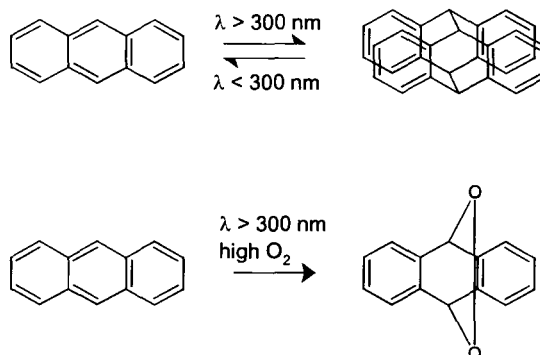


Figure 1-9. Dimerization of anthracene occurs at wavelengths over 300nm and de-dimerization under 300nm. Note that in the presence of oxygen endoperoxide is a competing reaction that may occur [74].

1.6 Hydrogel Polymers for Posterior Segment Drug Delivery

Hydrogels are hydrophilic polymer networks that are insoluble due to crosslink junctions but absorb large quantities of water, buffers and physiological fluids [24]. Their high water content resembles natural tissue making them widely investigated for drug delivery and well suited to the vitreous humour environment [89]. The vitreous humour consists largely of water (>98%) with collagen and hyaluronate (HA) [90]. The osmotic pressure and ionic properties of this physiologic gel may well match specific types of synthetic and natural hydrogels [90]. Hydrogel drug depot systems allow for the delivery of drug by diffusion through water filled pores.

Delivery of therapeutics from hydrogels is influenced by several factors. Their mesh size influences the microscopic space through which proteins and drugs can diffuse through after loading. Mesh size is influenced by the degree of crosslinking of a gel, the structure of the polymer backbones (and monomers) and external factors such as pH, temperature and ion concentrations [25,91] as illustrated in Figure 1-10. In addition to

predicting diffusivity of molecules, mesh size can also be a predictor of gel strength and degradation. The chemical structure of the polymer gel can introduce interactions such as ionic ones which can slow diffusion if the matrix and drug have opposite charges and increase diffusion if the matrix and drug have similar charges due to repulsion [92]. For non-porous hydrogels, the volume of liquid and flexibility of the chains within the gel can also influence diffusivity [91].

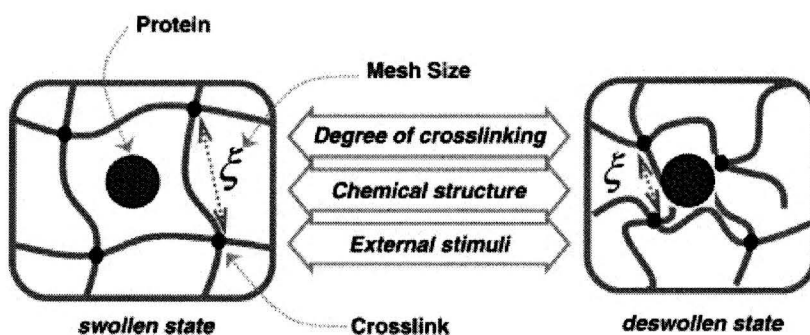


Figure 1-10. The factors that can affect protein and drug release from hydrogel matrices. Reprinted from [91], Copyright (2010) with permission from Elsevier.

Based on Fick's second law, an increase in the crosslink density of a hydrogel, decreases the diffusion coefficient of the solute within the matrix and hence the rate of delivery of the drug; decreasing the crosslinking density has the opposite effect [25]. It is believed that by incorporating a photosensitive crosslinking mechanism, crosslinking density and therefore diffusion can be controlled by light.

1.6.1 Alginate

Alginate is a non-toxic, degradable, linear copolymer of β -D-mannuronic acid (M) and its C-5 epimer, α -L-guluronic acid (G). As illustrated in Figure 1-11, these two acids

join to form 1-4 glycosidic linked blocks of M-M, G-G, and M-G [93]. Divalent ions, such as calcium, can be used to physically crosslink the G-G blocks through ionic interactions [94]. Alginate is a flexible, porous hydrogel whose mechanical properties may be altered by using alginates of different copolymer content. After crosslinking, significant amounts of water can be trapped within the alginate matrix [95]. Furthermore, the osmotic pressure of alginate has been shown to be high as a result of its negative groups influencing the infiltration of water in the presence of salt solutions [96]. The environment of the vitreous humour contains hyaluronate and its associated proteoglycans which have similar osmotic pressure and ionic properties as alginate.

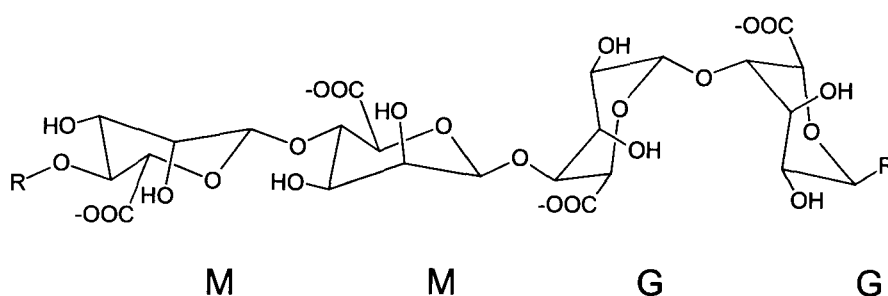


Figure 1-11. An illustration of the components of alginate. M= β -D-mannuronic acid, G= α -L-guluronic acid.

Physically crosslinked alginate has shown fast degradation and rapid release in ionic environments but reinforcement by associations with oppositely charged molecules or covalent modifications can increase its stability to increase delivery times [97,98]. Alginate can be reinforced with oppositely charged macromolecules such as chitosan [99], poly-L-lysine [100,101] and dipalmitoyl phosphatidylcholine liposomes [102]. Covalent modification of alginates with crosslinkers such as albumin [103], polyethylene

glycol [104,105], lysine [105], adipic dihydrazide [105] and glutaraldehyde [106] are effective at stabilizing its matrix to improve drug delivery properties [107]. For example, adipic dihydrazide-crosslinked alginate releases 60% of daunomycin (527.5 Da) over 40 days in Dulbecco's Modified Eagle's Medium [108] and alginate modification with a vinyl polymer resulted in an increased release time of N,N-diethyl-3-methylbenzamide to over 400 hours [109].

Previous studies have shown that physically crosslinked alginate can last over 2 weeks in the vitreous humour without any pathological or structural side effects [110]. Therefore, it is hypothesized that alginate will likely be well integrated into the vitreous humour over the long-term with minimal side-effects. There are no enzymes in humans that degrade alginate meaning that it can only be degraded via decrosslinking and hydrolysis [111]. Combined with its low cost and high availability, these properties make it an ideal candidate for drug delivery in the posterior eye.

1.6.2 Hyaluronate

Hyaluronate or hyaluronic acid (HA) is the predominant glycosaminoglycan constituent of the vitreous humour giving it potential as a relatively inert biomaterial delivery system in the posterior segment. As illustrated in Figure 1-12, HA is formed of alternating D-glucuronic acid and N-acetyl-D-glucosamine [76,112]. Human vitreous humour regularly contains 65-400 $\mu\text{g}/\text{mL}$ hyaluronate with an average molecular weight range of 2-4 million [76]. Hyaluronate solutions form coils generating highly viscoelastic networks at high concentrations. HA can be enzymatically degraded in vivo by

hyaluronidase (HAase) which is present on average at 20 turbidity reducing units (TRU) per mL in human vitreous humour [113] in the posterior segment of the eye.

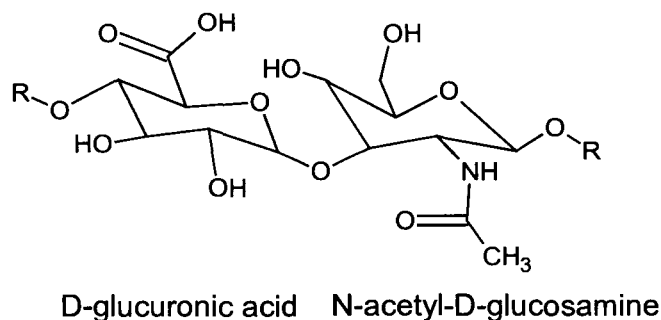


Figure 1-12. The components of HA.

Covalent modifications of HA can create stable crosslinked matrices ideal for drug delivery. Modifications with adipic dihydrazide [114,115], cellulose [116], amino acids [117], poly(ethylene oxide-star-propylene oxide) [118], disulfides [119], pluronics [120], methacrylates [121] and polyethylene glycol [122,123] are several examples that have been used to effect covalent crosslinking. Drug delivery systems composed of modified HA have also been investigated, although not widely. For example, BSA delivery from PEG crosslinked methacrylated HA has extended beyond 200 hours [122] and fibroblast growth factor delivery past 35 days from PEG crosslinked thiolated HA [124]. Since it forms a natural part of the vitreous humour, HA holds potential as a compatible drug delivery material for the posterior segment of the eye.

1.7 Scope of Work

The objective of this work was to create a photoresponsive hydrogel material that could deliver drugs at rates controlled by external light or laser stimuli. Photoresponsive

materials would well suit ophthalmic applications where the transparency of the eye would allow efficient penetration of light. There is a real need for delivery systems that can deliver drugs to the retina in a controlled, responsive manner at rates which can be altered to suit therapeutic targets. Delivery durations of months or years are desired. Potential drug targets include the anti-VEGF agents such as those currently used for the treatment of age related macular degeneration. Adjustments in release rate with light stimuli could be used to account for individual variations in disease progression and the diffusion-altering vitreous humour liquefaction that occurs with age [125]. In addition to potential applications in ophthalmology, photoresponsive materials would also suit other light-available delivery areas including those in gynaecology, dermatology, and gastroenterology [48]. A light responsive drug delivery platform that provides continual adjustable release over long terms (months/years) that is altered with light and laser stimuli according to disease progression would optimize disease treatment.

Hydrogels have high water contents similar to native vitreous humour and were chosen as materials for the delivery matrix. Anthracene was chosen as a light responsive moiety to be incorporated into the hydrogels since it undergoes dimerization at wavelengths > 300 nm and de-dimerization/dissociation at wavelengths < 300 nm (Figure 1-9) giving it the potential to act as a photoresponsive switch to alter hydrogel properties. Furthermore, anthracene was chosen for proof-of-concept studies since it is symmetrical and available in a variety of forms with substitutions at the ninth carbon which allows efficient and predictable dimerization in a head-to-tail form.

The hypothesis of this work is that the synthesis and subsequent grafting of water-soluble PEG-anthracene onto the backbone of various hydrogel polymers will introduce reversible photoinduced crosslinking due to the dimerization of anthracene, sufficient to cause alterations in the diffusion of drugs. In addition, it is hypothesized that the binding of anthracene to polyethylene glycol and its grafting to hydrogel materials will alter its toxicity profile due to the covalent modifications and due to the inaccessibility of anthracene to cells. Amine-terminated polyethylene glycol-anthracene (PEG-anthracene) is synthesized in this work, grafted to alginate and HA and optimized to produce photoresponsive hydrogel systems.

1.7.1 Photocrosslinkers

Critical to the development of the photogels was the ability to incorporate hydrophobic anthracene and other similar photoresponsive molecules onto hydrophilic polymers. Binding of anthracene to PEG was hypothesized to create a water-soluble anthracene-based macromolecule. Diamine PEG chains with one end protected were used for binding to anthracene-9-carboxylic acid using carbodiimide chemistry; removal of the protecting groups resulted in the desired amine terminated PEG-anthracene. Once these molecules are grafted along the backbone of polymers, anthracene dimerization effectively crosslinks the hydrogel. PEG chains of 3 and 11 units in length were investigated since short chains were desirable to allow changes in crosslinking density but long chains are required for anthracene solubilisation (Chapter 4). Once grafted, the PEG chain must be long enough for adequate mobility of the anthracene for dimerization to

occur but must be short enough for dimerization to effectively cause changes in crosslinking densities as investigated in Chapter 3.

1.7.2 Anthracene Photogels

Alginate is a non-toxic, hydrophilic polymer isolated from renewable plant-based sources making it an inexpensive and accessible delivery material. Alginate has numerous carboxyl groups available on its guluronic and mannuronic acid groups for the binding of PEG-anthracene via carbodiimide chemistry to create alginate photogels. In addition, PEG crosslinked hydrogels, physically crosslinked calcium alginate gels and calcium-reinforced photogels were synthesized as delivery matrices and compared. Star-PEG-anthracene was also incorporated into the gels to introduce additional anthracene groups. Covalent modification of alginate with either PEG or PEG-anthracene was found to create gels that have potential as long-term controlled delivery materials. Their diffusion properties were investigated using small and large model drugs. Varying light exposures, different large and small model compounds and different photogel formulations were investigated to assess the versatility of the system and methods to control its photosensitivity (Chapter 5). It was expected that factors such as increased light exposure would result in incremental changes in delivery since anthracene molecules must absorb 365 nm light to dimerize as opposed to photoinitiated reactions which propagate after absorption of light by the initiator molecules.

1.7.3 HA Photogels

HA photogels were also developed as potential vitreous delivery systems. It was expected that these materials would be compatible in this application since HA is present in human vitreous humour [90]. The HA also has a higher transparency than alginate so it was expected to have lower UV scattering to allow increased absorbance and therefore higher photosensitivity. HA has less available carboxyl groups for the grafting PEG-anthracene than alginate but differences in structure were expected to have potential for increases in grafting efficiency and therefore photosensitivity. Varying formulations were investigated to create crosslinkable loose gels or viscous solutions; these formulations of photogels and exposures to UV light were used to characterize their ability to alter release of small and large model drugs (Chapter 6). PEG crosslinked hydrogels and photogels containing star-PEG-anthracene were synthesized and investigated as additional delivery matrices for comparison. Laser studies with 248 nm dedimerizing/decrosslinking light were performed on previously crosslinked photogels to effect the release large and small model drugs as a proof-of-concept of the photoswitchability of these materials (Chapter 3 and 6). Since PEG-anthracene was bound to the HA, it was relatively inaccessible to the surrounding environment and was therefore hypothesized to be biocompatible with biological systems. Extensive cell studies were performed with human corneal epithelial cells and human retinal pigment epithelial cells grown with PEG-anthracene, photogels and photogel degradation products (Chapter 3 and 6).

1.7.4 Overview

While irreversible photopolymerizable and photodegradable materials have been investigated in the field of biomaterials to introduce alterations in material properties, these novel, reversibly photocrosslinked hydrogels using photodimerizing molecules have significant potential in drug delivery. By introducing a switchable mechanism to provide valuable reversible property changes in biomaterials, truly smart drug delivery is possible. To date, most smart drug delivery systems in literature are pulsatile, operating in an on/off fashion. The development of biomaterials with stimuli-induced adjustable properties and drug delivery rates would provide opportunities to fine-tune drug release profiles specific to disease progression and individual patients. While photodimerizing molecules have been introduced into polymer systems in past studies, the ability to control diffusion and release has been minimal with fast release times (≤ 120 hours) noted. By creating a versatile, graftable PEG-anthracene molecule, the introduction of high amounts of photodimerizing groups along the backbone has the potential to create a highly photosensitive matrix with photoreversible crosslinking and diffusion properties. In addition, using simple chemistries to create PEG-anthracene will allow for this mechanism to be applicable to other chromophores and other hydrogel systems, enabling the system to be fine tuned for a number of potential applications.

1.8 References

1. Klein R, Klein BE, Linton KL. Prevalence of age-related maculopathy. The Beaver Dam Eye Study. *Ophthalmol* 1992;99:933-943.
2. Hyman L. Epidemiology of AMD. In: Hampton GR, Nelson PT, editors. Age-related macular degeneration: principles and practice. New York: Raven Press, 1992.
3. Schmidt-Erfurth U, Hasan T. Mechanisms of action of photodynamic therapy with verteporfin for the treatment of age-related macular degeneration. *Surv Ophthalmol* 2000;45:195-213.
4. Brown GC, Brown MM, Sharma S, Stein JD, Roth ZR, Campanella J, Beauchamp GR. The burden of age-related macular degeneration: a value-based medicine analysis. *Trans Am Ophthalmol Soc* 2005;103:173-186.
5. Cruess A, Zlateva G, Xu X, Rochon S. Burden of illness of neovascular age-related macular degeneration in Canada. *Can J Ophthalmol* 2007;42:836-843.
6. Jaffe GJ, Ashton P, Pearson PA. Intraocular drug delivery. NY: Taylor & Francis, 2006.
7. Molokhia SA, Sant H, Simonis J, Bishop CJ, Burr RM, Gale BK, Ambati BK. The capsule drug device: Novel approach for drug delivery to the eye. *Vision Res* 2010;50:680-685.
8. Blick SKA, Keating GM, Wagstaff AJ. Ranibizumab. *Drugs* 2007;67:1199-1206.
9. Ahmadi MA, Lim JJ. Pharmacotherapy of age-related macular degeneration. *Expert Opin Pharmacother* 2008;9:3045-3052.
10. Asif M, Siddiqui A, Keating GM. Pegaptanib in exudative age-related macular degeneration. *Drugs* 2005;65:1571-1577.
11. Landa G, Amde W, Doshi V, Ali A, McGevna L, Gentile RC, Muldoon TO, Walsh JB, Rosen RB. Comparative study of intravitreal bevacizumab (Avastin) versus ranibizumab (Lucentis) in the treatment of neovascular age-related macular degeneration. *Ophthalmologica* 2008;223:370-375.
12. Chappelov AV, Kaiser PK. Neovascular age-related macular degeneration. Potential therapies. *Drugs* 2008;68:1029-1036.

13. Anderson OA, Bainbridge JWB, Shima DT. Delivery of anti-angiogenic molecular therapies for retinal diseases. *Drug Discovery Today* 2010;15:272-282.
14. Garber K. Biotech in a blink. *Nature Biotech* 2010;28:311-314.
15. Lang JC. Ocular drug delivery conventional ocular formulations. *Adv Drug Deliver Rev* 1995;16:39-43.
16. Urtti A. Challenges and obstacles of ocular pharmacokinetics and drug delivery. *Adv Drug Deliver Rev* 2006;58:1131-1135.
17. del Amo EM, Urtti A. Current and future ophthalmic drug delivery systems. A shift to the posterior segment. *Drug discovery today* 2008;13:135-143.
18. Yasukawa T, Ogura Y, Tabata Y, Kimura H, Wiedemann P, Honda Y. Drug delivery systems for vitreoretinal diseases. *Prog Ret Eye Res* 2004;23:253-281.
19. Fletcher EC, Lade RJ, Adewoyin T, Chong NV. Computerized model of cost-utility analysis for treatment of age-related macular degeneration. *Ophthalmology* 2008;115:2192-2198.
20. Kurz D, Ciulla TA. Novel approaches for retinal drug delivery. *Ophthalmol Clin N Am* 2002;15:405-410.
21. Ladas ID, Karagiannis DA, Rouvas AA, Kotsolis AI, Liotsou A, Vergados I. Safety of repeat intravitreal injections of bevacizumab versus ranibizumab. *Retina* 2009;29:313-318.
22. Saltzman WM. Drug delivery. Engineering principles for drug delivery. New York: Oxford University Press Inc, 2001.
23. Aulton ME. *Pharmaceutics. The science of dosage form design*. 2nd ed. UK: Elsevier Science Limited, 2002.
24. Peppas NA, Bures P, Leobandung W, Ichikawa H. Hydrogels in pharmaceutical formulations. *Eur J Pharm Biopharm* 2000;50:27-46.
25. Peppas NA, Lustig SR. The role of cross-links, entanglements, and relaxations of the macromolecular carrier in the diffusional release of biologically active materials. *Ann N Y Acad Sci* 1985;446:26-41.
26. Thacharodi D, Panduranga Rao K. Rate-controlling biopolymer membranes as transdermal delivery systems for nifedipine: Development and in vitro evaluations. *Biomaterials* 1996;17:1307-1311.

27. Weiner A. Drug delivery systems in ophthalmic applications. In: Yorio T, Clark AF, Wax MB, editors. *Ocular therapeutics: eye on new discoveries*. New York: Academic Press, 2008. p. 7-30.
28. Yasukawa T, Ogura Y. Medical devices for the treatment of eye diseases. *Handbook of Experimental Pharmacology* 2010;197:469-489.
29. Mohammad DA, Sweet BV, Elnor SG. Retisert: is the new advance in treatment of uveitis a good one? *Ann Pharm* 2007;41:449-455.
30. Kane FE, Burdan J, Cutino A, Green KE. Iluvien: a new sustained delivery technology for posterior eye disease. *Expert Opin Drug Deliv* 2008;5:1039-1046.
31. Campochiaro PA, Hafiz G, Shah SM, Bloom S, Brown DM, Busquets M, Ciulla T, Feiner L, Sabates N, Billman K, Kapik B, Green K, Kane F. Sustained Ocular Delivery of Fluocinolone Acetonide by an Intravitreal Insert. *Ophthalmology* 2010;117:1393-1399.e3.
32. Lee SS, Hughes P, Ross AD, Robinson MR. Biodegradable implants for sustained drug release in the eye. *Pharm Res* 2010.
33. Tan DTH, Chee S, Lim L, Lim ASM. Randomized clinical trial of a new dexamethasone delivery system (surodex) for treatment of post-cataract surgery inflammation, *Ophthalmology* 1999;106:223-231.
34. Dugel PU, Elliott D, Cantrill HL, Mahmoud T, Avery R, Erickson SR. I-vation™ TA: 24-month clinical results of the phase I safety and preliminary efficacy study. ARVO abstract 2009.
35. Emerich DF, Thanos CG. NT-501: An ophthalmic implant of polymer-encapsulated ciliary neurotrophic factor-producing cells. *Curr Opin Mol Ther* 2008;10:506-515.
36. Booth BA, Denham LV, Bouhanik S, Jacob JT, Hill JM. Sustained-release ophthalmic drug delivery systems for treatment of macular disorders. Present and future applications. *Drugs Aging* 2007;24:581-602.
37. Yasukawa T, Ogura Y, Sakurai E, Tabata Y, Kimura H. Intraocular sustained drug delivery using implantable polymeric devices. *Adv Drug Deliver Rev* 2005;57:2033-2046.
38. Choonara YE, Pillay V, Danckwerts MP, Carmichael TR, duToit LC. A review of implantable intravitreal drug delivery technologies for the treatment of posterior segment eye diseases. *J Pharm Sci* 2010;99:2219-2239.

39. Holz FG, Korobelnik J, Lanzetta P, Mitchell P, Schmidt-Erfurth U, Wolf S, Markabi S, Schmidli H, Weichselberger A. The Effects of a flexible visual acuity-driven ranibizumab treatment regimen in age-related macular degeneration: outcomes of a drug and disease model. *Invest Ophthalmol Vis Sci* 2010;51:405-412.
40. Lalwani GA, Rosenfeld PJ, Fung AE, Dubovy SR, Michels S, Feuer W, Davis JL, Flynn Jr HW, Esquiabro M. A variable-dosing regimen with intravitreal ranibizumab for neovascular age-related macular degeneration: year 2 of the PRONTO study. *Am J Ophthalmol* 2009;148:43-58.e1.
41. Bawa P, Pillay V, Choonara YE, dT,L.C. Stimuli-responsive polymers and their applications in drug delivery. *Biomed Mater* 2009;4:1-15.
42. Andresen TL, Jensen SS, Jørgensen K. Advanced strategies in liposomal cancer therapy: Problems and prospects of active and tumor specific drug release. *Prog Lipid Res* 2005;44:68-97.
43. Nanjawade BK, Manvi FV, Manjappa AS. In situ-forming hydrogel for sustained ophthalmic drug delivery. *J Control Rel* 2007;122:119-134.
44. Smolensky MH, Peppas NA. Chronobiology, drug delivery, and chronotherapeutics. *Adv Drug Deliver Rev* 2007;59:828-851.
45. Qiu Y, Park K. Environment-sensitive hydrogels for drug delivery. *Adv Drug Deliver Rev* 2001;53:321-339.
46. Kost J, Langer R. Responsive polymeric delivery systems. *Adv Drug Deliver Rev* 2001;46:125-148.
47. Alvarez-Lorenzo C, Bromberg L, Concheiro A. Light-sensitive intelligent drug delivery systems. *Photochem photobio* 2009;85:848-860.
48. Gibson KF, Kernohan WG. Lasers in medicine - a review. *J Med Eng Tech* 1995;17:51-57.
49. Schmaljohann D. Thermo- and pH- responsive polymers in drug delivery. *Adv Drug Deliver Rev* 2006;58:1655-1670.
50. Chan W, Lim T, Pece A, Silva R, Yoshimura N. Verteporfin PDT for non-standard indications—a review of current literature. *Graefes Arch Clin Exp Ophthalmol* 2010;248:613-626.

51. QLT. Visudyne (verteporfin for injection). Prescription information 2005:1-2.
52. Kumar GS, Neckers DC. Photochemistry of azobenzene-containing polymers. *Chem Rev* 1989;89:1915-1925.
53. Minkin VI. Photo-, thermo-, solvato-, and electrochromic spiroheterocyclic compounds. *Chem Rev* 2004;104:2751-2776.
54. Smets G. Photochemical reactions in polymeric systems. *Pure and Appl Chem* 1975;42:509-526.
55. Tomer R, Florence AT. Photo-responsive hydrogels for potential responsive release applications. *Int J Pharma* 1993;99:R5-R8.
56. El Halabieh RH, Mermut O, Barrett CJ. Using light to control physical properties of polymers and surfaces with azobenzene chromophores. *Pure Appl Chem* 2004;76:1445-1465.
57. Suzuki T, Shinkai S, Sada K. Supramolecular crosslinked linear poly(trimethylene iminium trifluorosulfonimide) polymer gels sensitive to light and thermal stimuli. *Adv Mater* 2006;18:1043-1046.
58. Patnaik S, Sharma AK, Garg BS, Gandhi RP, Gupta KC. Photoregulation of drug release in azo-dextran nanogels. *Int J Pharmaceut* 2007;IN PRESS.
59. Thompson KP, Ren QS, Parel JM. Therapeutic and diagnostic application of lasers in ophthalmology. *Proc IEEE* 1992;80:838-860.
60. Zheng Y, Micic M, Mello SV, Mabrouki M, Andreopoulos FM, Konka V, Pham SM, Leblanc RM. PEG-based hydrogel synthesis via the photodimerization of anthracene groups. *Macromol* 2002;35:5228-5234.
61. Andreopoulos FM, Beckman EJ, Russell AJ. Light-induced tailoring of PEG-hydrogel properties. *Biomaterials* 1998;19:1343-1352.
62. Zheng Y, Andreopoulos FM, Micic M, Huo Q, Pham SM, Leblanc RM. A novel photoscissile poly(ethylene glycol)-based hydrogel. *Adv Funct Mater* 2001;11:37-40.
63. Trenor SR, Long TE, Love BJ. Photoreversible chain extension of poly(ethylene glycol). *Macromol Chem Phys* 2004;205:715-723.
64. Ishigama T, Murata T, Endo T. The solution photodimerization of (E)-*p*-nitrocinnamates. *Bull Chem Soc Jap* 1976;49:3578-3583.

65. Ziffer H, Bax A, Highet RJ, Green B. Investigation by two-dimensional NMR of the structure and stereochemistry of a methyl *p* -nitrocinnamate photodimer. *J Org Chem* 1988;53:895-896.
66. Trenor SR, Shultz AR, Love BJ, Long TE. Coumarins in polymers: from light harvesting to photo-cross-linkable tissue scaffolds. *Chem Rev* 2004;104:3059-3077.
67. Bouas-Laurent H, Castellan A, Desvergne J, Lapouyade R. Photodimerization of anthracenes in fluid solutions: (part 2) mechanistic aspects of the photocycloaddition and of the photochemical and thermal cleavage. *Chem Soc Rev* 2001;30:248-263.
68. Greene FD, Misrock SL, Wolfe JRJ. The structure of anthracene photodimers. *J Am Chem Soc* 1955;77:3852-3855.
69. Bouas-Laurent H, Castellan A, Desvergne J-, Lapouyade R. Photodimerization of anthracene in fluid solution: structural aspects. *Chem Soc Rev* 2000;29:43-55.
70. Andreopoulos FM, Beckman EJ, Russell AJ. Photoswitchable PEG-CA hydrogels and factors that affect their photosensitivity. *J Polym Sci A: Polym Chem* 2000;38:1466-1476.
71. Andreopolous FM, Roberts MJ, Bentley MD, Harris JM, Beckman EJ, Russell AJ. Photoimmobilization of organophosphorus hydrolase within a PEG-based hydrogel. *Biotechnol bioeng* 1999;65:579-588.
72. Andreopoulos FM, Deible CR, Stauffer MT, Weber SG, Wagner WR, Backman EJ, Russell AJ. Photoscissable hydrogel synthesis via rapid photopolymerization of novel PEG-based polymers in the absence of photoinitiator. *J Am Chem Soc* 1996;118:6235-6240.
73. Sirpal S, Gattas-Asfura KM, Leblanc RM. A photodimerization approach to crosslink and functionalize microgels. *Coll Surf B Bioint* 2007;58:116-120.
74. Nakayama Y, Matsuda T. Preparation and characteristics of photocrosslinkable hydrophilic polymer having cinnamate moiety. *J Polym Sci A Polym Chem* 1992;30:2451-2457.
75. Andreopoulos FM, Persaud I. Delivery of basic fibroblast growth factor (bFGF) from photoresponsive hydrogel scaffolds. *Biomater* 2006;27:2468-2476.

76. Micic M, Zheng Y, Moy V, Zhang XH, Andreopolous M, Leblanc RM. Comparative studies of surface topography and mechanical properties of a new, photo-switchable PEG-based hydrogel. *Colloids Surf B* 2002;27:147-158.
77. Gattas-Asfura KM, Weisman E, Andreopoulos FM, Micic M, Muller B, Sirpal S, Pham SM, Leblanc RM. Nitrocinnamate-functionalized gelatin: synthesis and "smart" hydrogel formation via photo-cross-linking. *Biomacromol* 2005;6:1503-1509.
78. Matsui J, Ochi Y, Tamaki K. Photodimerization of anthryl moieties in a poly(methylacrylic acid) derivative as reversible cross-linking step in molecular imprinting. *Chem Lett* 2006;35:80-81.
79. Nowakowska M, Zapotoczny S, Sterzel M, Kot E. Novel water-soluble photosensitizers from dextrans. *Biomacromol* 2004;5:1009-1014.
80. Ide N, Tsujii Y, Fukuda T, Miyamoto T. Gelation processes of polymer solutions. 1. Photodimerization of free and polymer-bound anthryl groups. *Macromol* 1996;29:3851-3856.
81. Bratschkov C, Karpuzova P, Mullen K, Klapper M. Synthesis and photochemical transformations of an anthracene containing methacrylic copolymer. *Polymer Bull* 2001;46:345-349.
82. Coursan M, Desvergne JP. Reversible photodimerization of w-anthrylpolystyrenes. *Macromol Chem Phys* 1996;197:1599-1608.
83. Goldbach JT, Russell TP, Penelle J. Synthesis and thin film characterization of poly(styrene-*block*-methyl methacrylate) containing an anthracene dimer photocleavable junction point. *Macromol* 2002;35:4271-4276.
84. Peppas NA, Keys KB, Torres-Lugo M, Lowman AM. Poly(ethylene glycol)-containing hydrogels in drug delivery. *J Controlled Release* 1999;62:81-87.
85. Bhawalkar JD, He GS, Prasad PN. Nonlinear multiphoton processes in organic and polymeric materials. *Rep Prog Phys* 1996;59:1041-1070.
86. Hartner S, Kim HC, Hampp N. Phototriggered release of photolabile drugs via two-photon absorption-induced cleavage of polymer-bound dicoumarin. *J Polym Sci Part A: Polym Chem* 2007;45:2443-2452.
87. Hargreaves JS, Webber SE. Photophysics of anthracene polymers: fluorescence, singlet, energy migration and photodegradation. *Macromol* 1984;17:235-240.

88. Bouas-Laurent H, Castellan A, Desvergne JP. From anthracene photodimerization to jaw photochromic materials and photocrowns. *Pure & Appl Chem* 1980;52:2633-2648.
89. Soman N, Banerjee R. Artificial vitreous replacements. *Biomed Mater Eng* 2003;13:59-74.
90. Bishop PN. Structural macromolecules and supramolecular organization of the vitreous gel. *Prog Ret Eye Res* 2000;19:323-344.
91. Li CC, Metters AT. Hydrogels in controlled release formulations: Network design and mathematical modeling. *Adv Drug Deliver Rev* 2006;58:1379-1408.
92. Wells LA, Sheardown H. Extended release of high pI proteins from alginate microspheres via a novel encapsulation technique. *Eur J Pharm Biopharm* 2007;65:329-335.
93. Shilpa A, Agrawal SS, Ray R. Controlled delivery of drugs from alginate matrix. *J Macromol Sci* 2003;C43:187-221.
94. Morris ER, Rees DA, Thom D. Chiroptical and stoichiometric evidence of a specific primary dimerization process in alginate gelation. *Carbohydr Res* 1978;66:145-154.
95. Gombotz WR, Wee SF. Protein release from alginate matrix. *Adv Drug Deliver Rev* 1998;31:267-285.
96. Wang X, Spencer HG. Calcium alginate gels: formation and stability in the presence of an inert electrolyte. *Polymer* 1998;39:2759-2764.
97. Augst AD, Kong HJ, Mooney DJ. Alginate hydrogels as biomaterials. *Macromol Biosci* 2006;6:623-633.
98. Tonnesen HH, Karlsen J. Alginate in drug delivery systems. *Drug Dev Ind Pharm* 2002;28:621-630.
99. Lee KW, Yoon JJ, Lee JH, Kim SY, Jung HJ, Kim SJ, Joh JW, Lee HH, Lee DS, Lee SK. Sustained release of vascular endothelial growth factor from calcium-induced alginate hydrogels reinforced by heparin and chitosan. *Transplant Proc* 2004;36:2464-2465.
100. Quong D, Neufeld RJ. Electrophoretic extraction and analysis of DNA from chitosan or poly-L-lysine-coated alginate beads. *Appl Biochem Biotech* 1999;81:67-77.

101. Ferreiro MG, Tillman LG, Hardee G, Bodmeier R. Alginate/poly-L-lysine microparticles for the intestinal delivery of antisense oligonucleotides. *Pharm Res* 2002;19:755-764.
102. Monshipouri M, Rudolph AS. Liposome-encapsulated alginate: controlled hydrogel particle formation and release. *J Microencapsulation* 1995;12:117-127.
103. Tada D, Tanabe T, Tachibana A, Yamauchi K. Albumin-crosslinked alginate hydrogels as sustained drug release carrier. *Mater Sci Eng C* 2007;27:870-874.
104. Eiselt P, Lee KY, Mooney DJ. Rigidity of two-component hydrogels prepared from alginate and poly(ethylene glycol)-diamines. *Macromol* 1999;32:5561-5566.
105. Lee KY, Rowley JA, Eiselt P, Moy EM, Bouhadir KH, Mooney DJ. Controlling mechanical and swelling properties of alginate hydrogels independently by cross-linker type and cross-linking density. *Macromol* 2000;33:4291-4294.
106. Kulkarni AR, Soppimath KS, Aralaguppi MI, Aminabhavi TM, Rudzinski WE. Preparation of cross-linked sodium alginate microparticles using glutaraldehyde in methanol. *Drug Dev Ind Pharm* 2000;26:1121-1124.
107. Cathell MD, Szewczyk JC, Schauer CL. Organic modification of the polysaccharide alginate. *Mini-Rev Org Chem* 2010;7:61-67.
108. Bouhadir KH, Kruger GM, Lee KY, Mooney DJ. Sustained and controlled release of daunomycin from cross-linked poly(aldehyde guluronate) hydrogels. *J Pharm Sci* 2000;89:910-919.
109. Xiao C, Zhou M, Lin X, Li R. Chemical modification of calcium alginate gel beads for controlling the release of insect repellent N,N-diethyl-3-methylbenzamide. *J Appl Mater Sci* 2006;102:4850-4855.
110. Kumar MT, Rajeswari C, Balasubramaniam J, Pandit JK, Kant S. In vitro and in vivo characterization of scleral implant of indomethacin: role of plasticizer and cross-linking time. *Drug Delivery* 2003;10:269-275.
111. Lee KY, Yuk SH. Polymeric protein delivery systems. *Prog Polym Sci* 2007;32:669-697.
112. Liao YH. Hyaluronan: pharmaceutical characterization and drug delivery. *Drug Delivery* 2005;12:327-342.

113. Schwartz DM, Shuster S, Jumper MD, Chang A, Stern R. Human vitreous hyaluronidase: isolation and characterization. *Curr Eye Res* 1996;15:1156-1162.
114. Prestwich GD, Marecak DM, Marecek JF, Vercruyse KP, Ziebell MR. Controlled chemical modification of hyaluronic acid: synthesis, applications, and biodegradation of hydrazide derivatives. *J Controlled Release* 1998;53:93-103.
115. Liu Y, Zheng Shu X, Prestwich GD. Biocompatibility and stability of disulfide-crosslinked hyaluronan films. *Biomaterials* 2005;26:4737-4746.
116. Sannino A, Pappada S, Madaghiele M, Maffezzoli A, Ambrosio L, Nicolais L. Crosslinking of cellulose derivatives and hyaluronic acid with water-soluble carbodiimide. *Polymer* 2005;46:11206-11212.
117. Crescenzi V, Francescangeli A, Taglienti A, Capitani D, Mannina L. Synthesis and partial characterization of hydrogels obtained via glutaraldehyde crosslinking of acetylated chitosan and of hyaluronan derivatives. *Biomacromol* 2003;4:1045-1054.
118. Dhanasingh A, Salber J, Moeller M, Groll J. Tailored hyaluronic acid hydrogels through hydrophilic prepolymer cross-linkers. *Soft Matter* 2010;6:618-629.
119. Liu Y, Zheng Shu X, Prestwich GD. Biocompatibility and stability of disulfide-crosslinked hyaluronan films. *Biomaterials* 2005;26:4737-4746.
120. Kim MR, Park TG. Temperature-responsive and degradable hyaluronic acid/pluronic composite hydrogels for controlled release of human growth hormone. *J Controlled Release* 2002;80:69-77.
121. Hirakura T, Yasugi K, Nemoto T, Sato M, Shimoboji T, Aso Y, Morimoto N, Akiyoshi K. Hybrid hyaluronan hydrogel encapsulating nanogel as a protein nanocarrier: New system for sustained delivery of protein with a chaperone-like function. *J Controlled Release* 2010;142:483-489.
122. Leach JB, Schmidt CE. Characterization of protein release from photocrosslinkable hyaluronic acid-polyethylene glycol hydrogel tissue engineering scaffolds. *Biomaterials* 2005;26:125-135.
123. Segura T, Anderson BC, Chung PH, Webber RE, Shull KR, Shea LD. Crosslinked hyaluronic acid hydrogels: a strategy to functionalize and pattern. *Biomaterials* 2005;26:359-371.

124. Cai S, Liu Y, Zheng Shu X, Prestwich GD. Injectable glycosaminoglycan hydrogels for controlled release of human basic fibroblast growth factor. *Biomaterials* 2005;26:6054-6067.
125. Laude A, Tan LE, Wilson CG, Lascaratos G, Elashry M, Aslam T, Patton N, Dhillon B. Intravitreal therapy for neovascular age-related macular degeneration and inter-individual variations in vitreous pharmacokinetics. *Prog Ret Eye Res* 2010;XXX:1-10. In press.

2.0 Methods

The approach to synthesize anthracene-modified hydrogels first focused on the solubilization of hydrophobic anthracene through its binding to polyethylene glycol (PEG) chains to make “PEG-anthracene” photoactive crosslinkers which were then grafted onto the backbone of various hydrogel polymers. First PEG-anthracene photocrosslinker molecules were synthesized and analyzed. This was followed by their grafting to alginate and hyaluronic acid (HA) to create photogels which were tested for gel property and drug delivery alterations following exposure to UV light.

2.1 Photocrosslinker Synthesis

To make low polydispersity, highly substituted anthracene terminated PEG molecules that would also graft to the carboxyl-containing bulk polymers alginate and HA, protecting group and carbodiimide chemistries were used with a highly purified protected form of PEG-diamine and anthracene-9-carboxylic acid.

2.1.1 Carbodiimide Chemistry

Carbodiimide chemistry is a well understood reaction that forms amide bonds. PEG-anthracene molecules were created through the reaction of an amine-terminated PEG and carboxyl substituted anthracene. Illustrated in Figure 2-1 is a general reaction of 1-ethyl-(dimethylaminopropyl) carbodiimide hydrochloride (EDC) with and without N-hydroxysuccinimide (NHS). NHS can be used to promote the reaction and reduce side products.

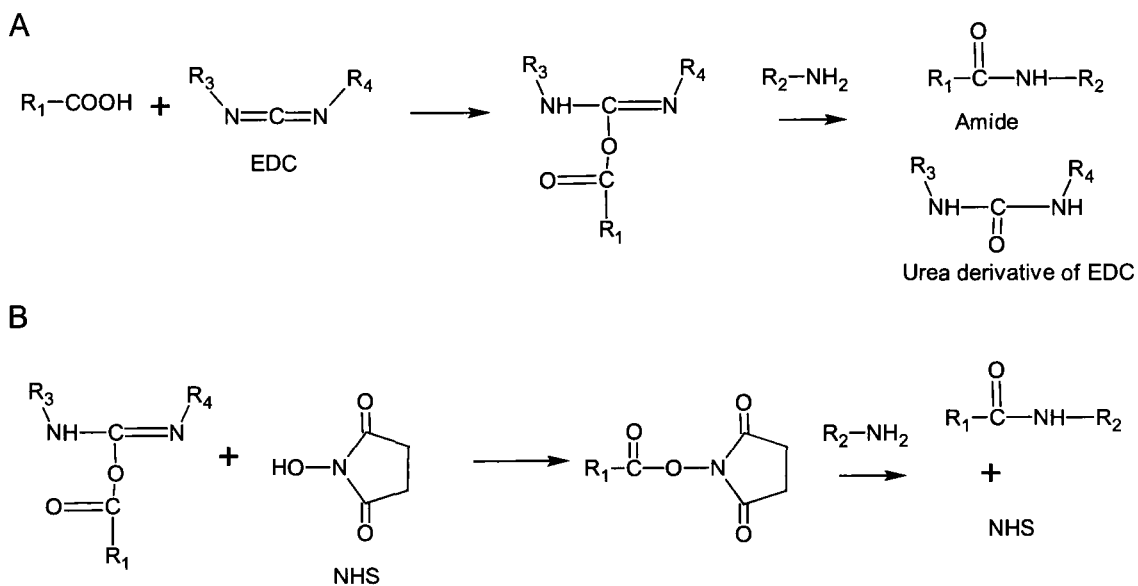


Figure 2-1. The reaction between carboxyl terminated R_1 with amine terminate R_2 using EDC. A: Without NHS. B: With NHS. Adapted from [1].

2.1.2 Protecting Groups

Protecting groups can increase the specificity of the reactions by temporarily blocking one end from reacting. Triphenylmethyl (trt) and *tert*-butyloxycarbonyl (tBoc) are common amine protecting groups that can be removed with strong acids in a reversible reaction to produce carbocations. Carbocation scavengers promote the reaction towards the removal of the protecting group to drive fast and complete removal [2]. Otherwise concentrated carbocation groups may react to other functional groups in close proximity. Triethylsilane and triisopropylsilane scavengers were used in this work to ensure that once the deprotecting groups are removed, they will react with any other groups [3].

In addition to the advantageous specificity of protecting group chemistry, its relative simplicity allows for simple modifications to be made to create similar molecules

with varying end groups and functionality. For example in the synthesis of photocrosslinkers, by using similar sized PEG with alternate end groups, different chromophores maybe be introduced to one end and a different binding/grafting group may be protected on the other end. Therefore, photocrosslinkers with different chromophores and alterable functionality made be synthesized using the same simplistic chemistry.

2.1.3 PEG-anthracene

O-(2-Aminoethyl)-O'-[2-(Boc-amino)ethyl]decaethylene glycol (tBoc-PEG-amine, 644.79 Da, n=11) and smaller O-(N-Trt-3-aminopropyl)-O'-(3-aminopropyl)-diethyleneglycol (trt-PEG-amine, 462.62 Da, n=3) are diamine PEG molecules with one group protected with either tBoc or trt groups respectively. In dichloromethane (DCM), their unprotected amine groups can be reacted with anthracene-9-carboxylic acid using EDC as illustrated in Figure 2-2. The blocking groups can then be removed in DCM using trifluoroacetic acid (TFA) with the addition of triisopropyl silane (TIPS) as a scavenger [4]. Concentrations and molar ratios of the different reagents were optimized as described in Chapter 4 to produce 3 and 11 unit PEG-anthracene macromolecules.

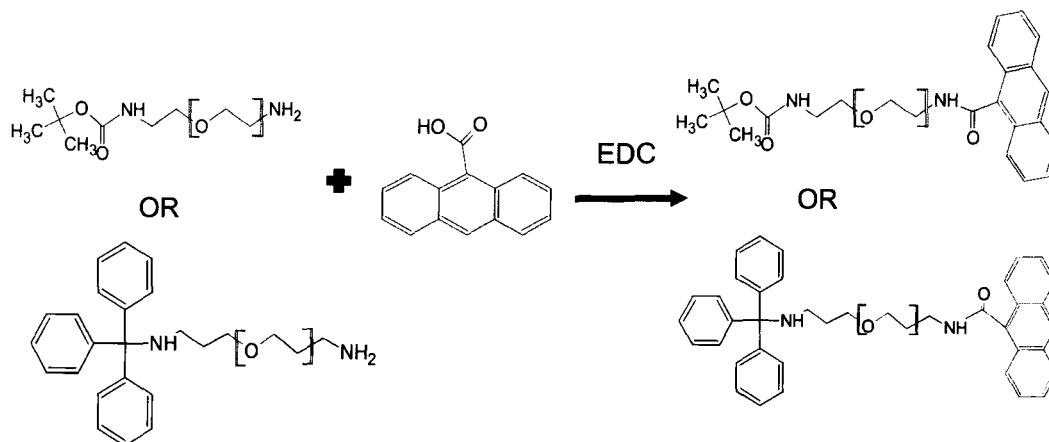


Figure 2-2. Carbodiimide chemistry to create anthracene-terminated PEG from either boc-PEG-amine or trt-PEG-amine.

Due to its higher solubility and yields, 11 unit amine-terminated PEG-anthracene (Figure 2-3) was the focus of most of the photogel studies. Details of its optimal synthesis are described in Appendix 1.

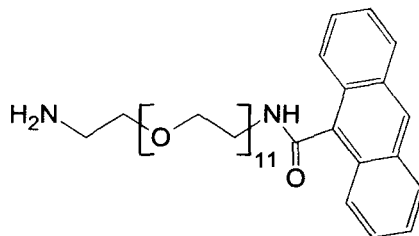


Figure 2-3. 11 unit amine-terminate PEG-anthracene was the photocrosslinker used in the majority of the studies.

2.2 Hydrogel Synthesis

Alginate and HA have carboxyl groups available for reaction with amine-terminated PEG-anthracene using carbodiimide chemistry. MES buffer (0.1 M 4-morpholinoethanesulfonic acid, 0.5 M NaCl at pH 6) was used in all reactions to promote

EDC activity [5,6]. Specific details for the grafting of PEG-anthracene onto HA, as an example, can be found in Appendix 2. Gels were cast between glass slides with 1 mm slide spacers and subsequently punched into 0.5 cm diameter disks. Different types of photogels and control gels were synthesized and are described in Table 2-1. Gels were stored air-dried over the long term since freeze drying was found to introduce a porous structure unsuitable for future drug delivery studies.

Table 2-1. Different types of photogels and control gels used in various studies.

| Bulk | Name | Crosslinker |
|----------|---|---|
| Alginate | Photogel | PEG-anthracene |
| | Control PEG Hydrogel | PEG-diamine |
| | Star-PEG-anthracene containing Photogel | PEG-anthracene with loose Star-PEG-anthracene |
| | Calcium alginate gel | Calcium ions |
| | Calcium-reinforced photogel | PEG-anthracene with calcium ions after grafting |
| HA | Photogel | PEG-anthracene |
| | Control PEG hydrogel | PEG-diamine |
| | Self-gel | No external crosslinker. |

2.3 Light Sources for PEG-anthracene and Photogels Stimuli

2.3.1 UV Source

For the ultraviolet (UV) treatment of photogels, UV sources must be powerful enough to cause anthracene dimerization and de-dimerization while not causing destruction to high-water content hydrogels by heat or chain scission. UV lights have

different tissue penetration/absorption; hydrogel penetration is expected to be similar since they also have high water contents (Table 2-2). Specifically, UV-A light will cause dimerization and UV-B/UV-C de-dimerization of anthracene.

Table 2-2. Description of the absorption of various UV and IR wavelengths. Adapted from [7].

| Spectral Band | Wavelength | Characteristics (tissue) |
|---------------|----------------------|------------------------------------|
| UV-C | 100 - 280 nm | Superficial absorption |
| UV-B | 280 - 315 nm | Penetration |
| UV-A | 315 - 400 nm | Deeper penetration |
| Visible Light | 380 - 780 nm | Day and night vision |
| IR-A | 780 - 1400 nm | Deep penetration |
| IR-B | 1400 - 3000 nm | Slight penetration (water absorbs) |
| IR-C | 3-1000 μm | Very superficial absorption |

Dose can be described by radiant exposure which is the density of energy from an optical source onto an area as described with equation 2-1. This is distinct from fluence which is the absorption into a specific spherical area as illustrated in Figure 2-4.

$$\text{Radiant exposure} = \frac{\text{power (W)} \times \text{time (s)}}{\text{area (cm}^2\text{)}} \quad (2-1)$$

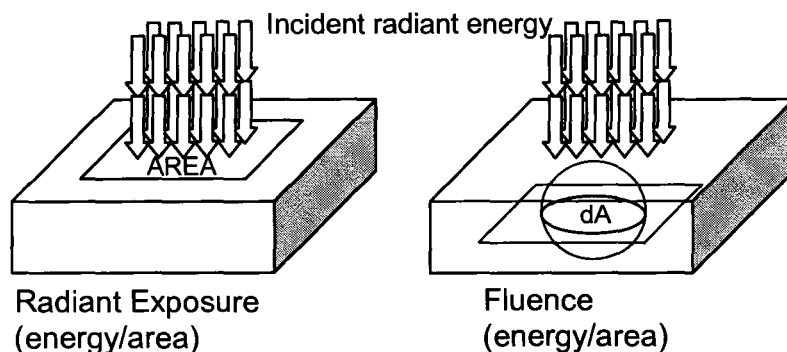


Figure 2-4. The difference between exposure and fluence. Adapted from [7].

For lamps, exposure is dependent on both the light source (mW/cm^2) and the time of exposure (s). UVA lamp sources generally range from $0.5\text{--}10 \text{ mW}/\text{cm}^2$ and higher with a defined spectral range that can be further limited to narrow ranges with UV filters. Since lamps are of a comparatively lower power, for anthracene dimerization, longer time frames of 10-40 minutes at $10 \text{ mW}/\text{cm}^2$ are required for dimerization to occur. Therefore exposures were to hydrogels in buffer solution to ensure that gels remained hydrated during the treatment.

Moderately powered UV sources of lower wavelengths under 300 nm that are required for anthracene de-dimerization/dissociation are less common, making lasers a more appropriate choice to achieve adequate power and wavelength specificity. Lasers also provide a proof-of-concept for their use *in vivo* on photogels in future applications. Excimer lasers are able to provide UV-range wavelengths for the dimerization and

dedimerization of anthracene although it is recognized that ultimately two-photon lasers will be required to achieve adequate *in vivo* tissue penetration. The name excimer comes from “excited dimers” that emit in the UV range. Pulsing laser systems are often used with excimer lasers to reach higher energies [8]. Figure 2-5 illustrates some UV-B/UV-C excimer laser systems with the krypton fluoride (KrF) laser output showing high specificity at a wavelength appropriate for anthracene de-dimerization. Therefore a KrF excimer laser operating at its lower range of 50-60 mJ/cm² at 5 Hz was used for 248 nm treatments since those settings provide adequate power over short time frames without causing hydrogel destruction. The exposure is a function of the pulse energy and number of pulses (equation 2-2) and radiant exposure is a function of pulse energy over the laser exposure area.

$$\begin{aligned} \text{Energy} &= \text{pulse energy (J)} \times \text{repetition rate (Hz)} \times \text{time (s)} \\ &= \text{pulse energy (J)} \times \text{number of pulses} \end{aligned} \quad (2-2)$$

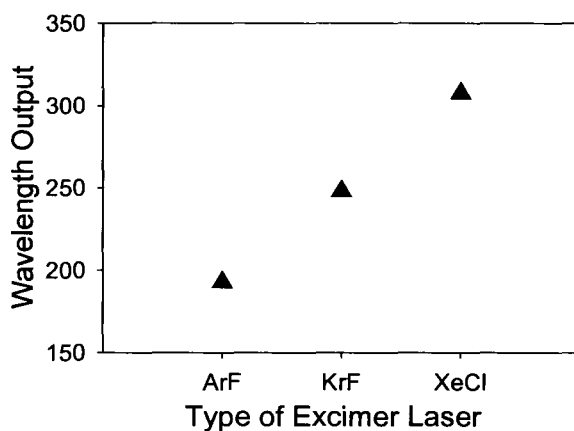


Figure 2-5. Peak wavelengths of some common excimer lasers. KrF lasers were used since they have a specific wavelength under 300 nm ideal for the de-dimerization of anthracene.

2.3.2 UV Treatment Procedure Specifics

The Curezone II UV lamp from CON-TROL-CURE (Chicago,IL) (400 W, 120 VAC, 60Hz, 8 amps max) was used for 365 nm treatments at 10 mW/cm^2 . The 254 nm source (0.63 mW/cm^2) which also provided 365 nm (0.5 mW/cm^2) was an EL Series UVLS-28 UV lamp from UVP (Upland, CA) (8 W). Curezone II is a UV chamber so samples must be placed within, on ice to prevent heat from the UV lamp from altering their properties. Exposure was to PEG-anthracene in solution or photogels sitting in 1 mL of PBS in 48 well plates. Thin layers of parafilm were used to contain samples since it was found to allow the transmission of light. Exposures/doses were altered by varying exposure times.

A KrF excimer laser operating from 50 mJ/cm^2 to 58 mJ/cm^2 at 5 Hz was used to irradiate gels. The power and frequency were at the low end of the laser specifications. For laser treatments, gels were carefully placed on glass slides then consistently placed within the center of an area that the laser projected to ensure matched exposures. The radiant exposures were altered by varying the numbers of pulses, for example 20 pulses at 50 mJ/cm^2 results in 1000 mJ/cm^2 whereas 240 pulses at 50 mJ/cm^2 results in $12,000 \text{ mJ/cm}^2$. Control PEG-crosslinked hydrogels demonstrated no changes in swelling and HA release (no degradation) after varying exposures versus controls with no exposure to the laser. Therefore 5 Hz is a sufficiently low frequency to allow relaxation between pulses to minimize heat induced destruction.

2.4 Analysis Techniques

2.4.1 NMR and FTIR

Nuclear magnetic resonance spectroscopy (NMR) was used to provide information on the type and number of chemical groups in synthesis samples. Both proton NMR (hydrogen-1) and carbon NMR (carbon-13) were used with deuterated DMSO as a solvent to monitor reaction products. For PEG-anthracene synthesis, some common shifts were at 7.5-8.3 ppm for anthracene and 3.2-3.9 for PEG. The tBoc protecting group peak at 1.4ppm disappears after its removal. Carbon NMR was used to investigate anthracene dimerization within alginate photogels. Alginate gels were synthesized with buffers containing 10% deuterated water and gelled within quartz NMR tubes to allow carbon NMR measurements before and after UV exposures to monitor dimerization/dedimerization within the gels. Fourier transform infrared spectroscopy (FTIR) was used to interrogate the PEG-anthracene by sandwiching the gel as a thin layer between two salt plates.

2.4.2 Spectrophotometry

Light absorption/transmission was determined spectrophotometrically. Since photodimerizing molecules absorb specific light when undimerized, dimerization may be monitored by spectral scans or observation of specific wavelengths, such as those observed between 300-400 nm for undimerized anthracene-9-carboxylic acid as illustrated in Figure 2-6 that disappear upon dimerization. Spectrophotometry was therefore used to verify the ability of the anthracene end groups to dimerize when bound

to PEG and compared to anthracene-9-carboxylic acid dimerization. Layers of swollen, transparent HA photogels and hydrogels were also scanned by adhering them to the edge of a cuvette, however, quantitative measurements could not be made since they could become loose between UV treatments.

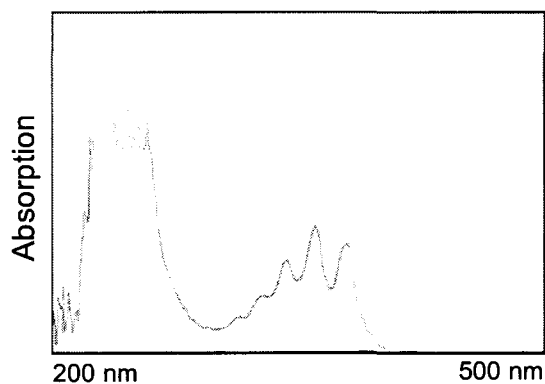


Figure 2-6. Scan of un-dimerized anthracene-9-carboxylic acid.

2.4.3 PEG Grafting

Grafting of amine-terminated PEG molecules can be monitored by detecting unreacted primary amine groups after the reaction. The colourimetric ninhydrin assay effectively detects primary amines through reactions with a solution of dissolved ninhydrin and hydrindantin that occur to produce Ruhemann's Purple. Ninhydrin causes oxidative decarboxylation of primary amines. Then the reduced form reacts with liberated ammonia to form Ruhemann's Purple which is detected via spectrophotometric absorption at 570 nm (Figure 2-7) [10]. The reagent used (Sigma-Aldrich, Oakville, ON), contained ninhydrin and hydrindantin in lithium acetate buffer and DMSO at an optimal

pH of 5.2 [11]. 1 mL of the sample was mixed with 0.5 mL of ninhydrin reagent solution and heated in an oil bath at 100°C for 10 minutes. After cooling, the sample were then mixed with 2.5 mL of 95% ethanol and read at 540 or 595 nm. Hydrogels were run by soaking in 1 mL of water then the solution with the gel was tested using the same procedure since the gels did not absorb the reagent or Ruhemann's Purple. Standard solutions of glycine were used as a calibration. The detection limit was less than 0.1 $\mu\text{mol/mL}$ of primary amine groups.

Grafting was calculated by subtracting the detected unreacted moles of primary amines from the amounts of amine-terminate PEG molecules added during the grafting reaction (theoretical grafting). The grafting efficiencies of amine-terminate PEG molecules onto alginate or HA were calculated by dividing the actual amount grafted (theoretical minus unreacted) by the theoretical amount grafted.

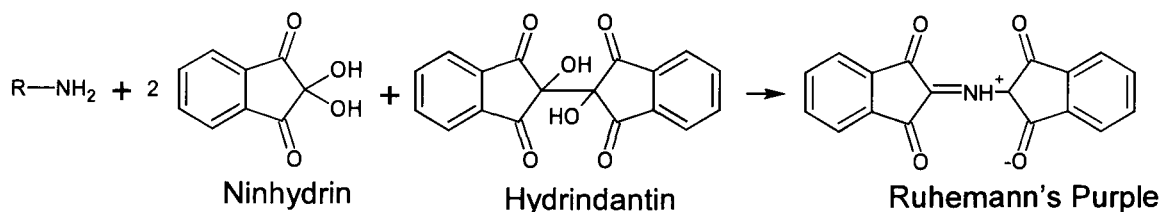


Figure 2-7. Ninhydrin reacts to produce Ruhemann's purple with the presence of primary amines.

2.4.4 Swelling and Effective Crosslinking Density

Swelling of dried gels by water or buffers indicates their liquid content which can also be used to determine relative effective crosslinking densities. Using a version of the

Flory-Rehner equation for hydrogels crosslinked in solution, established by Bray and Merrill [12-14], effective crosslinking densities (v_e) may be compared with different gels and with and without UV treatments (see equations 2-3 and 2-4).

$$\frac{1}{Mc} = \frac{2}{Mn} - \frac{(\bar{v}/V_1) [\ln(1 - v_{2,s}) + v_{2,s} + \chi_1(v_{2,s})^2]}{v_{2,r} [(v_{2,s}/v_{2,r})^{1/3} - 0.5(v_{2,s}/v_{2,r})]} \quad (2-3)$$

$$v_e = \frac{\rho_p}{M_c} \quad (2-4)$$

Mc = average molecular weight between crosslinks

ρ_p = polymer density

v = specific volume of dry polymer, 0.60 cm³/g alginate [15], 0.814 cm³/g for HA [16] and 0.89 cm³/g for PEG [17]

$v_{2,s}$ = volumetric polymer fraction at maximum swelling

$v_{2,r}$ = volumetric polymer fraction in a relaxed state,

V_1 = molar volume of solvent \approx 18 mol/cm³ for PBS and water

χ = Flory polymer-solvent interaction parameter \approx 0.473 for HA, alginate [16] and PEG [17]

Mn = number average molecular weight of the polymer

Due to the high water content of the gels (>90%), dried gels are difficult to manoeuvre. Therefore massing was performed by pre-weighing vial containers then adding gels that were gently dried with kim-wipes and their wet masses were determined by subtracting the vial mass from the gel + vial mass. After air drying the in open vials for 72 hours, they were weighed again to determine the dry mass. Freeze drying was avoided to prevent the creation of macroscopic pores which dramatically alter the properties of the gel matrix upon reswelling.

2.5 Enzymatic Degradation

While alginate only degrades via decrosslinking and slow hydrolysis in animals; HA may be degraded *in vivo* by the enzyme hyaluronidase which may ultimately influence its properties. Bovine testes hyaluronidase (hyaluronate 4-glycanohydrolase) is an endo- β -N-acetylhexosaminidase that cleaves at the β -N-acetylhexosamine bonds (N-acetylglucosamine β -(1 \rightarrow 4)-glucuronic acid) randomly along the backbone of HA resulting in glucuronic acid-terminated tetra- and hexa-sacharrides [18]. It is approximately 55 kDa in size consisting of 4 x 14 kDa subunits [19]. The activity of the purchased lot was 801 Units/mg; one unit causes a 0.330 per minute change in absorption (0.2 to 0.1 mg HA) at 600 nm at 37°C, pH 5.7 in a 2 mL mixture over 45 minutes (Sigma Aldrich, Oakville ON) [20].

For testing the influence hyaluronidase may have on HA gel degradation, 100 Unit/mL solutions were prepared by dissolving hyaluronidase in phosphate buffer containing 3.871 g of sodium citrate, 10.647g of disodium hydrogen phosphate and 4.383 g of sodium chloride in 500 mL of water with its pH was adjusted to 6.3 (1N NaOH/1N HCl). After swelling the gels in PBS (pH 7.4) for 24 hours, some gels were exposed to 365 nm UV light. Then all of the gels were put in 0.5 mL of 100 Units/mL hyaluronidase (total 50 Units), at 37°C, with regular solution changes to maintain the enzyme activity. Degradation was monitored over time until disks were no longer present. Experiments were performed in milk protein-blocked vials to prevent hyaluronidase adsorption to surfaces which may lower its activity.

2.6 Release Studies

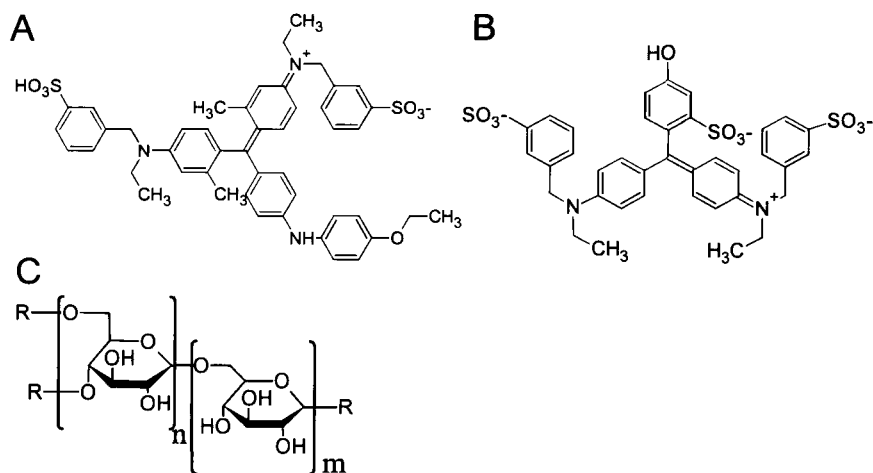
2.6.1 Model Drug Compounds

Small and large model compounds, illustrated in Table 2-3, were loaded and released from photogels to investigate the potential for UV treatment of the photogels to induce changes in drug release. The small molecules were chosen for their similar molecular weights but somewhat different structures. Coomassie Blue and Fast Green have a variety of aromatic groups that may possibly interact with the aromatic groups on anthracene (Figure 2-8). Dextran is a linear/branched chain which may entangle within hydrogel matrices. The proteins were chosen as representatives of large molecule drugs with a variety of molecular weights and isoelectric points (pI). Lysozyme is positive and bovine serum albumin (BSA) is negative at neutral pHs so they may ionically interact and be attracted or repelled respectively by negatively charged alginate and HA. Myoglobin with an isoelectric point at 7.3 (and minor 6.8) should remain relatively neutral.

Solutions of Coomassie blue and Fast Green were detected spectrophotometrically at 595 nm and 630 nm. Dextran was detected by precipitation in ethanol and read spectrophotometrically at 405 nm. Proteins were detected using the Bradford assay read at 595 nm. Details can be found in Appendix 3.

Table 2-3. The various model compounds used for release studies.

| Name | Molecular Weight | Detection |
|----------------------------------|------------------|--------------------------|
| Coomassie Blue | 833 Da | Absorption at 595 nm |
| Fast Green | 766 Da | Absorption at 630 nm |
| Dextran | 1000 Da | Precipitation in ethanol |
| Lysozyme (pI 9.3) | 14,400 Da | Bradford assay |
| Myoglobin (pI 7.3, minor 6.8) | 17,600 Da | Bradford assay |
| BSA (pI 4.9) | 67,000 Da | Bradford assay |

**Figure 2-8.** The structures of (A) Coomassie Blue, (B) Fast Green and (C) dextran.

2.6.2 Release Study Protocol

Molecules were loaded into hydrogels by soaking of dried gels into 0.5 mg/mL solutions in PBS for 24 hours followed by rinses with PBS to remove residual compounds. Release was into 1 mL of PBS (pH 7.4) at 37°C. Periodically the PBS was removed for quantification and replaced with fresh PBS at intervals selected to ensure

sink conditions. At specified times, groups of gels were treated with UV light as described in detail in Appendix 4. Release studies from physically crosslinked calcium alginate gels were into TRIS buffered saline (TBS) to slow decrosslinking to allow for adequate observations as the phosphate in PBS sequesters calcium ions resulting in rapid calcium alginate gel degradation.

The Ritger and Peppas model was used to evaluate the diffusion mechanisms of the molecules from the different hydrogels. The gel disks were treated as slabs since their diameters are over 4 times their thickness [21,22]. The transport mechanisms within the photogels after varied light treatments may be estimated with diffusional exponents. The diffusion exponent from slabs may be summarized by the simplified expression in equation 2-5 [23],

$$\frac{M_t}{M_\infty} = kt^n \quad (2-5)$$

Where, M_t and M_∞ are amount of drug released at time t and ∞ , t is time, k is the proportionality constant and n is the diffusional exponent. By correlating the natural logarithms of M_t/M_∞ versus t , the diffusional exponents were estimated and transport elucidated according to Table 2-4.

Table 2-4. The transport mechanisms associated with the diffusional exponents in slabs.

| Diffusional Exponent | Mechanism |
|----------------------|-------------------|
| $n \leq 0.5$ | Fickian |
| $0.5 < n < 1$ | Anomalous |
| $n = 1$ | Case II transport |
| $n > 1$ | Super case II |

Diffusion coefficients represent the speed of diffusion of model compounds through materials allowing comparison between different systems. The beginning of release of molecules from the photogels was found to be Fickian. Therefore the Ritger and Peppas model for slabs was used to compare the systems during these time periods (Equation 2-6) [23]. Regression of M_t/M_∞ versus $t^{0.5}$ can be used to determine the diffusion coefficient D_{iL} , where l is the thickness of the slab.

$$\frac{M_t}{M_\infty} = 4\sqrt{\frac{D_{iL}t}{\pi l^2}} \quad (2-6)$$

2.7 Cytocompatibility Studies

Human retinal pigment epithelial (RPE) cells from ATCC (Manassas, VA) and human corneal epithelial (HCE) cells from hybrid immortalized cell lines [24] were chosen as representative ophthalmic cell lines to test photogel compatibility. Cell culture protocols can be found in Appendix 5.

2.7.1 MTT Assay

The MTT assay tests cell viability through the conversion of MTT (3-[4,5-dimethylthiazol-2-yl]-2,5-diphenyl tetrazolium bromide) to a formazan precipitate by viable cell mitochondria (Figure 2-9) and was used to assess cell population and viability when cells were grown with photogels versus controls. Formazan can be dissolved in DMSO and detected spectrophotometrically at 595 nm and 700 nm (background). Specific protocols can be found in Appendix 6.

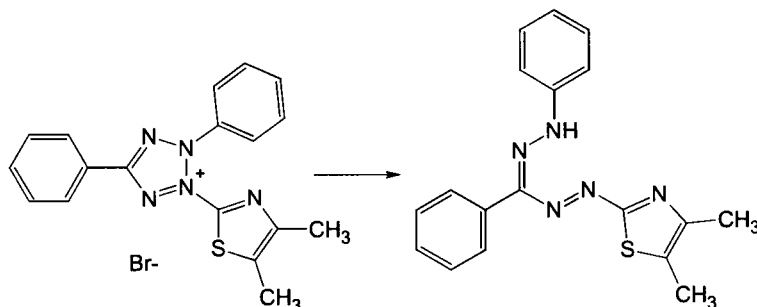


Figure 2- 9. MTT is converted to formazan by mitochondrial reductase.

2.7.2 Cell Tests

As summarized in Table 2-5, a variety of tests were used to assess the compatibility of RPE and HCE cells with gels in indirect contact, with degradation products and with solutions of crosslinkers or polymers. The details of the different types of tests can be found in Appendix 7. Solutions of PEG-anthracene and HA were sterile filtered for cell culture and dried hydrogel disks were sterilized by treatment with ethanol (also described in Appendix 7).

Table 2-5. The types of cell tests that were performed to investigate photogel compatibility.

| Name | Gel Form | Cell Type | Times | Measurements |
|--------------------------|--|-------------|------------------|--------------|
| Indirect Contact | Gels and cells separated by insert. | RPE and HCE | 3 days or 7 days | MTT assay |
| Degradation products | Long term degradation products. | RPE | 3 days | |
| PEG anthracene solutions | Solutions of PEG-anthracene (varying concentrations) | RPE | 3 days or 7 days | |
| HA solutions | Solutions of HA. | RPE and HCE | 3 days or 7 days | |

2.8 References

1. Sehgal D, Vijay IK. A method for the high efficiency of water-soluble carbodiimide-mediated amidation. *Anal Biochem* 1994;218:87-91.
2. Fields GB, Tian Z, Barany G. Principles and practice of solid-phase peptide synthesis. In: Grant GA, editor. *Synthetic peptides. A user's guide* United States of America: W.H. Freeman and Company, 1992. p. 77-183.
3. Pearson DA, Blanchette M, Baker ML, Guindon CA. Trialkylsilanes as scavengers for the trifluoroacetic acid deblockers of protecting groups in peptide synthesis. *Tetrahedron Letters* 1989;30:2739-2742.
4. Kocienski PJ. *Protecting groups*. 3rd ed. NY: Stuttgart, 2004.
5. Gilles MA, Hudson AQ, Borders CL, Jr. Stability of water-soluble carbodiimides in aqueous solution. *Anal Biochem* 1990;184:244-248.
6. Nakajima N, Ikada Y. Mechanism of amide formation by carbodiimide for bioconjugation. *Bioconjugate Chem* 1995;6:123-130.
7. Blume Y, Durzan DJ, Smertenko P. *Cell biology and instrumentation: UV radiation, nitric oxide and cell death in plants*. : IOS Press, 2006.
8. Baxter D. *Therapeutic lasers*. UK: Longman Group, 1994.
9. Basting D, Marowsky G. *Excimer Laser Technology*. Germany: Springer-Verlag Berlin Heidelberg, 2005.
10. MacFayden DA, Fowler N. On the mechanism of the reaction of ninhydrin with α -amino acids. *JBC* 1950:13-22.
11. Moore S. Amino acid analysis: aqueous dimethyl sulfoxide as solvent for the ninhydrin reaction. *J Biol Chem* 1968;243:6281-6283.
12. Bray JC, Merrill EW. Poly (vinyl alcohol) hydrogels. Formation by electron beam irradiation of aqueous solutions and subsequent crystallization. *J Apply Poly Sci* 1973;17:3779-3794.
13. Flory PJ, Rehner J. Statistical mechanics of cross-linked polymer networks II. Swelling. *J Chem Phys* 1943;11:521-526.
14. de Jong SJ, van Eerdenbrugh B, van Nostrum CF, Kettenes-van den Bosch JJ, Hennink WE. Physically crosslinked dextran hydrogels by stereocomplex formation

- of lactic acid oligomers: degradation and protein release behavior. *J Controll Rel* 2001;71:261-275.
15. Amsden B, Turner N. Diffusion characteristics of calcium alginate gels. *Biotech Bioeng* 1999;65:605-610.
 16. Leach JB, Bivens KA, Patrick CW, Schmidt CE. Photocrosslinked hyaluronic acid hydrogels: natural, biodegradable tissue engineering scaffolds. *Biotechnol Bioeng* 2003;82:578-589.
 17. Li CY, Birnkrant MJ, Natarajan LV, Tondiglia VP, Lloyd PF, Sutherland RL, Bunning TJ. Polymer crystallization/melting induced thermal switching in a series of holographically patterned Bragg reflectors. *Soft Mat* 2005;1:238-242.
 18. Kakizaki I, Ibori N, Kojima K, Yamaguchi M, Endo M. Mechanism for the hydrolysis of hyaluronan oligosaccharides by bovine testicular hyaluronidase. *FEBS Journal* 2010;277:1776-1786.
 19. Khorlin AY, Vikha IV, Milishnikov AN. Subunit structure of testicular hyaluronidase. *FEBS Lett* 1973;31:107-110.
 20. Bailey LC, Levine NA. Optimization of the USP assay for hyaluronidase. *J Pharma Biomed Anal* 1993;11:285-292.
 21. Leach JB, Schmidt CE. Characterization of protein release from photocrosslinkable hyaluronic acid-polyethylene glycol hydrogel tissue engineering scaffolds. *Biomater* 2005;26:125-135.
 22. Chorny RC, Krasuk JH. Extraction for different geometries. Constant diffusivity. *Ind Eng Chem Process Des Dev* 1966;5:206-208.
 23. Ritger PL, Peppas NA. A simple equation for description of solute release. 1. Fickian and non-fickian release from non-swellable devices in the form of slabs, spheres, cylinders or discs. *J Controll Rel* 1987;5:23-36.
 24. Griffith M, Osborne R, Munger R, Xiong X, Doillon CJ, Laycock NLC, Hakim M, Song Y, Watsky MA. Functional human corneal equivalents constructed from cell lines. *Science* 1999;286:2169-2172.

3.0 Graftable PEG-Anthracene to Generate Photoresponsive Hydrogels for Drug Delivery

Authors: Laura A. Wells, Michael A. Brook and Heather Sheardown

Publication Information: To be submitted to Macromolecular Bioscience

Objectives:

To create a water-soluble form of anthracene that may be generically grafted to different polymers to introduce photosensitive properties to allow photoswitchable crosslinking and drug delivery.

Main Scientific Contributions:

1. Synthesis and analysis of generic water-soluble, dimerizing photocrosslinker PEG-anthracene that retain its reversible photodimerizing properties with UV light exposure above and below 300 nm.
2. The grafting of PEG anthracene onto alginate and HA polymers to produce “photogels”.
3. Property testing of photogels to investigate the ability for light to cause changes in crosslinking. Initial proof-of-concept release studies of small Coomassie Blue and larger myoglobin.
4. Initial cell studies of human corneal epithelial cells grown with HA and alginate photogels versus controls were performed as an initial cytocompatibility evaluation.

**Graftable PEG-Anthracene to Generate Photoresponsive Hydrogels for Drug
Delivery**

Laura A. Wells¹, Michael A. Brook² and Heather Sheardown^{1*}

Departments of ¹Chemical Engineering and ²Chemistry
McMaster University, Hamilton ON Canada

* to whom correspondence should be addressed

sheardow@mcmaster.ca

Phone: 905-525-9140 x. 24794

Fax: 905-521-1350

Department of Chemical Engineering
McMaster University
1280 Main Street West
Hamilton ON
L8S 4L8
Canada

Abstract

Light-responsive polymers with controllable, reversible crosslink mechanisms have the potential to create unique biomaterials with stimulus-controlled swelling, degradation and diffusion properties useful in tissue engineering and drug delivery applications. Model photoresponsive materials for smart delivery of therapeutics using anthracene-based light-controlled crosslinking and decrosslinking mechanisms have been developed. PEG-based photodimerizing molecules were synthesized and grafted onto the backbone of hydrogel polymers effectively introducing photoresponsive properties into hyaluronate and alginate. The resulting photogels were demonstrated to be cytocompatible. The effective crosslinking densities of the photogels could be incrementally increased with exposure to light at 365 nm; delivery rates from the photogels could be altered with 365 nm and 248 nm wavelength light and laser treatments. This tuneable crosslinking can therefore be used to manipulate the delivery rates of therapeutics resulting in control over treatment profiles and may lend itself to various applications which may benefit from light induced changes in crosslinking.

Keywords:

Photoresponsive

Anthracene

Hyaluronic acid

Alginate

Drug delivery

1. Introduction

Responsive polymer-based drug delivery can benefit the treatment of ophthalmic diseases through the alteration of release rates via stimuli to suit disease progression.^{1, 2} While long-term controlled drug delivery lowers the risk of toxicity, increases efficacy and patient compliance versus conventional therapies³, the fixed release profiles obtainable from most systems do not follow the progression of chronic diseases that require lifetime treatment.¹ Temperature and pH have been established as valuable stimuli in responsive systems, but changes in temperature are dependent on thermal diffusion while pH is dependent on ion diffusion leading to lagged response times.⁴ The transparency of ocular tissue may present an ideal opportunity to use light as a stimulus. Light has significant potential as a stimulus for controlling drug release since its activation is instantaneous and both its intensity and focal point can be highly controlled.⁵⁻⁷ The ability to control the delivery of precise wavelengths to induce specific results is also an attractive component of light activated systems.

Photoresponsive systems can lead to irreversible or reversible property changes in polymers.⁶ Irreversible changes include for example photolabile polyethylene glycol materials⁸ or photoinduced microcapsule rupture.⁹ However, for long term controlled drug delivery for a chronic disease, a reversible system would be a valuable approach. Many reversible reactions involve light activation, inducing secondary reactions which cause changes in a system. For example light can cause reversible changes in chromophores that produce heat or ionic groups to alter the swelling/volume of polymer

networks.¹⁰⁻¹³ While activation of these systems is instantaneous, again the reaction depends on the transfer of heat or diffusion of ions which slows response times. Reversible direct changes have included photo-induced isomerizations that alter polymer chain properties¹⁴ causing for example micelles to solubilise/desolubilise⁶ and some research has shown the potential for photodimerizing molecules to introduce reversible properties.¹⁵⁻¹⁷

Anthracene¹⁸, cinnamylidene acetate¹⁵, nitrocinnamate¹⁹, and coumarin^{20,21} are popular dimerizing molecules investigated for the photocrosslinking of polymers. Anthracene undergoes dimerization through (4 π -4 π) photocycloaddition with UV wavelengths above 300 nm and de-dimerization/dissociation with UV wavelengths below 300 nm.²² By attaching photodimerizing molecules to polymers, a photocrosslinkable system with minimal side-product formation¹⁸ and a low risk of photosensitizer leaching can be created.⁵ The most promising research looks at the covalent incorporation of photosensitive nitrocinnamate molecules to the ends of star polymers. Release studies of growth factors from these materials showed UV-induced decreased release with 50-70% delivery at 120 hours.¹⁶ A drug delivery system with increased photosensitivity and better control of the sustained release of macromolecules would be beneficial for long-term drug delivery applications.

In the current work, a versatile polyethylene glycol-anthracene (PEG-anthracene) photosensitive crosslinker was synthesized. By binding this crosslinker along the

backbone of a polymer chain, instead of only at the polymer ends, a highly photosensitive system can be created. Anthracene was selected as the model light responsive functional group in this work, although other photoactive groups could also be used to generate alternative graftable crosslinkers. PEG-anthracene was grafted to the backbone of hydrogel polymers to create a cytocompatible, sensitive, photoresponsive crosslinking system, as illustrated in Figure 1, which is capable of altering long-term diffusion and drug release properties. Incorporation of PEG-anthracene onto the backbone of both hyaluronate and alginate as model crosslinkable hydrogels was found to control the effective crosslinking density of the gels and as a result the release of model compounds in response to different light/laser wavelengths of varying intensity.

2. Materials and Methods

2.1. Materials and Equipment

Sodium hyaluronan (hyaluronate) (MW 132.3 kDa and 31 kDa) was purchased from Lifecore Biomedical (Chaska, MN). Low viscosity sodium alginate produced by *Macrocystis pyrifera* (61% Mannuronic acid, 39% guluronic acid, MW=12-80 kDa), O-(2-Aminoethyl)-O'-[2-(Boc-amino)ethyl]decaethylene glycol (Boc-PEG-amine) and O,O'-Bis(2-aminoethyl) octadecaethylene glycol (PEG-diamine), assays (Ninhydrin and 3-[4,5-dimethylthiazol-2-yl]-2,5- diphenyl tetrazolium bromide or MTT) and other reagents were purchased from Sigma-Aldrich (Oakville, ON). Buffer chemicals were purchased from EM Science (Gibbstown, NJ). Cell culture supplies were from Invitrogen (CA). NMR spectra (^1H) were obtained using a Bruker AV 200. The Curezone II UV

lamp from CON-TROL-CURE (Chicago,IL) (400 W, 120 VAC, 60Hz, 8 amps max) was used for 365 nm treatments at 10 mW/cm^2 and a krypton fluoride excimer laser operating at 58 mJ/cm^2 at 5 Hz was used for 248 nm treatments.

2.2. PEG-anthracene Crosslinker Synthesis

Boc-PEG-amine of molecular weight 644.79 Da is a diamine terminated polyethylene glycol with one terminal group protected with tert-butoxycarbonyl (t-boc). The Boc-PEG-amine (200 mg) was reacted with anthracene-9-carboxylic acid (288 mg) using 1-ethyl-(dimethylaminopropyl) carbodiimide hydrochloride (EDC) (268 mg) in 20 mL of dry dichloromethane (DCM). The reaction proceeded for 24 hours at room temperature under nitrogen. After drying off the DCM in a rotating evaporator under vacuum at 40°C , unreacted EDC and by products were removed by extraction of ethyl acetate from water and then the ethyl acetate phase was dried in a rotating evaporator under vacuum at 60°C . The blocking group from Boc-PEG-anthracene was subsequently removed in DCM (16 mL) using trifluoroacetic acid (TFA) (2 mL) with triisopropyl silane (4 mL) as a scavenger.²³ Dark synthesis conditions prevented premature dimerization.

Purification was performed by drying the final reaction solution under vacuum in a rotating evaporator at 40°C , then dissolving it in water followed by centrifugation and filtration through a 0.2 micron filter to remove water insoluble residual deprotection products, anthracene and non-deprotected PEG. While the diamine PEG may aid in the overall properties of subsequent gels, it may also be separated out using silica columns

that are loaded using hexane/DCM and run using methanol/DCM. The deprotection reaction was monitored with ^1H NMR through the disappearance of the Boc singlet at 1.4 ppm which indicated 4 hours was adequate for deprotection. The resulting molecule shown in Figure 1b was found to have high solubility in aqueous solutions. The reaction was optimized to obtain yields of 81% with over 82% substitution (NMR). ^1H NMR (200MHz, DMSO) showed peaks at 7.5-8.3 ppm for anthracene and 3.2-3.9 for PEG and ^{13}C NMR (200 MHz, D_2O) showed $\delta = 130.5, 128.2, 125.6, 69.4, 41.9, 39.0$ ppm. FT-IR (KBr) had $\nu = 3500\text{-}3000$ (N-H and aromatic C-H stretch), 2880 (C-H stretch), 1677 (C=O stretch), 1522, 1457 (aromatic C=C stretch), 1201, 1132 (C-O stretch), 799, 721 cm^{-1} .

2.3. Photogel Synthesis

Photogels made of grafted PEG-anthracene and control PEG hydrogels made of grafted PEG were synthesized by mixing EDC, N-hydroxysuccinimide (NHS) and 6% HA or alginate with PEG-anthracene or PEG-diamine in MES buffer^{24,25} as illustrated in Figure 2. Low viscosity, 6% alginate and HA solutions in 4-morpholinoethanesulfonic acid (MES) buffer containing 0.1 M MES with 0.5 M NaCl (pH=6) were mixed with a solution of EDC and NHS in a COOH:EDC:NHS in molar ratio of 0.8:2:1 for alginate and HA photogel synthesis. The ratio of PEG-anthracene to carboxyl groups on the HA polymer backbone was 1.2:1 and on the alginate backbone was 0.84:1. For HA photogels, 0.353 mL of EDC (191.6 mg/mL) and NHS (57.5 mg/mL) were added to 0.443 mL PEG-anthracene (300 mg/mL plus NaOH to pH of 6.5) prior to the 6% HA to

prevent premature reaction whereas for alginate 0.353 mL of EDC (394.2 mg/mL) and NHS (118.3 mg/mL) were added to alginate to pre-activate the carboxyl groups prior to the addition of 0.443 mL of PEG-anthracene (428.3 mg/mL plus NaOH to pH of 6.5). A final concentration of 3% (w/v) alginate or HA resulted and after mixing for 5 minutes, the reaction solution was then placed between glass plates with a 1 mm glass spacer and allowed to react in the dark at 4°C for 72 hours. Control PEG-hydrogels were made with 20 unit PEG-diamine chain using the same method but with a ratio of PEG-diamine to carboxyl groups on the polymer backbone of 0.5:1, half as much PEG (0.443 mL of 180 mg/mL for HA and 346 mg/mL for alginate) was added versus the photogels to mimic the photocrosslinked photogels since both ends will react to the polymers. For swelling and drug release studies, the gels were cut into disks with a diameter of 0.5 cm and a thickness of 0.1 cm. Gels were soaked in de-ionized water for 24 hours to remove impurities and air-dried for 72 hours for long-term storage. Air drying of the disks over 72 hours for storage maintained the gel properties and was determined to be an adequate time-frame since insignificant differences in mass-loss during drying were noted between air dried versus freeze-dried gels ($p=0.066$). The physical properties of the various photogels were examined with swelling and drug release tests performed with a focus on the 132.1 kDa HA photogels and alginate photogels in these studies since they formed loose gels before UV treatments.

2.4. Ninhydrin Assay for Amines

Soaking solutions and photogels swollen in 1 mL of water were tested for primary amines using the ninhydrin assay. The 1 mL solutions were mixed with 0.5 mL of ninhydrin reagent (Sigma Aldrich) containing 2% ninhydrin and hydrindantin in dimethyl sulfoxide (DMSO) and lithium acetate buffer at pH 5.2. After heating at 100°C for 10 minutes, the solutions were cooled to room temperature and diluted with 2.5 mL of 95% ethanol. Primary amines were detected by measuring the solutions spectrophotometrically at 595 nm and concentrations were determined with a glycine calibration. The grafting density of the PEG-anthracene onto HA or alginate could then be calculated by dividing the actual amount grafted by the theoretical amount grafted.

2.5. Swelling and Effective Crosslinking Density

For swelling studies, dried gels were swollen in PBS for 24 hours and then weighed. Equilibrium swelling theory was used to estimate effective crosslinking density changes of alginate and HA photogels following UV exposure. An established version of the Flory-Rehner equation that had been previously modified by Bray and Merrill²⁶ to describe hydrogels crosslinked in solution²⁶⁻²⁸ was applied to estimate and compare the effective crosslinking densities (v_e) of the gels before and after UV treatment. Equation (1) relates the average molecular weight between crosslinks (M_c) to the specific volume of swollen and dry hydrogels while Equation (2) relates v_e to M_c and the polymer density (ρ_p).

$$\frac{1}{Mc} = \frac{2}{Mn} - \frac{(\bar{v}/V_1)[\ln(1 - v_{2,s}) + v_{2,s} + \chi_1(v_{2,s})^2]}{v_{2,r}[(v_{2,s}/v_{2,r})^{1/3} - 0.5(v_{2,s}/v_{2,r})]} \quad (1)$$

$$v_e = \frac{\rho_p}{M_c} \quad (2)$$

In the above equations, v is the specific volume of dry polymer ($v = 0.814 \text{ cm}^3/\text{g}$ for HA²⁹, $0.60 \text{ cm}^3/\text{g}$ alginate³⁰ and $0.89 \text{ cm}^3/\text{g}$ for PEG³¹), $v_{2,s}$ is the volumetric polymer fraction at maximum swelling, $v_{2,r}$ is the volumetric polymer fraction in a relaxed state, V_1 is the molar volume of solvent ($18 \text{ mol}/\text{cm}^3$) and χ is the Flory polymer-solvent interaction parameter ($\chi \approx 0.473$ for HA and alginate²⁹ and PEG³¹) and Mn is the number average molecular weight of the polymer. The calculations focused on HA or alginate with PEG assuming that both act as significant constituents based on their experimentally determined grafting densities.

2.6. Release Studies

For the release studies, air-dried disk gels were loaded by soaking in PBS solutions containing $0.5 \text{ mg}/\text{mL}$ of the model compounds Coomassie Blue or myoglobin. Prior to the release studies, the drug-loaded gels were rinsed with PBS buffer ($\text{pH}=7.4$). Disks of known mass were placed in 1 mL PBS ($\text{pH} 7.4$) and shaken in a water bath at 37°C . At preset times, the gels were exposed to UV, either light treatments of 365 nm or laser treatments of 248 nm . Gels were exposed to 365 nm light in 1 mL of PBS to maintain hydration and on ice to prevent heating over the long treatment times of 10-40 minutes

require for fluences $> 6000 \text{ mJ/cm}^2$ under the weak lamp. Gels were exposed to the 248 nm laser on slides without buffer since exposure times were shorter ($< 1\text{-}5$ minutes) due to the higher power of the laser and the frequency of pulses were kept low to prevent heating. Releasates were sampled at regular intervals and analyzed using a microplate reader with a 595nm filter. Coomassie Blue dye was detected at 595 nm and the Bradford assay³² was used to determine myoglobin concentration versus controls with no protein. Statistical analysis using two-tailed t-tests were used to assess cumulative and percent release changes.

2.7. Cytocompatibility Studies

Photogels were sterilized with a 2 hour ethanol soak followed by sterile air drying for 16 hours and a 1hour medium soak. Ethanol was used as the least destructive technique that did not require UV light which would alter the baseline crosslinking of the gels. Human corneal epithelial (HCE) cells from hybrid immortalized cell lines³³ were grown in keratinocyte-serum free medium (SFM) containing human recombinant epidermal growth factor 1-53 and bovine pituitary extract. After 24 hours of growth with seeding at 20,000 cells/well or 120,000 cells/well, HA or alginate photogels in inserts (1.0 micron pore-size, 1.6×10^6 pore density, polyethylene terephthalate) were respectively added to the cells and they were grown for 3 or 7 days. The MTT assay, a colorimetric assay that measures the reduction of a tetrazole molecule to formazan, was performed by spectrophotometrically measuring 595 nm and 700 nm absorption ratios after incubation of the cells in 0.4 mg/mL of MTT in medium for 4 hours.

3. Results

3.1. Photogel Synthesis

In order to introduce hydrophobic anthracene onto a hydrophilic polymer and to generate the versatile graftable photocrosslinker, anthracene was covalently attached to an 11 unit polyethylene glycol (PEG) chain creating a versatile water-soluble PEG-anthracene molecule of 748.9 Da that could ultimately be covalently grafted onto the backbone of various polymers to introduce a photocrosslinking mechanism as illustrated in Figure 1. Synthesis was optimized to obtain yields of 81%.

The ability of the PEG-anthracene to dimerize and de-dimerize was verified in solution by spectrophotometrically monitoring peaks between 300-400 nm that disappear with dimerization. For example, low fluences of 8100 mJ/cm² at 365 nm (270 minutes at 0.5 mW/cm²) allowed for 44% dimerization of PEG-anthracene in solution with a fluence of 1440 mJ/cm² at 254 nm (40 minutes at 0.6 mW/cm²) causing 9% dissociation in solution. This was slightly less efficient than anthracene-9-carboxylic acid that underwent 86% dimerization followed by 40% dissociation with the same exposures. In the design of the PEG-anthracene photocrosslinker molecules, the PEG chains were selected to give the anthracene mobility required for dimerization and de-dimerization after grafting.³⁴ The PEG chain likely caused a slight reduction in dimerization and de-dimerization efficiency, consistent with past literature which indicates that bound groups can lower anthracene

photoreactivity.²² Importantly, the PEG-anthracene still underwent dimerization and de-dimerization.

The grafting efficacy of PEG-anthracene and PEG-diamine on the hydrogels was estimated by measuring unreacted primary amine groups in both soaking solutions and swollen hydrogels using a ninhydrin assay.³⁵ On average, 50% of added PEG-anthracene bound to alginate when added at a 0.84:1 ratio of PEG-anthracene to polymer carboxyl groups resulting in 42% overall grafting (0.42:1 ratio). The measured grafting efficiencies for HA were higher with over 96% of the added PEG-anthracene binding to the HA polymers resulting in approximately 100% grafting (1:1 ratio). EDC and NHS were added last in the HA photogel synthesis to minimize self-crosslinking that may occur via ester bond formation between carboxyl and hydroxyl groups.³⁶ Since alginate has more carboxyl groups available (198.1g sodium alginate/mol_{COOH} versus 401.3g of sodium HA/mol_{COOH}), 42% grafting on alginate and 100% grafting on HA result in approximately the same number of anthracene groups per gram of gel (2.22mmol/g alginate gel versus 2.49 mmol/g HA gel) to create photogels with approximately the same potential photosensitivity.

3.2. Photogel Properties

Grafting of PEG-anthracene to HA resulted in either viscous liquids or hydrogels whose properties were monitored before and after 365 nm light exposures. Grafting of PEG-anthracene onto 31 kDa HA (100% theoretical grafting ratio) resulted in a viscous liquid

that gelled with exposure to 365 nm light as shown in Figure 3a; control solutions of HA in PBS did not gel with UV light. Alginate formed hydrogels that were slightly translucent presumably due to impurities in the alginate or due to the arrangements in the copolymer units resulting in light scattering. This will likely lower alginate photogel light-absorption due to the scattering of UV light making these gels less sensitive to light and therefore less responsive.

Irradiation of alginate and HA photogels with 365 nm light at 10 mW/cm² resulted in increases in effective crosslinking density (Figure 3b). In comparison, irradiation of HA control PEG-hydrogels resulted in no significant increases in crosslinking with exposure up to 18,000 mJ/cm² of 365 nm light (30 minutes at 10mW/cm²) (data not shown) demonstrating that the effective crosslinking results were due to PEG-anthracene grafting. This is in agreement with spectrophotometry scans (Figure 3c) that show lowering of absorption peaks of HA photogels, which is indicative of dimerization of the anthracene groups, but no changes with control HA PEG hydrogels with 365 nm UV treatments (30 minutes at 10mW/cm²).

3.3. Release Studies

A model low molecular weight compound (Coomassie Blue, 854 Da) and a model protein (myoglobin, 17.6 kDa, pI=7.3 and minor 6.8) were released from the photogels into PBS (37°C, pH=7.4) with and without UV light and laser treatments. Treatment of HA photogels with 365 nm UV light at a fluence of 12,000 mJ/cm² (20 minutes at 10

mW/cm²) at 1.5 hours of Coomassie Blue release resulted in decreased release rates relative to control HA photogels exposed to no UV light, as shown in Figure 4a, with significantly different amounts released by 3505 hours ($p=0.002$). A similar albeit lesser effect was noted with the alginate photogels when treated with 365 nm UV light at a fluence of 24,000 mJ/cm² (40 minutes at 10 mW/cm²) at 1.5 hours presumably due to the lower UV transparency of these materials (Figure 4b). However, alginate photogels treated with 365 nm UV light showed significantly lower amounts of released Coomassie Blue versus controls by 1708 hours ($p=0.046$). Furthermore, as shown in Figure 4a, a small but noteworthy increase in the rate of release from the gel was observed following 248 nm laser treatment (207 pulses at 58mJ/cm³, 5Hz, 12,000 mJ/cm²) of the photogels at 6530 hours. However, the changes in release noted after 365 nm light exposures were larger than those seen with the 248 nm laser. A burst was not noted at this time, presumably due to the previously lengthy release period from the gels.

The release of myoglobin from HA and alginate photogels into PBS with and without UV treatment is shown in Figure 5a and b. Of note, myoglobin release from HA photogels showed an “off effect” and stopped releasing when the photogels were irradiated with 365 nm light at 18,000 mJ/cm² (30 minutes for 10 mW/cm²) at 1.5 hours versus controls with no UV light exposure with significantly different amounts of released protein at 5.5 hours ($p=0.034$). Myoglobin release from alginate photogels slowed to a great extent with significantly lower release noted 20 hours after 365 nm treatments ($p=0.040$), although the “off effect” was not observed with these gels. When the myoglobin-containing HA-

photogels were further exposed to a 248 nm excimer laser for 18,000 mJ/cm² (310 pulses of 58 mJ/cm² at 5 Hz) at 2900 hours the protein release “turned on” (Figure 5a).

In all cases, control studies ensured that the observed changes in properties and release rates after UV treatment were due to grafted PEG-anthracene crosslinkers and not due to UV effects on the HA/alginate or model compounds. Control studies on unloaded HA control PEG hydrogels showed that they maintained their swelling properties with exposure to 248 nm excimer laser fluences from 200-24,000 mJ/cm² (50 mJ/cm² pulses at 5 Hz) and with 365 nm light up to 18,000 mJ/cm² (30 minutes at 10 mW/cm²). Therefore, the laser and UV light sources likely did not cause substantial degradation to the HA polymers which could lead to increased release. Release of Coomassie blue from control PEG-hydrogels did not significantly change with exposure to 18,000 mJ/cm² of 365 nm light and 248 nm laser treatments (310 pulses at 58 mJ/cm² at 5Hz). In addition, there were no apparent spectrophotometric changes in either Coomassie Blue or myoglobin when treated with 365 nm light (18,000 mJ/cm²) or 254 nm light (1080 mJ/cm²).

3.4. Cytocompatibility of Photogel Systems

Human corneal epithelial (HCE) cells were chosen to test the photogels since they are a well-understood model ocular cell line. HCE cells were seeded in 24 well plates with sterilized HA photogels and alginate photogels added following 24 hours of culture using cell inserts with pore sizes of 1.0 microns. HCE cells were then grown for periods of 3 or

7 days to assess cytotoxic effects. MTT assays were used to compare cellular effects in the presence of the photogels or control PEG hydrogels with those observed when no gel was present. The results shown in Figure 6 show that the HA and alginate photogels and the HA and alginate control PEG hydrogels did not cause significant changes in the viability of the HCE cells versus controls grown with no gels as measured by the MTT assay. Specifically, no significant differences were noted between the control cells (no gel) versus the HA photogels (3 days $p=0.377$, 7 days $p=0.0832$) and the HA control PEG hydrogels (3 days $p=0.263$, 7 days $p=0.362$) ($n=4$, single factor Anova). There is no data for 7 days of growth with alginate gels. However, no significant difference were noted between the control gels versus the alginate photogels (3 days $p=0.059$) or alginate control PEG hydrogels (3 days $p=0.111$) ($n=3$, single factor Anova).

4. Discussion

Swelling, crosslinking and release studies demonstrate the ability for the grafting of PEG-anthracene onto hydrogel polymers to effect changes in the photogels dependent on UV exposure, potentially allowing for the fine-tuning of their properties using light. The PEG-anthracene was grafted onto both hyaluronate (HA) (MW 31 and 132.3 kDa) and alginate (12-80 kDa) in this work. Formed of alternating units of D-glucuronic acid and N-acetyl-D-glucosamine³⁷, HA is present mostly in skin, lungs, intestines, synovial fluid, umbilical cords and vitreous humour³⁸ and has been widely demonstrated to be compatible *in vivo*. The low molecular weights were selected for relative ease of solubilisation and lower viscosity although higher molecular weights of over 1 million Da

exist naturally *in vivo*.³⁹ Alginate is a block copolymer of β -D-mannuronic and α -L-guluronic acid that forms high water content hydrogels.⁴⁰ It was selected based both on chemical properties as well as its previous application in both drug delivery and biomedical applications.^{41, 42} HA and alginate both have carboxyl groups available for grafting of the amine-terminated molecules via carbodiimide chemistry^{24, 35, 38, 43} although this is not a limiting factor in polymer selection. After PEG-anthracene grafting, the release of model compounds from the resulting HA and alginate photogels with and without UV treatment was used to assess the ability for the resulting photo-induced crosslinking to lead to changes in diffusion and release of model compounds from the gels. The 365 nm UV treatment of alginate and HA photogels effectively slowed the release of small model drugs and could greatly slow or shut down the release of large model drugs.

The small increase in release rate of Coomassie blue from the HA photogels with 248 nm laser treatment may be explained by the ability of these HA gels to absorb UV light under 300 nm. The spectrophotometer scans in Figure 3c clearly show that the HA gels absorb UV wavelengths under 300 nm. Therefore, 248 nm would likely irradiate the surface of the gels but may not significantly penetrate the surface. Therefore it is likely that decrosslinking occurs at the surface of the photogels and any increases in release are due to changes at the surface which explains the observed small bursts. Their low magnitude short time scales are due to increases in release of model compounds at the surface and compounds deeper within the photogels would continue to migrate at the same rate as

prior to 248 nm laser treatments. Note that the absorption of the photogels above 300 nm occurs at the anthracene group and lowers with 365 nm exposure allowing the 365 nm light to penetrate the entire gel and cause bulk changes. Future studies will focus on different bulk materials or grafting techniques that will have minimal interference with light under 300nm as well as alternative photoactive groups. For example, in the eye, it may be useful to examine groups which respond to wavelengths outside of the UV range.

The diffusion of larger molecules such as proteins is expected to be more heavily influenced by changes in crosslinking density induced by light exposure.⁴⁴ Therefore larger changes in release profiles observed in Figure 5 are expected with UV treatment of the photogels. Myoglobin was chosen as a model protein in these studies due to its somewhat neutral charge at pH 7.4; however electrostatic interactions with the polymers is unlikely since the high grafting reduces the number of acidic carboxyl groups on the alginate and HA polymer backbones. The protein release from HA photogels became undetectable for long periods of time following 365 nm UV exposure, which is attributed to the increased crosslinking density inhibiting the diffusion of the larger protein molecule. The slowing but incomplete halting of protein release from alginate photogels following 365nm light treatments is likely due to the porous structure alginate can possess due to the differences in entanglements and stiffness of the copolymer block arrangements of the mannuronic and guluronic acid chains. Guluronic acid blocks can create microscopic pore features.⁴⁵ In addition, due to the lower grafting density of PEG-anthracene onto alginate, the alginate photogels may be slightly negative and ionically

repel myoglobin to a low degree since myoglobin may be slightly negative at a pH of 7.4. There was a small increase in release of myoglobin from HA photogels with 248 nm laser treatments and it is hypothesized that higher fluences at 248 nm will result in larger increases in the release and the laser is not penetrating the photogels completely due to HA absorption resulting in surface decrosslinking but not bulk decrosslinking. The effect of these levels of light exposure on relevant biological tissues and on the proteins must also be examined. However, the ability for HA photogels to act as on/off controls for protein delivery creates the potential for a unique photoresponsive hydrogel delivery system for large sized drugs. The crosslinking density of hydrogels is known to have an influence on molecular diffusion within the matrix with increases in crosslinking resulting in decreases in mesh size thereby inhibiting diffusion.⁴⁶ It is therefore not surprising that the size of the released molecule will have an impact on release properties, with release of larger molecules such as proteins being more affected by changes in the crosslinking density.⁴⁴

In vitro and *in vivo*, the coupling of the anthracene to the PEG is hypothesized to minimize any adverse effects of the photoactive agent. Furthermore, cells will not be considerably exposed to anthracene in the polymer bound form. To test this hypothesis, corneal epithelial cells were grown in the presence of photogels to evaluate their cytocompatibility and to determine the effect of any released degradation and side products. Cytocompatibility tests show the ability of the cells to grow and metabolize in

the presence of the photogels; future studies will focus on the effect of UV light on these systems.

Light exposures at 365 nm have clearly shown the ability to increase crosslinking and slow the diffusion and release of model compounds. With large molecule release, on-demand ability to turn off release would provide a safety mechanism to halt the release of drugs when adverse patient-drug reactions occur. While it is clear that exposure to UV light for extended periods of time is not likely to be considered a viable or convenient therapy for the patient, there is potential to adapt these materials for treating various diseases. For example, since laser therapy is already used extensively in medical treatments^{7, 47}, appropriate formulations of these gels may have the potential to be used with targeted laser therapy to elicit the release of such molecules on demand for treatment as a disease progresses. Laser use was demonstrated with the 248 nm excimer laser causing surface decrosslinking and increases in release. Laser use for 365 nm studies would lower the treatment time while maintaining the required exposures. Studies with other hydrogel systems may also provide information about the potential of these systems in alternative applications. Ultimately, formulation of these materials into other materials may be useful for controlling release.

5. Conclusions

The grafting of a generic PEG-anthracene crosslinker onto hydrogel polymer backbones has been shown to introduce photosensitive properties into the polymer allowing for

incremental photoinduced crosslinking with 365 nm light. Treatment with 365 nm wavelength light (12,000, 18,000 or 24,000 mJ/cm²) was found to slow the release of Coomassie blue and to “turn off” myoglobin release from the HA photogels. Release of Coomassie blue from alginate photogels was slowed to a lesser extent, presumably due to the translucency of this material. Excimer laser (248 nm wavelength light, 12,000 and 18,000 mJ/cm²) exposure resulted in a small but measurable increase in release rate from HA photogels relative to the controls. The ability to control drug release from these systems, both incrementally and in an on/off fashion, demonstrates their potential for use as a controllable and smart drug delivery system. Furthermore, demonstration of these effects with both alginate and hyaluronate as hydrogel polymer backbones suggests that these crosslinkers are generic and may be useful for the further development of responsive drug delivery systems.

Acknowledgements

NSERC and 20/20 NSERC Ophthalmic Materials Network are acknowledged for funding.

Figure Captions

Figure 1. Photogels based on anthracene dimerization.

(a) Anthracene dimerization and de-dimerization/dissociation and the proposed mechanism by which the anthracene is grafted to the backbone polymer chains via a PEG linker. This allows crosslinking and de-crosslinking of polymers to occur with dimerization and de-dimerization of anthracene upon irradiation at > 300 nm and < 300 nm. (b) The structure of the graftable, photosensitive PEG-anthracene crosslinker.

Figure 2. Synthesis of HA photogels.

The synthesis of HA photogels using EDC/NHS to create an amide bond between the HA and PEG-anthracene.

Figure 3. Photogel crosslinking.

(a) Grafting of PEG-anthracene onto 31 kDa HA results in a liquid that gels with 365 nm light exposure ($10\text{mW}/\text{cm}^2$ for 2.5 hours). (b) The effective crosslinking density of alginate and HA photogels with no UV treatment and with 365 nm UV treatments for 20 minutes (alginate photogels) or 30 minutes (HA photogels) ($10\text{ mW}/\text{cm}^2$). (c) Spectrophotometric scans of HA photogels and HA control PEG hydrogels. The photogels show decreases in absorption above 300 nm as the anthracene groups dimerize due to exposure to 365 nm light whereas there are no changes in the absorption of the control PEG hydrogels with 365 nm light (30 min at $10\text{mW}/\text{cm}^2$).

Figure 4. Release of Coomassie blue from photogels with UV treatments.

(a) Coomassie Brilliant Blue release from HA photogel disks into PBS (37°C , $\text{pH}=7.4$). At 1.5 hours two sets of gels ($n=3$) were irradiated with 365 nm at $10\text{mW}/\text{cm}^2$ for 20 minutes ($12,000\text{ mJ}/\text{cm}^2$). At ~ 6500 hours, one set of gels ($n=3$) was then exposed to a 248 nm excimer laser for $12,000\text{ mJ}/\text{cm}^2$ (207 pulses of $58\text{ mJ}/\text{cm}^2$ at 5 Hz). (b) Coomassie Brilliant Blue release from alginate photogel disks into PBS (37°C , $\text{pH}=7.4$).

At 1.5 hours one set (n=3) of alginate photogels was irradiated with 365 nm at 10mW/cm² for 40 minutes (24,000 mJ/cm²).

Figure 5. Release of proteins from photogels with UV treatments.

Myoglobin release from HA photogel disks into PBS (37°C, pH=7.4). At 1.5 hours two sets of gels (n=3) were irradiated with 365 nm at 10mW/cm² for 30 minutes (18,000 mJ/cm²). At 2900 hours one set of gels was then exposed to a 248 nm excimer laser for 18,000 mJ/cm² (310 pulses of 58 mJ/cm² at 5 Hz). (b) Myoglobin release from alginate photogel disks into PBS (37°C, pH=7.4). At 1.5 hours two sets of gels (n=3) were irradiated with 365 nm at 10mW/cm² for 30 minutes (18,000 mJ/cm²).

Figure 6. Cytocompatibility testing of cells grown with photogels.

HCE cells grown with alginate or HA control PEG-hydrogels and with alginate or HA photogels were tested versus controls HCE cells grown with no gels with the MTT assay after growth for 3 and 7 days.

Figures

Figure 1.

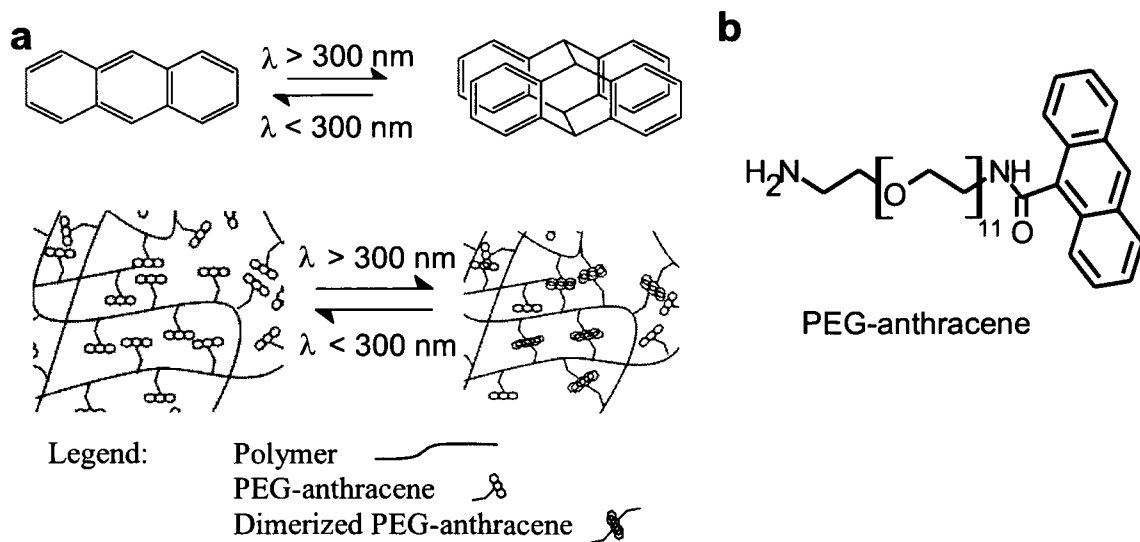


Figure 2.

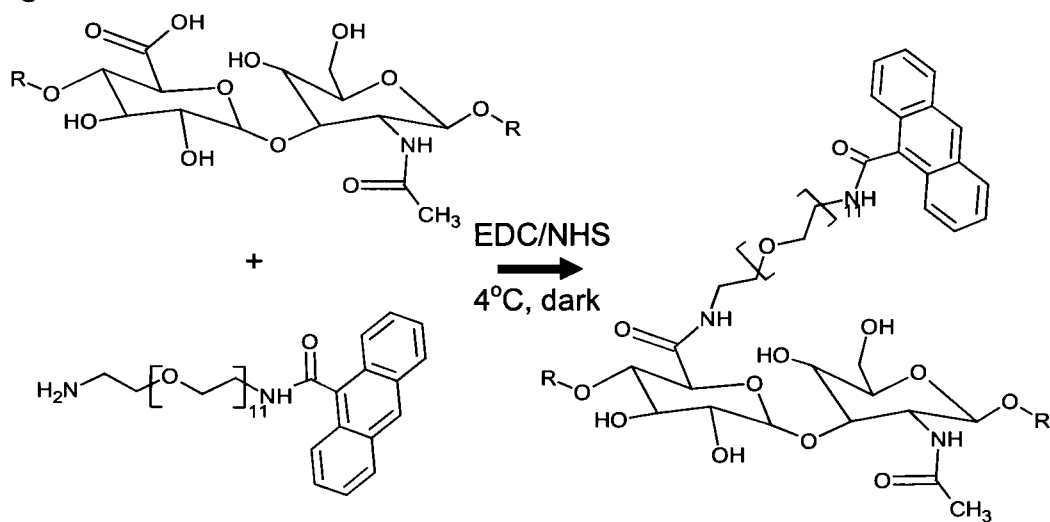
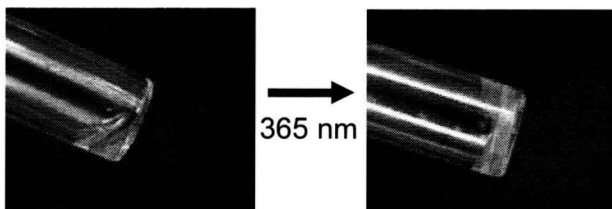
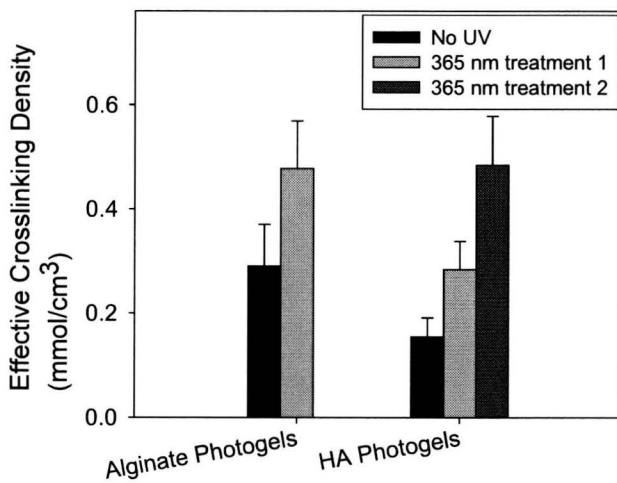


Figure 3.

a



b



c

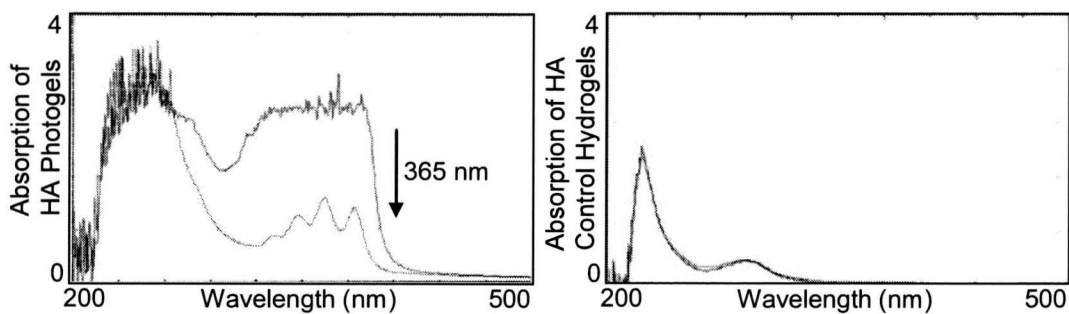


Figure 4.

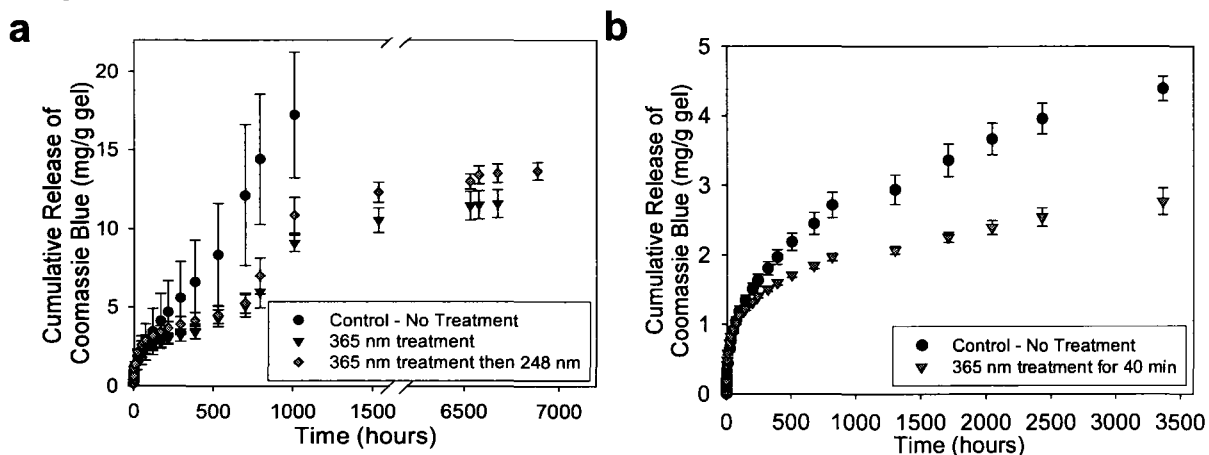


Figure 5.

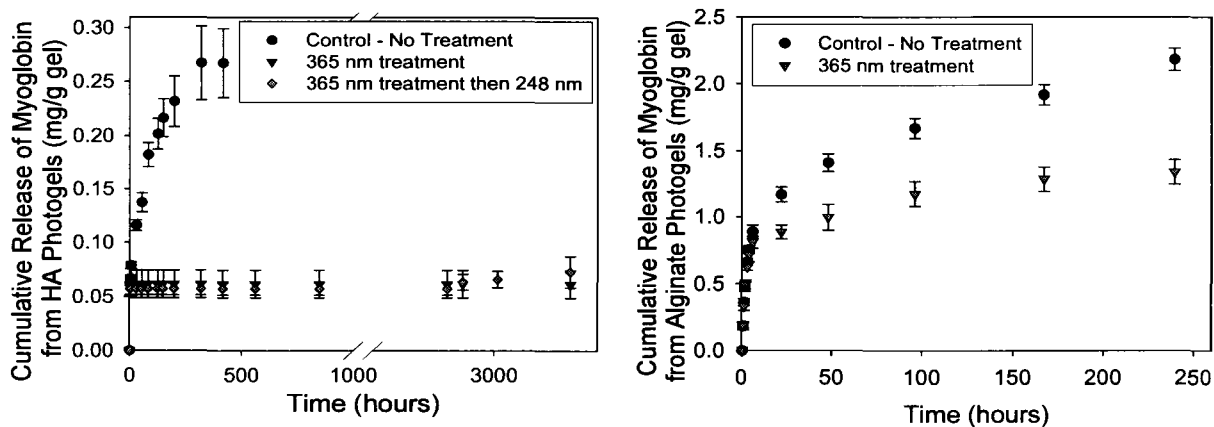
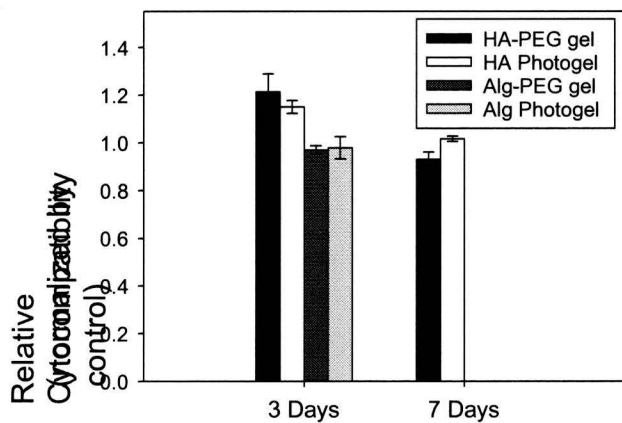


Figure 6.



References

1. Bawa P, Pillay V, Choonara YE, du Toit LC. Stimuli-responsive polymers and their applications in drug delivery. *Biomed Mater* 2009;4:1-15.
2. Youan BC. Chronopharmaceutics: gimmick or clinically relevant approach to drug delivery? *J Control Rel* 2004;98:337-353.
3. Peppas NA, Bures P, Leobandung W, Ichikawa H. Hydrogels in pharmaceutical formulations. *Eur J Pharm Biopharm* 2000;50:27-46.
4. Schmaljohann D. Thermo- and pH- responsive polymers in drug delivery. *Adv Drug Deliver Rev* 2006;58:1655-1670.
5. Qiu Y, Park K. Environment-sensitive hydrogels for drug delivery. *Adv Drug Deliver Rev* 2001;53:321-339.
6. Alvarez-Lorenzo C, Bromberg L, Concheiro A. Light-sensitive intelligent drug delivery systems. *Photochem Photobiol* 2009;85:848-860.
7. Gibson KF, Kernohan WG. Lasers in medicine - a review. *J Med Eng Technol* 1995;17:51-57.
8. Kloxin AM, Kasko AM, Salinas CN, Anseth KS. Photodegradable hydrogels for dynamic tuning of physical and chemical properties. *Science* 2009;324:59-63.
9. Kost J, Langer R. Responsive polymeric delivery systems. *Adv Drug Deliver Rev* 2001;46:125-148.
10. Suzuki A, Tanaka T. Phase transition in polymer gels induced by visible light. *Nature* 1990;346:345-347.
11. Mamada A, Tanaka T, Kungwachakun D, Irie M. Photo-induced phase transition of gels. *Macromolecules* 1990;23:1517-1519.
12. Gorelikov I, Field LM, Kumacheva E. Hybrid microgels photoresponsive in the near-infrared spectral range. *J Am Chem Soc* 2004;126:15938-15939.
13. Irie M, Kunwachakun D. Photoresponsive polymers. 8. Reversible photostimulated dilation of polyacrylamide gels having triphenylmethane leuco derivatives. *Macromolecules* 1986;19:2476-2480.
14. Satyakam P, Sharma AK, Garg BS, Gandhi RP, Gupta KC. Photoregulation of drug release in azo-dextran nanogels. *Int J Pharm* 2007;342:184-193.

15. Andreopoulos FM, Beckman EJ, Russell AJ. Light-induced tailoring of PEG-hydrogel properties. *Biomaterials* 1998;19:1343-1352.
16. Andreopoulos FM, Persaud I. Delivery of basic fibroblast growth factor (bFGF) from photoresponsive hydrogel scaffolds. *Biomaterials* 2006;27:2468-2476.
17. Andreopoulos FM, Beckman EJ, Russell AJ. Photoswitchable PEG-CA hydrogels and factors that affect their photosensitivity. *J Polym Sci Pol Chem* 2000;38:1466-1476.
18. Zheng Y, Micic M, Mello SV, Mabrouki M, Andreopoulos FM, Konka V, Pham SM, Leblanc RM. PEG-based hydrogel synthesis via the photodimerization of anthracene groups. *Macromolecules* 2002;35:5228-5234.
19. Zheng Y, Andreopoulos FM, Micic M, Huo Q, Pham SM, Leblanc RM. A novel photoscissile poly(ethylene glycol)-based hydrogel. *Adv Funct Mater* 2001;11:37-40.
20. Trenor SR, Long TE, Love BJ. Photoreversible chain extension of poly(ethylene glycol). *Macromol Chem Phys* 2004;205:715-723.
21. Trenor SR, Shultz AR, Love BJ, Long TE. Coumarins in polymers: From light harvesting to photo-cross-linkable tissue scaffolds. *Chem Rev* 2004;104:3059-3077.
22. Bouas-Laurent H, Castellan A, Desvergne JP, Lapouyade R. Photodimerization of anthracenes in fluid solutions: (part 2) mechanistic aspects of the photocycloaddition and of the photochemical and thermal cleavage. *Chem Soc Rev* 2001;30:248-263.
23. Kocienski PJ. *Protecting Groups*. 3rd ed. New York: Stuttgart; 2004.
24. Nakajima N, Ikada Y. Mechanism of amide formation by carbodiimide for bioconjugation. *Bioconjugate Chem* 1995;6:123-130.
25. Gilles MA, Hudson AQ, Borders CL, Jr. Stability of water-soluble carbodiimides in aqueous solution. *Anal Biochem* 1990; Feb 1;184(2):244-248.
26. Bray JC, Merrill EW. Poly (vinyl alcohol) hydrogels. Formation by electron beam irradiation of aqueous solutions and subsequent crystallization. *J Apply Polym Sci* 1973;17:3779-3794.
27. Flory PJ, Rehner J. Statistical mechanics of cross-linked polymer networks II. Swelling. *J Chem Phys* 1943;11:521-526.
28. de Jong SJ, van Eerdenbrugh B, van Nostrum CF, Kettenes-van den Bosch JJ, Hennink WE. Physically crosslinked dextran hydrogels by stereocomplex formation of

lactic acid oligomers: degradation and protein release behavior. *J Control Rel* 2001;71:261-275.

29. Leach JB, Bivens KA, Patrick CW, Schmidt CE. Photocrosslinked hyaluronic acid hydrogels: natural, biodegradable tissue engineering scaffolds. *Biotechnol Bioeng* 2003;82:578-89.

30. Amsden B, Turner N. Diffusion characteristics of calcium alginate gels. *Biotechnol Bioeng* 1999;65:605-610.

31. Li CY, Birnkrant MJ, Natarajan LV, Tondiglia VP, Lloyd PF, Sutherland RL, Bunning TJ. Polymer crystallization/melting induced thermal switching in a series of holographically patterned Bragg reflectors. *Soft Matter* 2005;1:238-242.

32. Bradford MM. A rapid and sensitive method for the quantitation of microgram quantities of protein utilizing the principle of protein-dye binding. *Anal Biochem* 1976;72:248-254.

33. Griffith M, Osborne R, Munger R, Xiong X, Doillon CJ, Laycock NLC, Hakim M, Song Y, Watsky MA. Functional human corneal equivalents constructed from cell lines. *Science* 1999;286:2169-2172.

34. Bratschkov C, Karpuzova P, Mullen K, Klapper M. Synthesis and photochemical transformations of an anthracene containing methacrylic copolymer. *Polym Bull* 2001;46:345-349.

35. Jeon O, Song SJ, Lee KJ, Park MH, Lee SH, Hahn SK, Kim S, Kim BS. Mechanical properties and degradation behaviors of hyaluronic acid hydrogels cross-linked at various cross-linking densities. *Carbohydr Polym* 2007;70:251-257.

36. Tomihata K, Ikada Y. Crosslinking of hyaluronic acid with water-soluble carbodiimide. *J Biomed Mater Res* 1997;37:243-251.

37. Liao YH. Hyaluronan: pharmaceutical characterization and drug delivery. *Drug Deliv* 2005;12:327-342.

38. Kuo JW. Practical aspects of hyaluronan based medical products. New York: Taylor and Francis Group CRC; 2006.

39. Garg HG, Hales CA. Chemistry and Biology of Hyaluronan. Oxford UK: Elsevier Ltd; 2004.

40. Erstesvag H, Valla S. Biosynthesis and applications of alginates. *Polym Degrad Stabil* 1998;59:85-91.

41. Augst AD, Kong HJ, Mooney DJ. Alginate hydrogels as biomaterials. *Macromol Biosci* 2006;6:623-633.
42. Wells LA, Sheardown H. Extended release of high pI proteins from alginate microspheres via a novel encapsulation technique. *Eur J Pharm Biopharm* 2007;65:329-335.
43. Hennink WE, van Nostrum CF. Novel crosslinking methods to design hydrogels. *Adv Drug Deliver Rev* 2002;54:13-36.
44. Li CC, Metters AT. Hydrogels in controlled release formulations: Network design and mathematical modeling. *Adv Drug Deliver Rev* 2006;58:1379-1408.
45. Draget KI, Skjak-Braek G, Smidsrod O. Alginate based new materials. *Int J Biol Macromol* 1997;21:47-55.
46. Peppas NA, Lustig SR. The role of cross-links, entanglements, and relaxations of the macromolecular carrier in the diffusional release of biologically active materials. *Ann NY Acad Sci* 1985;446:26-41.
47. Wright CHG, Barrett SF, Welch AJ. Laser-Tissue Interactions. In: Niemz MH, editor. *Medical Applications of Lasers*. Berlin, Germany: Springer-Verlag; 2007. p. 21-56.

4.0 Synthesis and Optimization of Graftable Polyethylene Glycol – Anthracene Macromolecules

Authors: Laura A. Wells, Heather Sheardown

Objectives:

To optimize the synthesis and grafting of PEG-anthracene.

Main Scientific Contributions:

1. The synthesis of PEG-anthracene was varied to obtain high anthracene functionalization and yields. Different sized PEG chains (n=3 and 11) were used and compared for PEG-anthracene synthesis.
2. Different ratios of PEG-diamine and PEG-anthracene were grafted onto alginate to determine their impact on its properties to optimize the gels.
3. Testing of release from initial model gels showed the first potential for these gels to influence release of Coomassie Blue and lysozyme. These model photogels were used as the first proof of concept with studies in Chapter 3 focused on photogels that were further optimized.

**Synthesis and Optimization of Graftable Polyethylene Glycol – Anthracene
Macromolecules**

L.A. Wells¹, M.A. Brook², H. Sheardown^{1*}

Departments of ¹Chemical Engineering and ²Chemistry

McMaster University, 1280 Main St. West, Hamilton ON, L8S 4L7

* to whom correspondence should be addressed sheardown@mcmaster.ca

Abstract

PEG-anthracene is known to introduce photosensitive properties when grafted to hydrogel polymers through its photoinitiated dimerization mechanism. The synthesis of the generic graftable photocrosslinker of two different lengths ($n=3$ and 11) is investigated and compared. 11 unit PEG-anthracene showed better solubility and provided mobility to allow for anthracene dimerization to occur so its synthesis was optimized. The water content of the alginate gels and the grafting density of either PEG-anthracene onto alginate for photogels or PEG-diamine onto alginate for control hydrogels are optimized to obtain gels with good handling properties. Loading and release of Coomassie Blue and lysozyme from alginate photogels show decreases in release with UV light exposure but the different grafting shows lower photosensitivity than photogels in previous studies. The varying grafting densities of PEG-anthracene onto alginate show ability to create both gels and viscous solutions which may be beneficial in the creation of various photosensitive materials.

1. Introduction

Smart biomaterials have potential to allow for the design of drug release and cell scaffold materials that can be altered to suit physiological and disease states. Thermal, pH, ionic, electric and photo mechanisms are examples of internal and external stimuli [1,2] that can be used to induce changes. Reversible photodimerizing molecules may introduce a reversible switching mechanism if effectively incorporated into polymer systems through covalent modifications on the ends or the backbone of the polymer chains. Hydrogels with their high water content resemble natural tissue ideal for creating compatible smart biomaterials [3]. The design of a hydrophilic, universal, reversible photocrosslinker that can be incorporated into these high water content systems is critical in the development of photoreversible hydrogels.

Anthracene is a known photodimerizing molecule whose detailed photochemistry has been investigated since the 1950's [4,5]. Furthermore, it is highly symmetrical making it an ideal starting point for the design of graftable photocrosslinking molecules. Its symmetry makes for predictable monitoring of dimerization with minimal side reactions. The $[4\pi+4\pi]$ photocycloaddition of anthracene is a reductive process forming an ortho-substituted benzene molecule [6] and once dimerized will not absorb light at wavelengths between 300-400 nm making the reaction easy to monitor spectrophotometrically [6]. Since well understood, it is evident that modifications at the ninth carbon will minimally lower its dimerization efficiency with dimerization predominantly occurring in a “head-to-tail” formation [4,5,7] as illustrated in Figure 1.

Anthracene is only soluble in organic solvents; to create an anthracene-hydrogel photoresponsive system anthracene needs to be modified to increase its solubility to allow for miscibility with hydrophilic polymers and buffers. Polyethylene glycol (PEG) is a polyether chain polymer with variable end groups that can be tailored to different molecule weights [8]. Not only can PEG be crosslinked on its own to form matrices [9], PEG chains have also been used in numerous occasions as crosslinkers through the modification of polymers with both ends of the PEG chains. Alginate [10-12], HA [13,14], collagen [15], and chitosan [15,16] are just a few examples of hydrogels that have been crosslinked with PEG to increase their degradation times. Lengthened release of various drugs and proteins has been noted upon crosslinking with PEG chains. For example, PEG modified alginate has shown delivery of Paclitaxel from over 3 weeks [17] and PEG modified thiolated HA has shown delivery of fibroblast growth factor past 35 days [18]. The length of PEG chains used will directly influence the swelling and crosslinking density [11] and therefore diffusion of molecules within the hydrogel matrix; shorter chains for example would be expected to decrease rates of release from crosslinked matrices. PEG has also been extensively used in the modification of biological macromolecules for their stabilization or immobilization using multiple chemistries [8], is soluble in both inorganic buffers and organic solvents and is relatively biologically inert [8]. Therefore, PEG chains well suit the modification of anthracene to allow for its incorporation into hydrophilic systems.

Attempts at modification of polymers with anthracene have mainly focused on direct alteration of hydrophobic polymers. Modification of polystyrene [19,20],

methacrylate [21-23] and polyoxazoline [24] with anthracene have demonstrated some photoresponsiveness. The most promising approach involves direct modification of star-PEG with anthracene to create thin sheets with hydrophobic aggregation that showed some photoresponsiveness [25].

In this study, a graftable anthracene-based soluble macromolecule, that was previously investigated was optimized since it a valuable photocrosslinker that allows for the modification of a variety of polymers with strict control of photosensitivity through modification of grafting density [23]. Two different PEG-anthracene molecules ($n=3$ and 11) were synthesized. As a starting point, PEG₁₁-anthracene was then grafted along the backbone of alginate and the synthesis and grafting conditions of PEG₁₁-anthracene were optimized with gels having high water content. Release of Coomassie blue and lysozyme from photogels created with a 1:1.3 molar ratio of anthracene to alginate carboxyl groups showed changes in release with UV light exposure creating a photoresponsive photogel with crosslinking driven by dimerization/de-dimerization not requiring any initiators or catalysts.

2. Methods

2.1 Materials

O-(2-Aminoethyl)-O'-[2-(Boc-amino)ethyl]decaethylene glycol (boc-PEG-amine), triisopropyl silane (TIPS), 1-ethyl-(dimethylaminopropyl) carbodiimide hydrochloride (EDC), N-hydroxysuccinimide (NHS), *N,N'*-dicyclohexylcarbodiimide (DCC), 4-morpholinoethanesulfonic acid, lysozyme and sodium alginate (MW=12-18

kDa, 61% mannuronic acid, 39% guluronic acid) were purchased from Sigma-Aldrich (Oakville, ON). Coomassie Blue G-250 was from Fluka Chemicals (Switzerland). Anthracene-9-carboxylic acid was purchased from Alfa Aesar (CA). O-(N-Trt-3-aminopropyl)-O'-(3-aminopropyl)-diethyleneglycol (trt-PEG-amine) was from EMD Biosciences through Merck KGaA (Darmstadt, Germany). ^1H NMR spectra were run on a Bruker AV 200. The UV sources were a Curezone II UV lamp (CON-TROL-CURE, Chicago, IL) (365 nm at 400 W, 120 VAC, 60Hz, 8 amps max) and an EL Series UVLS-28 lamp (UVP, Upland, CA) (254 nm at 0.63 mW/cm², 365 nm at 0.5 mW/cm², 8W).

2.2 PEG-anthracene Synthesis

Boc-PEG-amine and smaller trt-PEG-amine are diamine PEG molecules with one end group protected with tert-butoxycarbonyl or triphenylmethyl groups respectively (see Table 1). Boc-PEG-amine or trt-PEG-amine were reacted with anthracene-9-carboxylic acid using EDC in dry dichloromethane (DCM). The reaction proceeded with stirring for 24 hours at room temperature in a nitrogen atmosphere to ensure that the protecting group was not prematurely removed.

The blocking groups from boc-PEG-anthracene or trt-PEG-anthracene were subsequently removed in DCM using trifluoroacetic acid (TFA) [26] with the addition of triisopropyl silane (TIPS) as a scavenger as illustrated in Figure 2. Yields were calculated as the mg actual product/ mg theoretical product.

2.2.1 PEG₃-anthracene Synthesis Details

In 5 mL DCM under nitrogen, 200 mg of trt-PEG-amine was reacted with 48 mg of anthracene-9-carboxylic acid with 33.5 mg of EDC for 48 hours. The reaction solution was dried (rotating evaporator, 40°C under vacuum) then purified by extraction from water into ethyl acetate, then dried again (rotating evaporator, 60°C under vacuum). Deprotection was in 40 mL of DCM using 2 mL of TFA and 4 mL of TIPS. After drying (rotating evaporator, 40°C under pressure), silica columns and TLC with varying DCM and methanol ratios were used for separation. However the PEG₃-anthracene resulted in low yields after purification. Therefore, the focus was shifted towards PEG₁₁anthracene synthesis.

2.2.2 PEG₁₁-anthracene Synthesis

In 20 mL of DCM under nitrogen, 200 mg of boc-PEG₁₁-amine was reacted with 288-3950 mg of anthracene-9-carboxylic acid with 90-322 mg of EDC for 24 hours. The reaction solution was dried (rotating evaporator, 40°C under vacuum) then purified by extraction from water into ethyl acetate, followed by drying (rotating evaporator, 60°C under vacuum). Deprotection was carried out in 16-40 mL of DCM using 2 mL of TFA and 4 mL of TIPS. PEG₁₁-diamine was also synthesized by deprotecting the 100 mg of boc-PEG₁₁-amine by dissolution in 4 mL of DCM with 4 mL of TFA for 24 hours.

Purification was performed as described in Wells *et al.* 2010 [27] by drying the final reaction product, dissolving it in water followed by centrifugation and filtration

through a 0.2 micron filter to remove water insoluble residual anthracene and non-protected PEG. Residual unreacted PEG may be separated out using silica columns as described by Wells *et al.* 2010 by loading using hexane/DCM (1:1 ratio) and adequate separation by run with methanol/DCM (7:3 ratio) [27].

Spectrophotometric analysis was used to verify the dimerization capability of the NH₂-PEG-anthracene in solution after irradiation with 365 nm light by verifying peaks between 330-400 nm disappear after 365 nm UV to indicate dimerization [25].

2.3 Grafting

The available amine group on PEG₁₁-anthracene can be reacted onto the carboxyl group of alginate via carbodiimide chemistry. All reaction solutions were in MES buffer containing 0.1 M 4-morpholinoethanesulfonic acid and 0.5 M NaCl with slight amounts of 1N NaOH to adjust to pH 6 in order to increase the reactivity of EDC [28]. Different NaCl molarity MES solutions have been used in past studies for EDC chemistry with alginate [10,11]. Adipic dihydrazide was used as a model crosslinker to determine the optimal concentration of NaCl which was varied from 0.3 NaCl to 0.5 NaCl; 0.5 NaCl proved optimal grafting creating stronger gels so this concentration was used in all synthesis procedures.

To synthesize the photogels or control PEG hydrogels via grafting of PEG₁₁-anthracene or PEG₁₁-diamine, alginate was premixed with solutions of EDC (394 mg/mL)/NHS (118 mg/mL) for 5 minutes then mixed with PEG₁₁-anthracene/PEG₁₁-diamine and set between two glass plates with a 1 mm spacer for 16 hours at room

temperature. The percent alginate (2-3%) and ratios of alginate carboxyl groups to PEG amine groups were varied until gels with good handling properties were obtained. Photogel synthesis by PEG-anthracene grafting was then optimized by varying the ratio of PEG-anthracene (amine groups) with 3% alginate.

2.4 Release Studies

Photogels created with the PEG₁₁-anthracene (3% alginate, 1:1.3 molar ratio of COOH_{alginate}:NH₂ PEG) and hydrogels made with PEG-diamine were loaded with Coomassie Blue (833 Da) and lysozyme (14,400 Da, pI = 9.3). Loading was by soaking disks (0.5 cm diameter and 0.1 mm thick) in 0.5 mg/mL solutions for 24 hours followed by rinses with PBS. Discs of known weight were then placed in 0.75 mL of phosphate buffered saline (PBS) (0.8 M NaCl, pH 7.4) and released at 37°C. At 1.5 hours, gels were exposed to UV light. Coomassie blue was quantified spectrophotometrically at 595 nm while lysozyme release was measured using the Bradford assay.

3. Results and Discussion

3.1 PEG-anthracene Crosslinker Analysis

Naturally hydrophobic anthracene will not dissolve in aqueous media unless bound to a more hydrophilic moiety such as the water soluble PEG in the current study. PEG₃-anthracene showed low yields and low solubility likely due to the inability of the short PEG to overcome the water insolubility of the anthracene. Therefore the focus in the current work was the PEG₁₁-anthracene macromolecules. With the reaction of the

boc-PEG-amine and anthracene, ^1H NMR peaks appeared at 7.5-8.3 ppm for anthracene and 3.2-3.9 for PEG with substitution monitored by a ratio between the peaks. Any di-substituted PEG (anthracene-PEG-anthracene) was removed during the purification steps due to its insolubility in aqueous media. The deprotection reaction monitored through the disappearance of the Boc singlet at 1.4 ppm; the results indicated that 4-24 hours was adequate for deprotection.

Optimization of the reaction of anthracene-9-carboxylic acid with the longer boc-PEG₁₁-amine was performed by monitoring the anthracene to PEG peak ratio of the final product with ^1H NMR. The molar ratios of anthracene, EDC and Boc-PEG-amine were varied during synthesis. As illustrated in Table 2, reactions with anthracene:EDC:boc-PEG₁₁-amine(NH₂) molar ratios of 4.2:4.5:1 resulted in maximal substitution.

By optimizing the deprotection reaction, the yields could be somewhat increased, although insignificantly, as illustrated in Table 3. The high acidity of the reaction likely degraded some of the final product when run over periods of 24 or more hours.

In recent studies, solubility issues were noted after synthesis when the anthracene was coupled with 8-armed PEG [25] and to gelatin [29]. Presumably due to the linear and highly soluble nature of the PEG chain, the current synthesis method was found to yield very soluble NH₂-PEG-anthracene macromolecules with a reaction procedure that maintained reagent and reactive-intermediate solubility throughout the various required solvents. Anthracene is not expected to become water-soluble unless bound to PEG therefore the presence of the anthracene in the aqueous solutions is indicative of covalent reactions occurring. Past studies by Mikheev *et al.* (2006) have suggested that unbound

PEG can solubilize anthracene in aqueous solution [30]. In a control study, boc-PEG₁₁-amine deprotection in the presence of fresh, unbound anthracene-9-carboxylic acid showed that there was no interaction and that all of the free anthracene was removed by the purification steps based on the absence of peaks in proton NMR and spectrophotometry. It was found that for this series of reactions, covalent attachment to PEG was necessary for the anthracene to become soluble in water.

Spectrophotometric studies verified the ability for the PEG₁₁-anthracene crosslinker to dimerize following exposure to 365 nm light. As the synthesized NH₂-PEG-anthracene is irradiated with 365 nm light, the disappearance of peaks in the 300-400 nm range indicates that anthracene is present on the PEG chain and can dimerize in aqueous solution as shown in Figure 3. Previous studies by Wells *et al.* have demonstrated the ability for PEG₁₁-anthracene to dimerize with 365 nm light and de-dimerize with 254 nm light [27].

3.2 Photogel Synthesis

Grafting of PEG₁₁-diamine (544.68 Da) onto different concentrations of alginate with varying molar ratios of alginate carboxyl groups (COOH_{alg}) to PEG amine groups (NH₂_{PEG}) was performed in order to optimize the system and to obtain gels with good handling properties. Hydrogels with 3 % alginate were used since lowering the amount of alginate clearly reduced the quality of the gels (Table 4) likely due to the reduction of entanglements which may act to increase crosslinking. Low alginate concentrations may however offer the potential for future development of injectable, photogelling materials.

The synthesis of 3% photogels was optimized for the grafting of PEG₁₁-anthracene. The ratios of COOH_{alg} to NH₂ PEG-anthracene were altered with two ratios described in Table 5 forming gels with good handling properties. For release studies, a 1:1.3 molar ratio gel was used as a starting point to assess changes in properties that may occur with UV treatments in release studies.

3.3 Release Studies

Model compounds, Coomassie blue and lysozyme, were loaded and released to test the responsiveness of photogels of alginate and PEG₁₁-anthracene made with a 1:1.3 COOH_{alg}:NH₂ PEG-anthracene ratio. When grafted along the backbone of alginate, the PEG₁₁-anthracene introduced slight UV responsiveness with slight slowing of release (p=0.51). Illustrated in Figure 4 is Coomassie Blue release from photogels with and without UV treatments versus a control crosslinked with PEG₁₁-diamine. Control PEG hydrogels show a slower release of Coomassie blue since they are fully crosslinked versus the partially crosslinked photogels. All gels effectively sustained the release of Coomassie blue for over 60 hours.

Lysozyme release (Figure 5) showed slight changes with UV exposure that resulted in slowing of release at 56 hours (p=0.364). The control PEG hydrogels made with PEG₁₁-diamine with 2 different grafting synthesis molar ratios of 1:2.2 and 1:3.8 both released their contents by 20 hours. However the PEG₁₁-anthracene photogels showed extended release past 150 hours demonstrating their capability to act as sustained

release gels. The longer release times of lysozyme from the photogels may be due to interactions between the anthracene groups and the protein.

The photogels prepared with a grafting ratio of 1:1.3 demonstrated slightly altered release of Coomassie blue and lysozyme with UV light treatment. An important aspect of anthracene dimerization when it is bound to large molecules on its ninth carbon is its mobility to align for photochemical reactions. For the grafting of PEG-anthracene, the PEG chains must still be long enough to allow adequate mobility for dimerization [22] in addition to being present at high enough densities for interactions to allow dimerization to occur [22]. With $n=11$ units, the PEG was found to demonstrate enough flexibility for anthracene dimerization after grafting but remained sufficiently short to for changes in gel properties to occur upon photocrosslinking. The liquid content of the gels, which is approximately 97%, may also play an important role since liquid allows for the movement and alignment of anthracene [25]. Since PEG is soluble in both inorganic buffers and organic solvents, the resulting anthracene macromolecule may then be grafted into both types of systems.

Other published release studies of photogels made from 1:0.84 molar ratios of alginate carboxyl groups to PEG₁₁-anthracene demonstrated the ability to cause greater changes in release as described by Wells *et al.* 2010 [27]. It is possible that gels made with 1:1.3 COOH_{alg}:NH₂ PEG-anthracene ratios had excess PEG-anthracene within the gels so when dimerization occurred, the free PEG-anthracene would dimerize with grafted PEG-anthracene resulting in dimerization without changes in gel crosslinking and release.

4. Conclusions

PEG-anthracene was synthesized and is a valuable molecule for introducing photosensitive properties to alginate upon grafting along the bulk polymer backbone. PEG₁₁-anthracene grafted with COOH_{alg}:NH₂ PEG-anthracene ratios of 1:1.3 and 1:0.84 created gels. Altering the percent alginate or grafting ratio can create viscous liquids which may be useful for the development of injectable *in situ* polymerizable materials in future studies. Grafting of PEG₁₁-anthracene in a theoretical 1:1.3 ratio to alginate introduced some photosensitivity to the release of small and large molecules whereas previous studies with lower grafting demonstrate that PEG₁₁-anthracene can more effectively introduce photosensitivity. The PEG chains provide adequate mobility for efficient dimerization to occur. Future studies will focus on lower grafting of PEG₁₁-anthracene onto alginate since it seems that excess photocrosslinker may interfere with the crosslinking process lowering the overall changes in gel properties with UV light. PEG₁₁-anthracene synthesis was effectively optimized and will be used in further studies involving the synthesis of photogels with the grafting of universal PEG-anthracene to multiple polymer systems.

Legends

Tables

Table 1. The two types of protected PEG-diamines that were investigated.

Table 2. Anthracene binding to boc-PEG₁₁-amine was dependent on ratios of the anthracene-9-carboxylic acid groups, the EDC and the PEG-amine groups. A molar ratio of 4.2:4.5:1 of anthracene:EDC:PEG produced high amounts of incorporation with low amounts excess reagents.

Table 3. The volume of DCM and time were varied for the deprotection of boc-PEG₁₁-anthracene.

Table 4. Optimization of PEG-amine hydrogels by varying percent alginate and COOH:NH₂ ratios. Note that the ratio of COOH_{alg}:EDC is 1:2.4 in every case.

Table 5. Optimization of PEG-anthracene photogels by varying the COOH:NH₂ ratios. Note that the ratio of COOH_{alg}:EDC is 1:2.4 in every case.

Figures

Figure 1. Anthracene dimerization with a generic substitution on the ninth carbon. Dimerization occurs predominantly in the “head-to-tail” formation.

Figure 2. After anthracene-9-carboxylic acid is substituted on the boc-PEG-amine or trt-PEG-amine via amide bond formation using EDC, the protecting groups are removed by TFA using TIPS as a scavenger.

Figure 3. Spectrophotometer scans of PEG-anthracene before and after irradiation of 365nm (0.5mW/cm²). Note the peaks between 300-400nm diminish as the molecule absorbs less light at these wavelengths after dimerization.

Figure 4. Release of Coomassie blue from alginate grafted with PEG₁₁-anthracene (photogels) made with a 1 : 1.3 molar ratio and control PEG hydrogels crosslinked with PEG₁₁diamine. Release was into 0.75 mL of PBS buffer of pH 7.4 at 37°C, with UV of one group of photogels at t=1.5 hours.

Figure 5. Release of lysozyme from (A) control PEG hydrogels crosslinked with PEG₁₁diamine and (B) PEG₁₁-anthracene crosslinked alginate photogels. Release was into 0.75 mL of PBS buffer of pH 7.4 at 37°C, with UV of one group of photogels at t=1.5 hours.

Tables

Table 1.

| Name | Source | MW | Protecting group | PEG units (n=) | |
|---|--------------------------------|-------------------|------------------|---------------------|----|
| O-(2-Aminoethyl)-O'-[2-(Boc-amino)ethyl]decaethylene glycol | Boc-PEG ₁₁ -diamine | Sigma-Aldrich | 644.79 | tert-butoxycarbonyl | 11 |
| O-(N-Trt-3-aminopropyl)-O'-(3-aminopropyl)-diethyleneglycol | Trt-PEG ₃ -diamine | Novabiochem (EMD) | 462.62 | triphenylmethyl | 3 |

Table 2.

| Molar Ratios | | | NMR Integration | Percent Substitution |
|------------------------------|-----|---------------|-----------------|----------------------|
| Anthracene-9-carboxylic acid | EDC | Boc-PEG-amine | | |
| 5.6 | 4.5 | 1 | 0.42 | 84% |
| 4.2 | 4.5 | 1 | 0.43 | 86%* |
| 4.2 | 4.5 | 1 | 0.37 | 74%** |
| 6.7 | 4.5 | 1 | 0.33 | 66% |
| 6.7 | 5.4 | 1 | 0.19 | 38% |
| 1.9 | 1.5 | 1 | 0.18 | 35% |

* Reaction time 24 hours ** Reaction time 48 hours

Table 3.

| DCM mL | Deprotection time (hours) | Average yield |
|--------|---------------------------|---------------|
| 40 | 24 | 82.0 ± 4.9 |
| 16 | 24 | 83.4 ± 3.5 |
| 16 | 4 | 87.1 ± 8.7 |

Table 4.

| Percent Alginate (w/v) | COOH _{alg} :NH ₂ PEG ratio | Properties |
|------------------------|--|----------------|
| 3% | 1 : 3.8 | Bubbly gel |
| 3% | 1 : 1 | Bubbly gel |
| 3% | 1 : 2.2 | Gel |
| 2.6% | 1 : 2.2 | Loose gel |
| 2% | 1 : 2.2 | Viscous liquid |

Table 5.

| Percent Alginate | COOH _{alg} :NH ₂ PEG-anthracene ratio | Properties |
|------------------|---|----------------|
| 3% | 1 : 1.9 | Viscous liquid |
| 3% | 1 : 1.6 | Loose gel |
| 3% | 1 : 1.3 | Gel |
| 3% | 1 : 0.84 | Gel |

Figures

Figure 1.

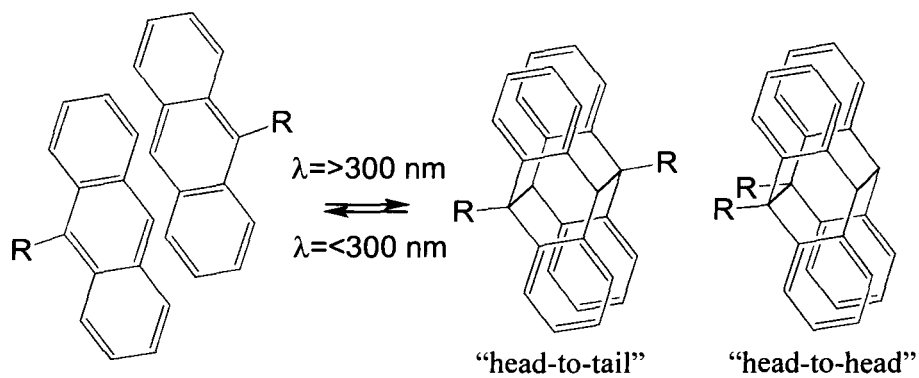


Figure 2.

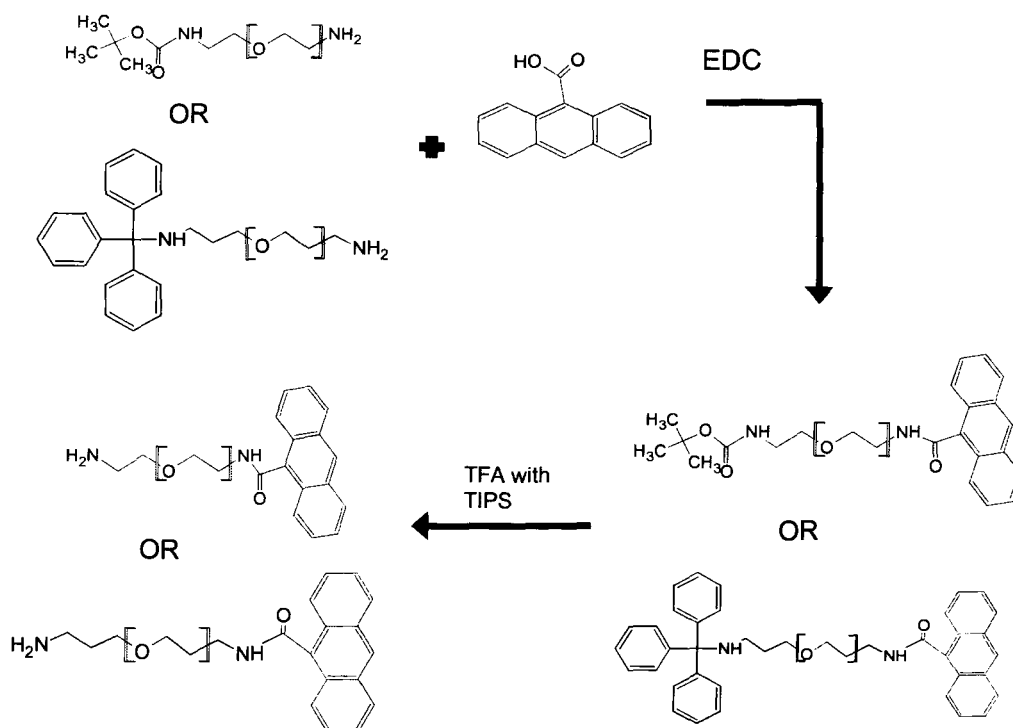


Figure 3.

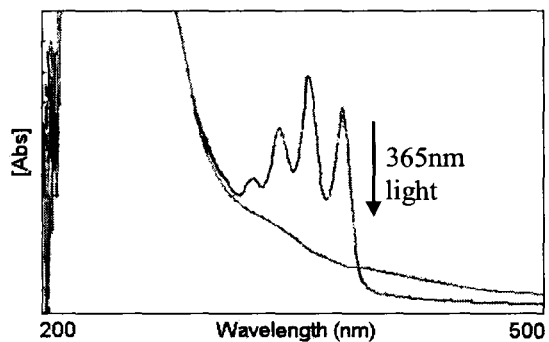


Figure 4.

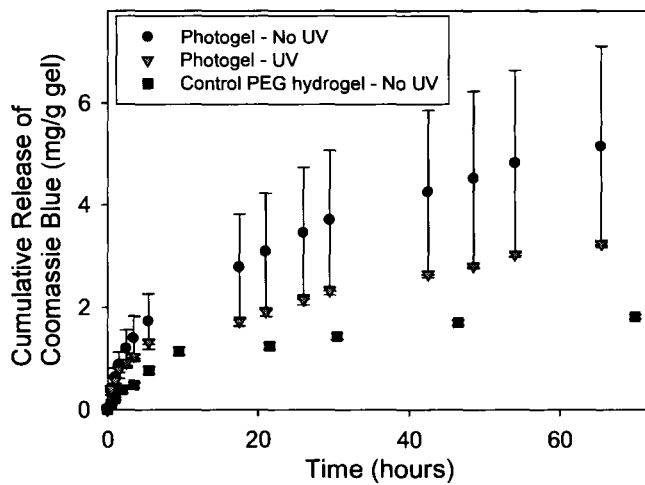
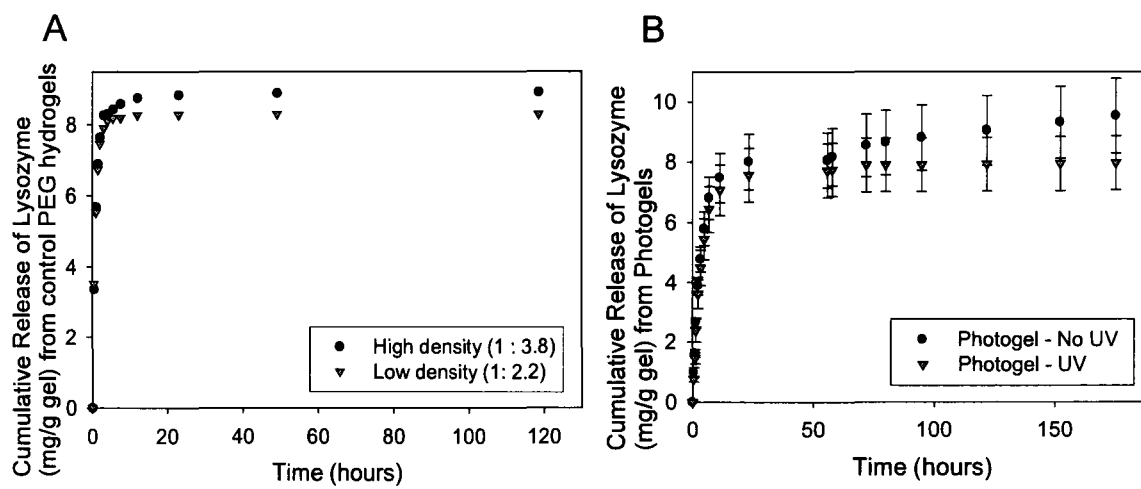


Figure 5.



References

1. Bawa P, Pillay V, Choonara YE, duToit LC. Stimuli-responsive polymers and their applications in drug delivery. *Biomed Mater* 2009;4:1-15.
2. Qiu Y, Park K. Environment-sensitive hydrogels for drug delivery. *Adv Drug Deliver Rev* 2001;53:321-339.
3. Peppas NA, Bures P, Leobandung W, Ichikawa H. Hydrogels in pharmaceutical formulations. *Eur J Pharm Biopharm* 2000;50:27-46.
4. Greene FD, Misrock SL, Wolfe JRJ. The structure of anthracene photodimers. *J Am Chem Soc* 1955;77:3852-3855.
5. Bouas-Laurent H, Castellan A, Desvergne JP, Lapouyade R. Photodimerization of anthracene in fluid solution: structural aspects. *Chem Soc Rev* 2000;29:43-55.
6. Bouas-Laurent H, Castellan A, Desvergne JP, Lapouyade R. Photodimerization of anthracenes in fluid solutions: (part 2) mechanistic aspects of the photocycloaddition and of the photochemical and thermal cleavage. *Chem Soc Rev* 2001;30:248-263.
7. Bouas-Laurent H, Castellan A, Desvergne JP. From anthracene photodimerization to jaw photochromic materials and photocrowns. *Pure & Appl Chem* 1980;52:2633-2648.
8. Roberts MJ, Bentley MD, Harris JM. Chemistry for peptide and protein PEGylation. *Adv Drug Deliver Rev* 2002;54:459-476.
9. Lin C, Anseth K. PEG hydrogels for the controlled Release of biomolecules in regenerative medicine. *Pharm Res* 2009;26:631-643.
10. Eiselt P, Lee KY, Mooney DJ. Rigidity of two-component hydrogels prepared from alginate and poly(ethylene glycol)-diamines. *Macromolecules* 1999;32:5561-5566.
11. Lee KY, Rowley JA, Eiselt P, Moy EM, Bouhadir KH, Mooney DJ. Controlling mechanical and swelling properties of alginate hydrogels independently by cross-linker type and cross-linking density. *Macromolecules* 2000;33:4291-4294.
12. Mahou R, Wandrey C. Alginate–poly(ethylene glycol) hybrid microspheres with adjustable physical properties. *Macromolecules* 2010;43:1371-1378.
13. Leach JB, Schmidt CE. Characterization of protein release from photocrosslinkable hyaluronic acid-polyethylene glycol hydrogel tissue engineering scaffolds. *Biomaterials* 2005;26:125-135.

14. Segura T, Anderson BC, Chung PH, Webber RE, Shull KR, Shea LD. Crosslinked hyaluronic acid hydrogels: a strategy to functionalize and pattern. *Biomaterials* 2005;26:359-371.
15. Rafat M, Li F, Fagerholm P, Lagali NS, Watsky MA, Munger R, Matsuura T, Griffith M. PEG-stabilized carbodiimide crosslinked collagen–chitosan hydrogels for corneal tissue engineering. *Biomaterials* 2008;29:3960-3972.
16. Kulkarni AR, Hukkeri VI, Sung H, Liang H. A novel method for the synthesis of the PEG-crosslinked chitosan with a pH-independent swelling behavior. *Macromol Biosci* 2005;5:925-928.
17. Livnat M, Beyar R, Seliktar D. Endoluminal hydrogel films made of alginate and polyethylene glycol: Physical characteristics and drug-eluting properties. *J Biomed Mater Res* 2005;75A:710-722.
18. Cai S, Liu Y, Zheng Shu X, Prestwich GD. Injectable glycosaminoglycan hydrogels for controlled release of human basic fibroblast growth factor. *Biomaterials* 2005;26:6054-6067.
19. Coursan M, Desvergne JP. Reversible photodimerization of w-anthrylpolystyrenes. *Macromol Chem Phys* 1996;197:1599-1608.
20. Goldbach JT, Russell TP, Penelle J. Synthesis and thin film characterization of poly(styrene-*block*-methyl methacrylate) containing an anthracene dimer photocleavable junction point. *Macromol* 2002;35:4271-4276.
21. Ishii T, Tezuka Y, Kawamoto S, Uno T. Photodecomposition of copolymers between 9-anthrylmethylmethacrylate and methymethacrylate by XeF excimer laser irradiation. *Journal of Photochemistry & Photobiology, A: Chemistry* 1994;83:55-62.
22. Bratschkov C, Karpuzova P, Mullen K, Klapper M. Synthesis and photochemical transformations of an anthracene containing methacrylic copolymer. *Polymer Bulletin* 2001;46:345-349.
23. Ide N, Tsujii Y, Fukuda T, Miyamoto T. Gelation processes of polymer solutions. 1. Photodimerization of free and polymer-bound anthryl groups. *Macromolecules* 1996;29:3851-3856.
24. Chujo Y, Sada K, Nomura R, Naka A, Saegusa T. Photogelation and redox properties of anthracene-disulfide-modified polyoxazolines. *Macromolecules* 1993;26:5611-5614.

25. Zheng Y, Micic M, Mello SV, Mabrouki M, Andreopoulos FM, Konka V, Pham SM, Leblanc RM. PEG-based hydrogel synthesis via the photodimerization of anthracene groups. *Macromol* 2002;35:5228-5234.
26. Kocienski PJ. *Protecting groups*. 3rd ed. NY: Stuttgart, 2004.
27. Wells LA, Brook MA, Sheardown H. Graftable PEG-Anthracene to Generate Photoresponsive Hydrogels for Drug Delivery . Submitted to the *Journal of Biomedical Materials Research Part A*;2010.
28. Gilles MA, Hudson AQ, Borders CL,Jr. Stability of water-soluble carbodiimides in aqueous solution. *Anal Biochem* 1990;184:244-248.
29. Gattas-Asfura KM, Weisman E, Andreopoulos FM, Micic M, Muller B, Sirpal S, Pham SM, Leblanc RM. Nitrocinnamate-functionalized gelatin: synthesis and "smart" hydrogel formation via photo-cross-linking. *Biomacromol* 2005;6:1503-1509.
30. Mikheev YA, Guseva LN, Davydov EY, Ershov YA. The thermodynamic and structural rules governing the solubilization of anthracene in aqueous solutions of polyethylene oxide. *Russ J Phys Chem* 2006;80:841-851.

5.0 Controlled Release with Polyethylene Glycol – Anthracene Modified Alginate

Authors: Laura A. Wells, Heather Sheardown

Publication Information: Submitted to the European Journal of Pharmaceutics and Biopharmaceutics.

Objectives: To thoroughly investigate the release of model drugs from alginate photogels. Different model compounds, formulations and exposure times were compared with PEG crosslinked and physically crosslinked alginate gels as controls.

Main Scientific Contributions:

1. Thorough investigations into the release properties of Coomassie Blue or Fast Green from alginate photogels with varying UV light exposures.
2. The interaction between loaded molecules and the photogels was investigated by effective crosslink density with and without loading versus release results.
3. Release from different formulations with different resulting photosensitivities and controls gels were compared to verify the observed effects of UV on the photogels. Diffusion coefficients were calculated to allow the direct comparison of different systems.

Controlled Release with Polyethylene glycol - Anthracene Modified Alginate

LA Wells and H Sheardown*

Department of Chemical Engineering

McMaster University, Hamilton ON Canada

*** to whom correspondence should be addressed**

sheardow@mcmaster.ca

Department of Chemical Engineering, JHE 374

McMaster University

1280 Main Street West

Hamilton, Ontario, Canada

L8S 4L8

Phone: 905-525-9140 x. 24794

Fax: 905-521-1350

Abstract

Covalent modification of alginate with polyethylene glycol conjugated anthracene molecules has the potential to both stabilize the alginate and act as a photosensitive crosslinker. Release studies with Coomassie Blue show lengthy release times from the alginate photogels that extend past 70 days with, for example, 17 % versus 27 % release at 1750 hours (73 days) for photogels with and without 365 nm UV light treatment for 30 minutes at $10\text{mW}/\text{cm}^2$ in the initial release period. Photocrosslinking of the photogels after loading effectively “locks” in drug compounds to control their release. Effective crosslinking densities and controls of polyethylene glycol-crosslinked alginate and physically crosslinked calcium alginate gels suggest strong interactions between Coomassie Blue and both alginate and anthracene. Photogels containing anthracene-capped star-polyethylene glycol show increased photosensitivity with modified release profiles. Ultimately, the covalent modification of alginate with photoactive crosslinkers has the potential to create a long-term, photosensitive, controlled release system.

Keywords

alginate; photoresponsive; anthracene; drug delivery; smart biomaterials

Abbreviations

PEG: polyethylene glycol

Photogel: PEG-anthracene grafted alginate

Control PEG hydrogel: PEG-diamine crosslinked alginate

Boc-PEG-amine: O-(2-Aminoethyl)-O'-[2-(Boc-amino)ethyl]decaethylene glycol

PEG-diamine: O,O'-Bis(2-aminoethyl)octadecaethylene glycol

EDC: 1-ethyl-(dimethylaminopropyl) carbodiimide hydrochloride

NHS: N-hydroxysuccinimide

MES: 4-morpholinoethanesulfonic acid

PBS: phosphate buffered saline

TBS: TRIS-buffered saline

UV: ultraviolet

1. Introduction

Alginate is a non-toxic, inert and hydrophilic polymer conducive to the storage and delivery of active proteins, drugs and cells [1,2]. Composed of linear copolymers of β -D-mannuronic and α -L-guluronic acid, alginate is generated by renewable resources such as kelp, algae and bacteria [1,3]. While commonly used physically crosslinked with divalent ions such as calcium, these gels can have weak mechanical properties and uncontrolled degradation kinetics since ions and chelators in solution can lead to their rapid dissolution [4]. Research has focused on the modification of alginate to produce stable, long-term delivery devices [2,4].

The reinforcement of calcium alginate microspheres with oppositely charged materials such as chitosan [5], poly-L-lysine [6,7] and dipalmitoyl phosphatidylcholine liposomes [8] are but a few examples of how researchers have tried to reinforce alginate to control drug delivery from microcapsules and gels. However, covalent modifications along the backbone of the polymer can stabilize the gel matrix and control pore-size to specifically control drug delivery [9]. There are several examples of covalent crosslinking of alginate to improve its mechanical and drug delivery properties using crosslinkers such as albumin [10], polyethylene glycol (PEG) [11,12], lysine [12], adipic dihydrazide [12], glutaraldehyde [13] or peptides that cause cellular crosslinking [14]. Hydrophobic modifications in particular have shown great promise in stabilizing the matrix and increasing the release times of various proteins and drugs [9,15-18]. These materials have increased release times versus calcium alginate controls and their

swelling/crosslinking properties can be altered with changes in grafting density and changes in the size of the crosslinking molecules [12].

Covalent modification of alginate with stimuli-sensitive molecules cannot only further improve its stability but also introduce other responsive properties to create smart gels. Alginate has already shown natural pH-sensitive properties in past studies with lower release times in lower pH buffers [19,20] making it well suited to oral delivery where gastric and intestinal fluids have varied pHs. However, pH does not typically vary significantly *in vivo* so the use of other stimuli may be more relevant. Recent examples show the ability for the grafting of or creation of interpenetrating networks of alginate with poly(N-isopropyl acrylamide) or hydroxypropyl cellulose to create thermosensitive drug delivery systems [21,21,22].

In our lab, where the focus is delivery of drugs to the eye, light has been targeted as a potential drug release stimulus. To produce stimuli-responsive hydrogels which respond to UV light and lasers, we have covalently modified hydrogels with a PEG-anthracene based graftable photocrosslinker [23] (see Figure 1) that has shown promise for the introduction of photosensitive properties to hydrogel polymers including alginate. Anthracene photodimerizes with other anthracene molecules upon exposure to 365 nm light and dedimerizes with 254/248 nm light treatment in a reversible reaction which causes crosslinking and potentially de-crosslinking when grafted along the backbone of

polymers. Alginate covalently linked to PEG-anthracene crosslinkers has been previously demonstrated to generate gels which respond light treatment.

Herein we report on the properties of PEG-anthracene grafted alginate “photogels”. Not only do these gels deliver over lengthy periods beyond 2000 hours, but different light treatment times, different model release compounds and different formulations can be used to alter the release characteristics of the photoresponsive alginate. Furthermore, this technique has the potential for loading of the photogels and locking the drug in place following loading with exposure to UV light.

2. Materials and Methods

2.1 Materials

Sodium alginate (61% β -D-mannuronic acid, 39% α -L-guluronic acid, MW=12-18 kDa, from *Macrocystis pyrifera*), O-(2-Aminoethyl)-O'-[2-(Boc-amino)ethyl]decaethylene glycol (Boc-PEG-amine, n=11), O,O'-Bis(2-aminoethyl)octadecaethylene glycol (PEG-diamine, n=20) and N-(3-dimethylaminopropyl)-N'-ethylcarbodiimide hydrochloride (EDC) were purchased from Sigma-Aldrich (Oakville, ON). Anthracene-9-carboxylic acid was from Alfa Aesar (CA). Coomassie Blue G-250 was purchased from Fluka Chemicals (Switzerland). Anthracene-terminated four-arm poly(ethylene oxide) made with a pentaerythritol core (star-PEG-anthracene) of 9500 Da (polydispersity of 1.15) with over 90% functionality was purchased from Polymer Source (Quebec). Fast Green and other reagents were purchased from Sigma-Aldrich (Oakville, ON) and EM Science

(Gibbstown, NJ). NMR spectra were obtained with a Bruker AV 200. The 365 nm lamp source was a 10 mW/cm² Curezone II UV lamp from CON-TROL-CURE (Chicago, IL) (400 W, 60Hz) and the 254 nm source (0.63mW/cm²) was an EL Series UVLS-28 UV lamp from UVP (Upland, CA) (8 W).

2.2 PEG-anthracene Crosslinker

Amine terminated PEG-anthracene molecules of molecular weight 748.9 g/mol are soluble, graftable universal photocrosslinkers that may be bound to different polymer backbones. As described in detail by Wells *et al.* 2010, they are created through the reaction of Boc-PEG-amine to anthracene-9-carboxylic acid followed by deprotection in trifluoroacetic acid with triisopropylsilane as a scavenger [23]. Specifically, under dark conditions, 200 mg of Boc-PEG-amine was reacted with 288 mg of anthracene-9-carboxylic acid with 268 mg of EDC in 20 mL of dry dichloromethane (DCM) under nitrogen. After removing unreacted reagents and side-products by extraction from water into ethyl-acetate, the protecting group was removed in 20 mL of DCM by 4 ml of trifluoroacetic acid with 2 mL of triisopropylsilane as a scavenger followed by purification with filtration or silica columns.

2.3 Hydrogel Synthesis

2.3.1 Photogels

As depicted in Figure 1 and as previously described [23], the amine group on the PEG-anthracene molecules was reacted to the carboxyl groups on the alginate. 6% alginate

was premixed with EDC (394 mg/mL) and N-hydroxysuccinimide (NHS) (118 mg/mL) which was then mixed with amine-terminated PEG-anthracene (428 mg/mL). The mixture was then placed between two glass plates using a 1 mm spacer and allowed to react for 16 hours at room temperature. All solutions were in 4-morpholinoethanesulfonic acid (MES) buffer at pH 6 (0.1 M MES and 0.5 M NaCl with 1N NaOH to pH 6) to promote EDC activity [24]. The COOH:EDC:NHS was at a molar ratio of 0.8:2:1. Per mL of 6% alginate, 0.443 mL of PEG-anthracene and 0.354 mL of EDC/NHS solution was added to obtain a ratio of PEG-anthracene to carboxyl groups on the alginate polymer backbones of 0.84:1. Previous work showed that under these conditions, the average grafting efficiency was 50%. In this case, the resulting gels had 42% grafting of PEG-anthracene [23]. The photogels were punched into disks 0.5 cm in diameter, soaked in de-ionized water overnight then dried at room temperature for 72 hours. Degradation via hydrolysis and decrosslinking was monitored with gel disks soaking in PBS buffer at 37°C under shaking. ¹³C NMR studies were performed on photogels crosslinked in quartz NMR tubes with and without UV light treatments to observe any changes in the carbon bonds.

2.3.2 Control PEG Hydrogels

Hydrogels made from alginate covalently crosslinked with PEG-diamine were used as controls. Note that in this case, a bifunctional PEG molecule which can bind to the alginate backbone at both ends was used. The same procedure as with the photogels was used except in this case, either 3 unit or 20 unit amine-terminated PEG molecules (PEG-

diamine) were grafted in a 1:1 amine to carboxyl molar ratio. The resulting control PEG hydrogels were punched into disks 0.5 cm in diameter, soaked in de-ionized water overnight then dried at room temperature for 72 hours.

2.3.3 High Alginate Concentration Photogels

To create photogels with a higher concentration of alginate, the same synthesis procedure as with the photogels was used except 12% alginate was substituted for the 6% alginate solution. The resulting high concentration alginate photogels were punched into disks 0.5 cm in diameter, soaked in de-ionized water overnight then dried at room temperature for 72 hours.

2.3.4 Calcium Alginate Gels and Calcium Reinforced Photogels

As an additional control, alginate gels crosslinked with calcium were prepared. To make these gels, approximately 0.1 mL of 3% alginate in water was placed between two glass plates with a 1 mm spacer. 0.1 M calcium chloride was then injected into the surrounding space and the solution was allowed to gel for 4 hours. At this time, the gels were punched and soaked in 0.1 M calcium chloride for 16 hours to ensure complete crosslinking.

Calcium-reinforced photogels were created by soaking water-swollen photogels in 0.1 M calcium chloride for 16 hours to allow calcium ions to diffuse and reinforce any unbound guluronate blocks with physical crosslinks.

2.3.5 Star-PEG-Anthracene Containing Photogels

During photogel synthesis, star-PEG-anthracene was incorporated by dissolving it into the initial PEG-anthracene solution followed by addition into the reactive solution of alginate and EDC/NHS. The anthracene molar ratio of grafted PEG-anthracene to star-PEG-anthracene was 10:1. To prepare these gels, 1 mL of 6 % alginate was mixed with 0.443 mL of PEG-anthracene, 0.354 mL of EDC/NHS solution and 60 mg of star-PEG-anthracene. The mixture was then gelled at 4°C for 72 hours. The resulting star-PEG-anthracene containing photogels were punched into disks 0.5 cm in diameter, soaked in de-ionized water overnight and subsequently dried at room temperature for 72 hours.

2.4 Drug Loading

Dried hydrogel disks were individually soaked in 1 mL of a 0.5 mg/mL solution of Coomassie Blue or Fast Green as model drugs in phosphate buffered saline (PBS) for 24 hours. The disks were then rinsed twice and soaked for 30 minutes prior to the release studies in order to remove any residual, loosely associated model compounds. Loading of the calcium alginate gels and the calcium-reinforced photogels was with pre-swollen gels in 0.5 mg/mL of Coomassie Blue in TRIS-buffered saline (TBS) for 24 hours followed by the described rinse procedure. TBS was selected for this loading procedure as it will have lower calcium alginate degradation rates than PBS since it has a lower sodium concentration, that remove and replace calcium, and it lacks calcium-binding phosphate ions. Drying was avoided to maintain the properties of the physical gels. Loading was estimated through solution depletion measurements. The UV absorbance of the soaking

solution remaining following loading was measured and compared to that of the initial solution to estimate the quantity of Coomassie Blue or Fast Green loaded into the hydrogel disks.

2.5 Effective Crosslinking Density

To assess potential interactions of the loaded model compounds with alginate, effective crosslinking densities of the gels were monitored with and without loading. Dry and swollen or loaded gel masses and polymer/liquid densities were used to calculate the volumetric polymer fraction at maximum swelling ($\nu_{2,s}$) and the volumetric polymer fraction in a relaxed state ($\nu_{2,r}$) which were used in the Flory-Rehner equation as modified by Bray and Merrill (equation 1) to determine the average molecular weight between crosslinks (M_c) of hydrogels crosslinked in solution [25-27].

$$\frac{1}{M_c} = \frac{2}{M_n} - \frac{(\bar{\nu}/V_1)[\ln(1 - \nu_{2,s}) + \nu_{2,s} + \chi_1(\nu_{2,s})^2]}{\nu_{2,r}[(\nu_{2,s}/\nu_{2,r})^{1/3} - 0.5(\nu_{2,s}/\nu_{2,r})]} \quad (1)$$

The known variables for calculating M_c are the molar volume of solvent ($V_1 = 18$ mol/cm³), the specific volume of dry polymer ($\nu = 0.60$ cm³/g alginate [28] and 0.89 g/cm³ for PEG [29]), the Flory polymer-solvent interaction parameter ($\chi = 0.473$ for alginate [30] and PEG [29]) and the average molecular weight of the polymer ($M_n = 46,000$ g/mol). The effective crosslinking density was then determined by dividing the density of alginate by M_c with and without loading.

2.6 Release Studies

The model drugs Coomassie Blue and Fast Green were released into PBS (pH=7.4) in a shaking water bath at 37°C and the buffer was periodically removed and replaced. Releasate concentrations were measured spectrophotometrically at 595 nm for Coomassie Blue and 630 nm for Fast Green. At 1.5 hours, some of the hydrogels were irradiated in PBS with 365 nm light for specified treatment times ranging from 10 to 40 minutes and compared to controls which had no UV treatment. Percent release was calculated using the measured loading in the individual gels. Two tailed t-tests were used to assess significant differences in release with and without UV treatments. To ensure that the absorbance of the Coomassie Blue and Fast Green were not altered by UV exposure, control solutions were irradiated and their absorption profile was noted to remain constant.

2.7 Diffusion Exponents and Coefficients

Diffusion exponents and coefficients were calculated and compared for the various gel systems before and after UV treatment. In the early stage of release when the release ratio M_t/M_∞ is under 0.6, according to the Ritger and Peppas model [31], release is dependent on $M_t/M_\infty=kt^n$, where M_t and M_∞ are released amounts at time t and at infinite time and n is the diffusion exponent which is indicative of the type of transport. The disks were treated as slabs since their diameter was over 4 times that of their thickness [32]. The diffusion coefficient (D) can be calculated from equation 2 using regression for Fickian release. In this case, l is the width of the slabs (1 mm).

$$\frac{M_t}{M_\infty} = 4 \left[\frac{Dt}{\pi l^2} \right]^{1/2} \quad (2)$$

3. Results and Discussion

3.1 Synthesis and Analysis

Grafting of PEG-anthracene to alginate was successful, resulting in high liquid content hydrogels. Swelling results showed that the gels swelled 96.3 ± 1.3 % in water or 97.3 ± 2.1 % in PBS ($p=0.307$). Carbon NMR showed alterations in the carbon bonds of alginate photogels with 365 nm irradiation. Gels showed characteristic anthracene peaks between 125-130 ppm. Previous studies show that a peak under 50 ppm is indicative of anthracene dimerization [33]. Following 365 nm UV irradiation for 80 minutes at 10 mW/cm^2 ($48,000 \text{ mJ/cm}^2$), a new peak at 32 ppm was observed corresponding to the carbon at the juncture of the anthracene dimer indicating dimerization occurred. This peak disappeared after irradiation with 254 nm light for 90 minutes at 0.6 mW/cm^2 (3240 mW/cm^2) corresponding to partial de-dimerization. Importantly, the appearance of a new peak at 32 ppm with 365 nm light exposure followed by disappearance with 254 nm light proves any observed changes in alginate gel properties from the application of UV light is due to PEG-anthracene dimerization within the gel matrix.

3.2 Degradation

Since there are no mammalian enzymes to break down alginate, its chains degrade slowly and its decrosslinking is thought to be the primary degradation mechanism for these gels. The control PEG hydrogels remained intact for over 800 hours and the photogels for over 2000 hours in PBS with or without 365 nm UV light treatment. Calcium alginate physical gels however, degraded in under 24 hours. Covalent modification with PEG and PEG-anthracene therefore is an effective method to stabilize alginate for a variety of long-term drug delivery and biological applications.

3.3 Effective Crosslinking Density and Loading

The crosslinking density of the different gels can be characteristic of the size of the crosslinking molecules and the level of crosslinking within the gels. Smaller crosslinkers lead to tighter crosslinks and therefore a higher crosslinking density. With grafted PEG-diamine crosslinkers, effective crosslinking density will be affected by the length (size) of the chains and when grafted with PEG-anthracene, effective crosslinking density of the photogels will be affected by the formation of linked-PEG chains due to the dimerization of the anthracene groups on the ends of the grafted PEG-anthracene molecules. From Figure 2, it can be seen that the calcium alginate gels have a lower crosslinking density than the PEG hydrogels, which is not surprising since the molecular weight of the calcium is 40.1 g/mol compared with the PEG-diamine which is 897.1 g/mol. The addition of calcium to photogels causes an increase in crosslinking density due to the formation of physical crosslinks of calcium with alginate guluronic acid block chains.

The photogels, shown in Figure 2, have a low crosslinking density since at this point they have not been exposed to UV light so the anthracene molecules have not dimerized and therefore the PEG-anthracene chains are not connected i.e. not photocrosslinked.

As illustrated in Table 1, during loading, the photogels uptake the most Coomassie Blue, likely due to their lower crosslinking density relative to the physically crosslinked calcium alginate gels and control PEG hydrogels. This could therefore provide a very effective and novel loading technique. Large amounts of drugs could be loaded into uncrosslinked photogels. UV exposure would then “lock” drugs within the then photocrosslinked matrix. This technique could increase loading amounts and decrease loading times, which are crucial parameters in delivery systems for water-labile drug compounds and proteins [1,34], as well as presumably alter the kinetics of drug release from the gels.

The lower loading of alginate crosslinked with short PEG (3 units) versus long PEG (20 units) further demonstrates that tighter, more highly crosslinked gels will absorb less Coomassie Blue due to their smaller mesh size. High concentration alginate photogels were also found to have lower loading of the dye, likely due to the high amount of alginate causing physical entanglements that act as connections to increase the overall crosslink density which will slow diffusion into the gels, decreasing loading. Therefore, not surprisingly, calcium alginate gels load low relative amounts of Coomassie Blue and the photogels reinforced with calcium load less than photogels without calcium. Since

their loading was into pre-swollen gels and not into dried gels there is also a lower driving force for Coomassie Blue uptake. The high overall loading of the relatively small Coomassie Blue into the different gels suggests the possibility that positive interactions between alginate and Coomassie Blue act to increase its absorption. In comparison, the loading of Fast Green into the photogels was on average 1.29 ± 0.11 mg/g gel which suggests there are little interactions occurring between Fast Green and the photogels.

To investigate the interactions between Coomassie Blue and alginate, effective crosslinking densities before and after loading were calculated and compared, since interactions may act to increase crosslinking to affect future release kinetics. Based on swelling data using the Flory-Rehner equation [25-27] and also illustrated in Figure 2, the effective crosslinking of the photogels, high alginate concentration photogels and PEG hydrogels show slight, but insignificant decreases after loading of Coomassie Blue. This indicates that Coomassie Blue likely interacts with alginate but not in its well-known crosslink-inducing mechanistic “egg box” formation [35]. It should also be noted that the calcium reinforced photogels have an increase in crosslinking as shown in Figure 2 because the gels in the buffer have no calcium reinforcement whereas the addition of calcium chloride in the Coomassie Blue loaded gels causes an overall increase in their crosslinking density.

3.4 Release Studies

3.4.1 Photogels and Control PEG Hydrogels

Release of Coomassie Blue from alginate photogels into PBS at 37°C following irradiation with 365 nm light (10 mW/cm²) at 1.5 hours for 10 and 30 minutes versus controls with no UV treatments is shown in Figure 3a. After an initial period of instability where high levels of release were observed, likely due to surface bound dye, irradiation of gels with 30 minutes of 365 nm light (18,000 mJ/cm²) resulted in decreases in release of the model drug Coomassie Blue from the photosensitive gels (p=0.036 at 606 minutes). Since anthracene photodimerization requires the molecules to absorb light, a minimal exposure is required for adequate dimerization of the grafted PEG-anthracene to cause observable changes in crosslinking and an effect on release. With an exposure of 6000 mJ/cm² obtained for 10 minute exposures at 10 mW/cm², there is insufficient energy to considerably alter the Coomassie Blue release (p=0.147 at 1711 minutes). This illustrates that increases in 365 nm UV exposure slow the release of Coomassie Blue to create a tuneable drug delivery material based on UV treatment times/exposures. Since the current alginate photogels are slightly cloudy with a refractive index of 1.348, it is not surprising that higher exposures of 365 nm light are necessary for an effect comparable to our previous studies with hyaluronic acid [23]. Furthermore, highly purified sources of alginate that have less light scattering, and therefore higher photosensitivity, may be more appropriate for future studies.

With 365 nm UV treatment, a slight increase in Coomassie Blue release was observed with the control PEG hydrogels (Figure 3b) ($p=0.01$ at 794 hours). This is thought to have a couple of possible explanations. Despite attempts to store the gels at cool temperatures while under the UV lamp, the slight induced increase in temperature may lead to faster diffusion during this time period. Furthermore, with the absence of anthracene in these systems, the alginate may absorb the 365 nm UV light, causing slight chain scission along the backbone of the polymer, a slight decrease in crosslinking and therefore slight increase in release. These explanations are further substantiated by the size of the increase which is miniscule in comparison to the large decreases in Coomassie Blue release observed with 365 nm UV treatment of photogels verifying the crosslinking effect that PEG-anthracene introduces into the alginate gel matrices.

The carbon NMR study, that proves anthracene dimerization occurs in the photogels, coupled with observed trends in drug release that show decreases upon 365 nm UV light exposure with photogels but not control PEG hydrogels, leads to the conclusion that the grafted PEG-anthracene chains act as crosslinkers, which upon dimerization with 365 nm light, can alter the physical properties of alginate gel matrices. Interestingly, the amount of Coomassie Blue release at approximately 800 hours is comparable between the control PEG hydrogels (14 % at 795 hours) and the photogels not treated with UV (19 % at 845 hours) indicating that interactions that slow Coomassie Blue diffusion and release are likely interactions with the alginate. There may also be interactions occurring between

Coomassie Blue and anthracene since the non-photocrosslinked photogels with no UV exposure also release in a controlled fashion over lengthy periods of time.

To ensure that the observed changes in release were repeatable with other model drugs, Fast Green was also loaded into the alginate photogels and released with and without 365 nm UV treatments. As illustrated in Figure 4, changes in release after 365 nm light treatment for 30 minutes appeared by 600 hours of release ($p=0.246$). The lower loading of Fast Green may have reduced the time for occurrence of changes in release to appear and significant differences are expected to occur past the times shown in Figure 4. However, importantly, the changes did occur with a different model release compound other than Coomassie Blue. Photoresponsive alginate is a release system that may work on multiple drugs/molecules.

3.4.2 High Alginate Concentration Photogels

Release of Coomassie Blue from photogels containing twice as much alginate but with a 50% lower PEG-anthracene grafting density, shown in Figure 5, demonstrates that while there is a trend of decreased release with 365 nm treatment, the decrease in release is not to the same degree as the previous photogels that had less alginate but a higher PEG-anthracene grafting density ($p=0.688$ at 1373 hours). This demonstrates that the control over the release is in fact due to the presence of anthracene in the gels. In addition, these high alginate concentration photogels released quite quickly in comparison to the other photogels with over 90% delivery at 1200 hours with or without UV treatment. This

demonstrates that a minimum amount of PEG-anthracene grafting is required for either dimerization to occur or for dimerization to significantly affect crosslinking density and drug release.

3.4.3 Calcium Alginate Gels versus Photogels in TBS

To directly compare and observe differences in physically crosslinked alginate gels versus photogels, some photogels were secondarily crosslinked with calcium chloride. Both calcium crosslinked alginate gels and calcium-reinforced photogels were loaded with Coomassie Blue which was subsequently released into TBS. PBS contains sodium and phosphate ions that quickly degrade calcium alginate gels by the replacement of calcium ions (Ca^{2+}) with 2 sodium ions (Na^+) to cause decrosslinking in conjunction with the presence of phosphate which combines with the freed calcium to produce calcium phosphate effectively removing any calcium ions to prevent re-crosslinking [36]. Therefore, TBS was used as a buffer that would slow this degradation and allow adequate observation of the release without the convoluting effects of the decrosslinking [36]. As shown in Figure 6a, the physically crosslinked calcium alginate gels quickly release the Coomassie Blue consistent with literature [37], and degrade with no observable changes in release with UV treatment ($p=0.139$ at 2.5 hours). However, release of Coomassie Blue from the calcium-reinforced photogels, depicted in Figure 6b, show large decreases in release following 365 nm UV treatment with significant decreases noted at 867 hours ($p=0.003$). The addition of calcium to these photogels temporarily increased the crosslinking density of the photogels (Figure 2). Therefore, during UV treatment at 1.5

hours, the anthracene molecules along the backbone of the alginate were likely closer together, thereby increasing the likelihood of dimerization. Hence there are more significant decreases in percent release following UV treatment. Any calcium introduced into the calcium-reinforced photogels releasing Coomassie Blue in Figure 6b is likely to have migrated from the photogels after first 24 hours. Overall, this demonstrates that increased stability is provided to the alginate gels with covalent grafting of PEG-anthracene and shows that calcium can be used to reinforce alginate photogels in a formulation to increase their photosensitivity.

3.4.4 Star-PEG-Anthracene Containing Photogels

Star-PEG-anthracene was successfully incorporated into the photogels, introducing additional photodimerizing groups into the system in order to increase its overall photosensitivity. As shown in Figure 7a, a statistically significant decrease in release was observed with 365 nm light treatments of 20 or 40 minutes after a period of release at approximately 1857 hours (approximately 77 days, $p=0.064$) or 1183 hours (approximately 49 days, $p=0.018$) respectively. Therefore, longer treatment times resulted in more rapid changes in release. By removing the initial burst, shown in Figure 7b, the changes in the release can be more readily observed with significant decreases noted at 176 hours with 20 minute UV gel treatments ($p=0.026$). This burst is thought to be due to contraction of the star-PEG-anthracene within the photogel system causing changes in pore-structure. Overall, the photosensitivity increased but different types of release curves are noted with the presence of the additional photosensitive molecules.

3.5 Diffusion Coefficients

Diffusion coefficients are indicative of the rate and the mechanism by which the molecules diffuse through the gels, providing a good method of directly comparing gels of different compositions with and without UV treatments. Diffusion coefficients for early release from 3-4 hours after UV treatment up to 1700 hours for photogels and star-containing photogels or up to 380 hours for high alginate concentration photogels were compared by calculating the percent reduction of the diffusion coefficient that occurs with 365 nm UV treatments. As illustrated in Table 2, the percent reduction increased with additional UV treatment time by 54% to 67% for 10 and 30 minute treatments of photogels indicating increasing in UV doses do change the release kinetics. The alginate photogels are tuneable dependent on UV times/exposures. Calcium-reinforced photogels had the highest decrease of 79% with 365 nm UV treatment for 30 minutes for reasons described earlier, specifically calcium tightening the gels to allow for more efficient dimerization of anthracene with UV treatments. The 29% decrease in diffusion coefficient with 30 minute 365 nm treatments in high alginate concentration photogels is likely due to the lower overall grafting density compared to regular photogels, demonstrating that grafting may be altered to change photosensitivity.

Control PEG-hydrogels have equal diffusion exponents of 0.44. However there is a slight increase in the diffusion coefficient by 20% with 365 nm UV treatment. The physical calcium alginate gels demonstrated a similar trend over a shorter period of time. There are two possible reasons for this. As previously discussed it might be due to slight

heating in the system or, because there are no anthracene molecules to absorb the light, it may be absorbed by the alginate leading to slight alginate break down and a resulting increase in release. Overall, the control gels in comparison to the photogels demonstrate that the slowing of the release of compounds from the photogels is due to dimerization and crosslinking.

The star-PEG-anthracene containing photogels had overall decreases in diffusion coefficients of 48% and 57% with UV treatments of 20 and 40 minutes respectively. However, as described in Table 3, after the initial burst, the decrease in the diffusion coefficient is 57% and 72% with 20 minute and 40 minute UV treatments respectively, demonstrating the possibility that an increase in the number of anthracene groups due to the presence of the star-PEG-anthracene may increase the overall photosensitivity of the photogels.

Taken together, the results suggest that the photogels, control PEG hydrogels and variations thereof have the potential to act as effective long-term alginate based drug delivery systems. There have been several examples in the literature that have shown extended release and degradation with covalently modified alginate. Some hydrophilic modifications include, for example, adipic dihydrazide as a covalent crosslinker to produce alginate gels that release 60% of daunomycin (527.5 Da) over 40 days in Dulbecco's modified Eagle's medium [38]. Hydrophobic modifications have shown much promise since hydrophobicity may improve alginate stability and lengthen release times

[9,15,16]. For example, alginate with 25% methacrylation was shown to degrade over 5 weeks after photocrosslinking [39] while modification with butyl methacrylate led to systems that can deliver albumin into TBS for over 60 hours [15]. Modification with a vinyl polymer increased release of N,N-diethyl-3-methylbenzamide to over 400 hours [40]. Alginate modified with long alkyl chains produce gels that show release into TBS (pH=9.2) varying from 5% - 45% at 122 hours dependent on loading [41]. However, while sustained release has been shown in previous studies, the release profiles in Figures 3, 4, 5, 6b and 7 are considerably lengthier than those in the literature, with some showing controlled release for up to 2000 hours (83 days). For example photogels releasing Coomassie Blue had 17% or 27% release at 1750 hours (73 days) for photogels with and without 365 nm UV light treatment for 30 minutes at $10\text{mW}/\text{cm}^2$. Since anthracene is quite hydrophobic, the covalent modification of alginate with PEG-anthracene likely lowers the hydrophilicity of the alginate gels, increasing their stability and allowing for controlled release. In addition, it is thought that the Coomassie Blue interacts to both increase loading and release times. While not as dramatic, increased release durations were also observed with Fast Green demonstrating the potential of these systems. Therefore, not only do the photogels produce a light-sensitive system, they also present an effective modification method to extend the life time of alginate drug delivery materials.

4. Conclusions

PEG-anthracene grafting introduces light-sensitive crosslinking into alginate photogels in a controllable manner dependent on light treatment time/exposure, the model drug compound being released and the photogel formulation. Covalent modification with both PEG-diamine and PEG-anthracene increases the lifetime of alginate hydrogels even when releasing into high ion containing buffers, such as PBS, which are known to cause high swelling and known to decrosslink physical alginate gels. Decreases in release of Coomassie Blue with 365 nm treatments were tuneable with larger decreases in release with longer photogel UV treatment times/exposures. Changes in release can occur with a variety of different small molecules however Coomassie Blue interacts with alginate in a non-crosslinking fashion resulting in long-term controlled release into high ion containing buffers. The photosensitivity of the photogels to 365 nm UV light can be increased by changing the formulation of the photogels to contain calcium or star-PEG-anthracene and by increasing the amount of grafted PEG-anthracene. Furthermore, the light sensitivity of these materials lends itself to the possibility of a novel loading mechanism that involves absorption of model drug compounds into uncrosslinked photogels followed by photocrosslinking to “lock” the drugs within the gel matrix. Ultimately, the ability to slow the release of small model drugs from alginate photogels presents a long-term, smart delivery material that can be tailored *in vitro* or *in situ* to slow drug release.

Acknowledgements

NSERC and 20/20 NSERC Ophthalmic Materials Network are acknowledged for funding. Keith Oxby is acknowledged for lab assistance.

Legends

Figures

Figure 1. PEG-anthracene photoreversible dimerization and alginate.

PEG-anthracene can dimerize and de-dimerize with 365 nm and 254 nm light. Alginate contains β -D-mannuronic acid (M) and α -L-guluronic acid (G). PEG-anthracene can be grafted onto the carboxyl group of alginate to crosslink it via dimerization.

Figure 2. Effective crosslinking density of gels before and after loading.

The effective crosslinking density of the various gels had a trend of decreases after loading with Coomassie Blue (photogels $p=0.217$, high alginate concentration photogels $p=0.157$, PEG gel $p=0.192$, Calcium gel $p=2.69 \times 10^{-10}$). Calcium-reinforced photogels have an increase in effective crosslinking density because the Coomassie Blue loaded gels also have calcium which causes an overall increase in crosslinking (calcium-reinforced photogel $p=0.136$). In the Figure, Photogels = alginate photogels, High Alg Photo = high alginate concentration photogels, PEG Gel = control PEG hydrogels, Ca Gel = calcium alginate gels, Ca Photogel = calcium reinforced photogels.

Figure 3. Coomassie Blue release from photogels and control PEG hydrogels.

(a) Coomassie Blue release from photogels into PBS (pH=7.4) at 37°C. 1 mL samples were taken and replenished with fresh PBS periodically. At 1.5 hours gels were irradiated with either no light or 365nm light ($10\text{mW}/\text{cm}^2$) for either 30 or 10 minutes. Loading for the 30 minute study was on average 25.5 ± 2.1 mg/g gel. Loading for the 10 minutes study was on average 18.3 ± 1.3 mg/g gel.

(b) Coomassie Blue release from control PEG hydrogels into PBS (pH=7.4) at 37°C. 1 mL samples were taken and replenished with fresh PBS periodically. At 1.5 hours gels were irradiated with either no light or 365nm light ($10\text{mW}/\text{cm}^2$) for 30 minutes. Loading was on average 10.5 ± 1.7 mg/g gel.

Figure 4. Fast Green release versus Coomassie Blue release from photogels.

Coomassie Blue and Fast Green release from photogels into PBS (pH=7.4) at 37°C. 1 mL samples were taken and replenished with fresh PBS periodically. At 1.5 hours gels were irradiated with either no light or 365nm light (10mW/cm²) for 30 minutes. Loading for Fast Green was on average 1.29 ± 0.11 mg/g gel. Loading for Coomassie Blue was on average 25.5 ± 2.1 mg/g gel and is the cumulative release representation of the percent release graph shown in Figure 3 (a).

Figure 5. Coomassie Blue release from high alginate concentration photogels.

Coomassie Blue release from high alginate concentration photogels into PBS (pH=7.4) at 37°C. 1 mL samples were taken and replenished with fresh PBS periodically. At 1.5 hours gels were irradiated with either no light or 365nm light (10mW/cm²) for 30 minutes. Loading was on average 8.80 ± 3.0 mg/g gel.

Figure 6. Coomassie Blue release from calcium alginate gels and calcium-reinforced photogels.

(a) Coomassie Blue release from calcium alginate gels into TBS (pH=7.4) at 37°C. 1 mL samples were taken and replenished with fresh TBS periodically. At 1.5 hours gels were irradiated with either no light or 365nm light (10mW/cm²) for 30 minutes. Loading was on average 3.03 ± 1.65 mg/g gel.

(b) Coomassie Blue release from calcium-reinforced photogels into TBS (pH=7.4) at 37°C. 1 mL samples were taken and replenished with fresh TBS periodically. At 1.5 hours gels were irradiated with either no light or 365nm light (10mW/cm²) for 30 minutes. Loading was on average 16.83 ± 2.84 mg/g gel.

Figure 7. Coomassie Blue release from star-PEG-anthracene containing photogels.

(a) Coomassie Blue release from star-PEG-anthracene containing photogels into PBS (pH=7.4) at 37°C. 1 mL samples were taken and replenished with fresh PBS periodically. At 1.5 hours gels were irradiated with either no light or 365 nm light (10mW/cm²) for 20

or 40 minutes. Loading for the 20 minute study was on average 20.71 ± 1.22 mg/g gel. Loading for the 40 minutes study was on average 16.10 ± 1.27 mg/g gel.

(b) The same release studies as in Figure 7a but with the release calculations starting at 100 hours.

Tables

Table 1. Coomassie Blue loading.

Loading of Coomassie Blue into the different types of gels estimated by solution depletion.

Table 2. Changes in the diffusion coefficients with and without UV treatments.

The diffusion coefficients and exponents of the different gels with and without UV treatments. The percent-decreases in diffusion of 365 nm UV treated gels versus control with no UV treatments are described as a direct comparison between the different systems. All gels are releasing Coomassie Blue.

Table 3. Changes in the diffusion coefficients of star-PEG-anthracene containing photogels with and without UV treatments.

The diffusion coefficients and exponents of the gels with and without UV treatments. Both the total release time and release after the burst (after 100 hours) were investigated to fully explore the changes in release that occur with these gels. All gels are releasing Coomassie Blue.

Figures

Figure 1.

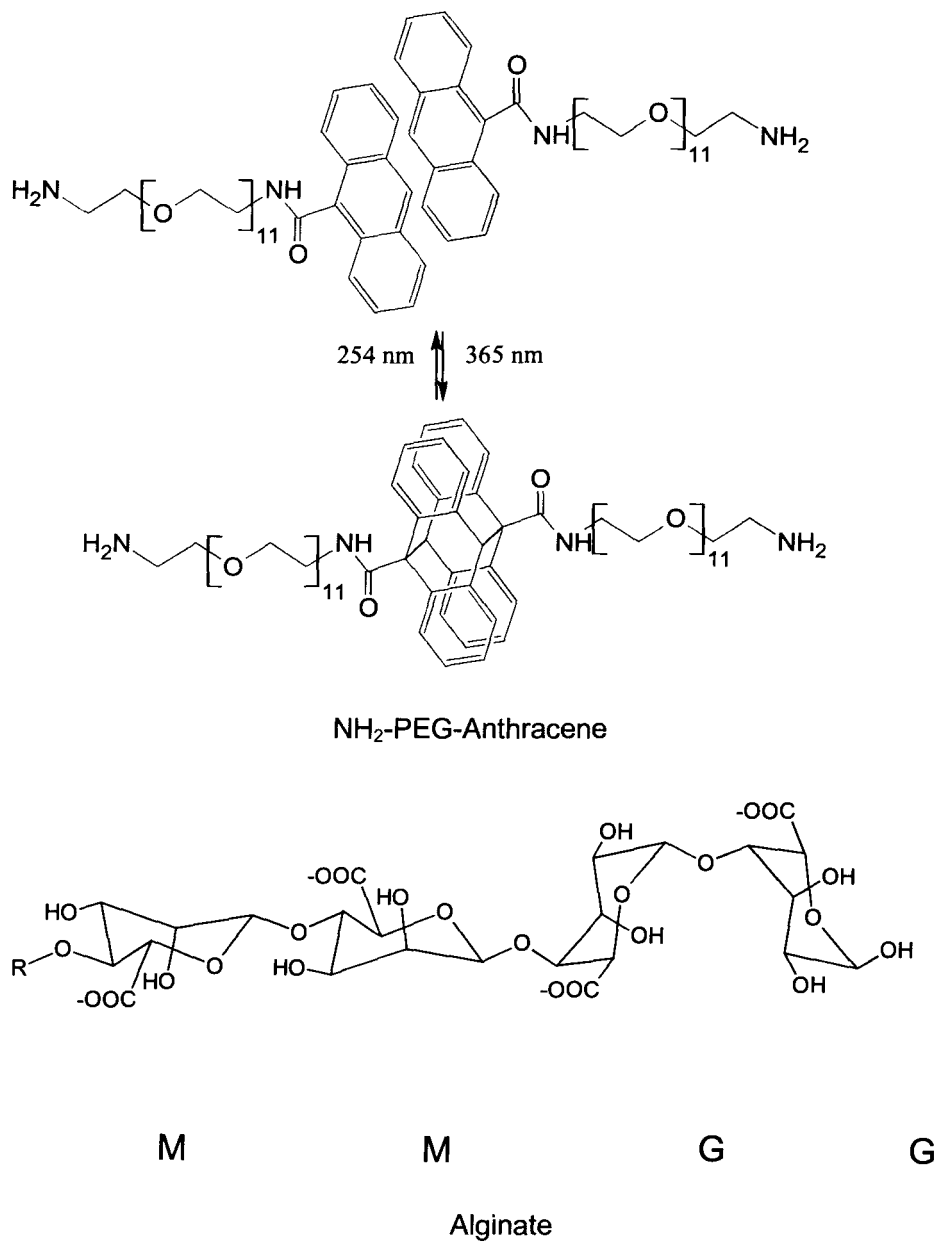


Figure 2.

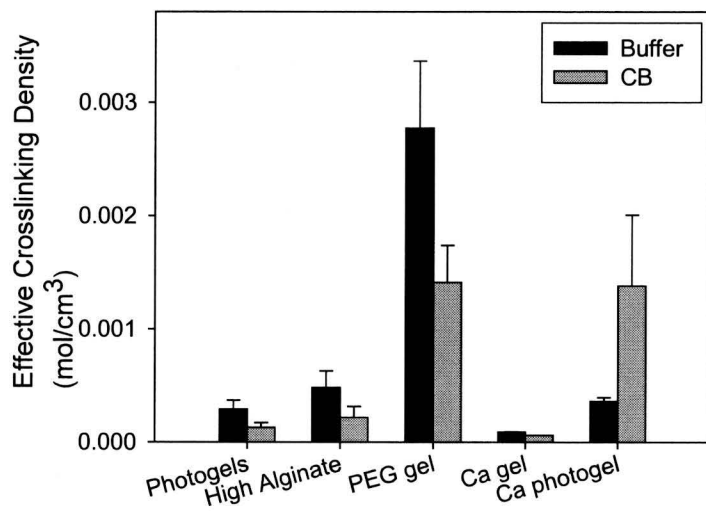
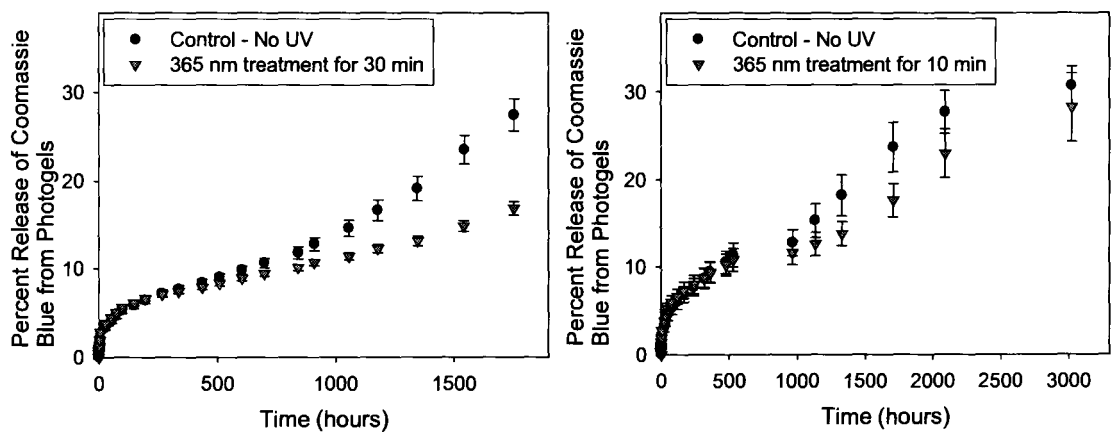


Figure 3.

A



B

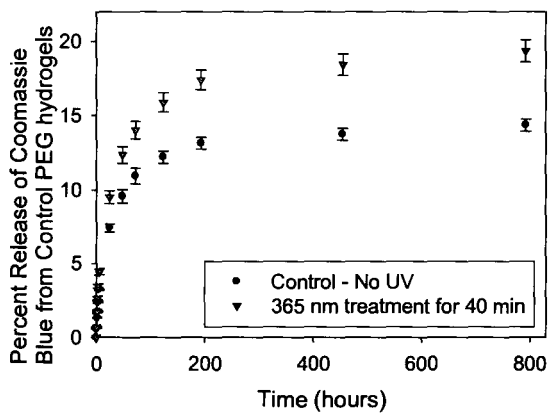


Figure 4.

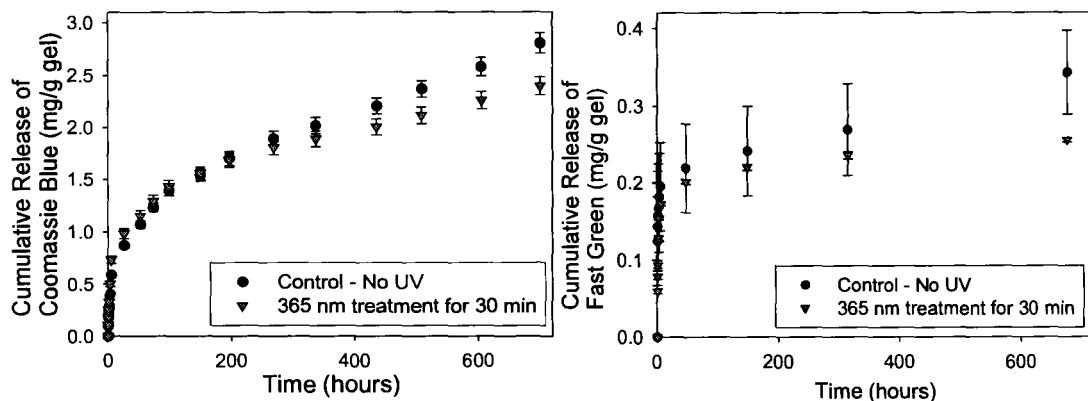


Figure 5.

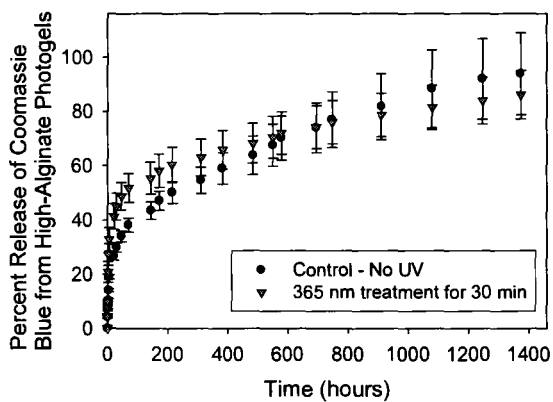


Figure 6,

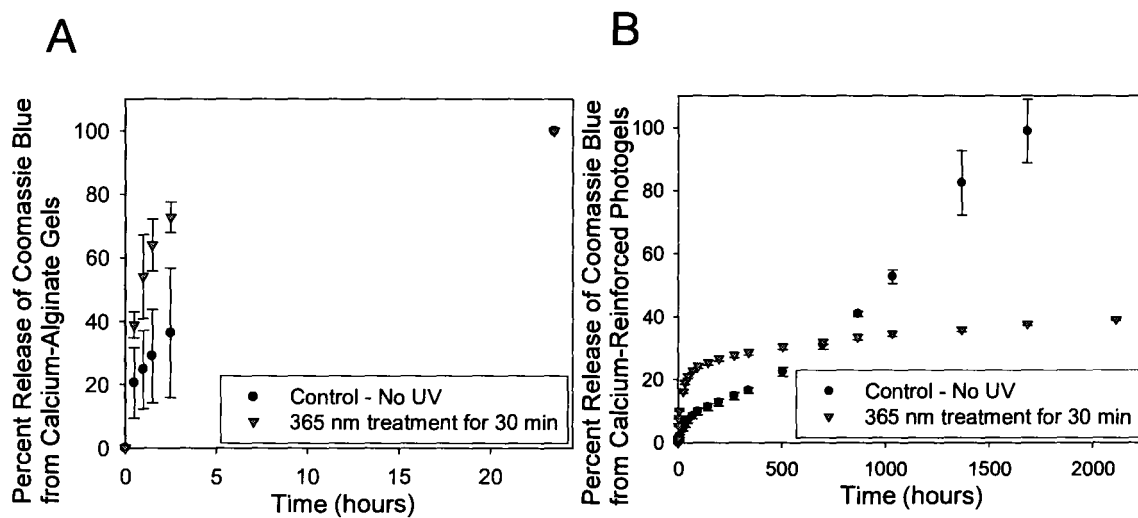
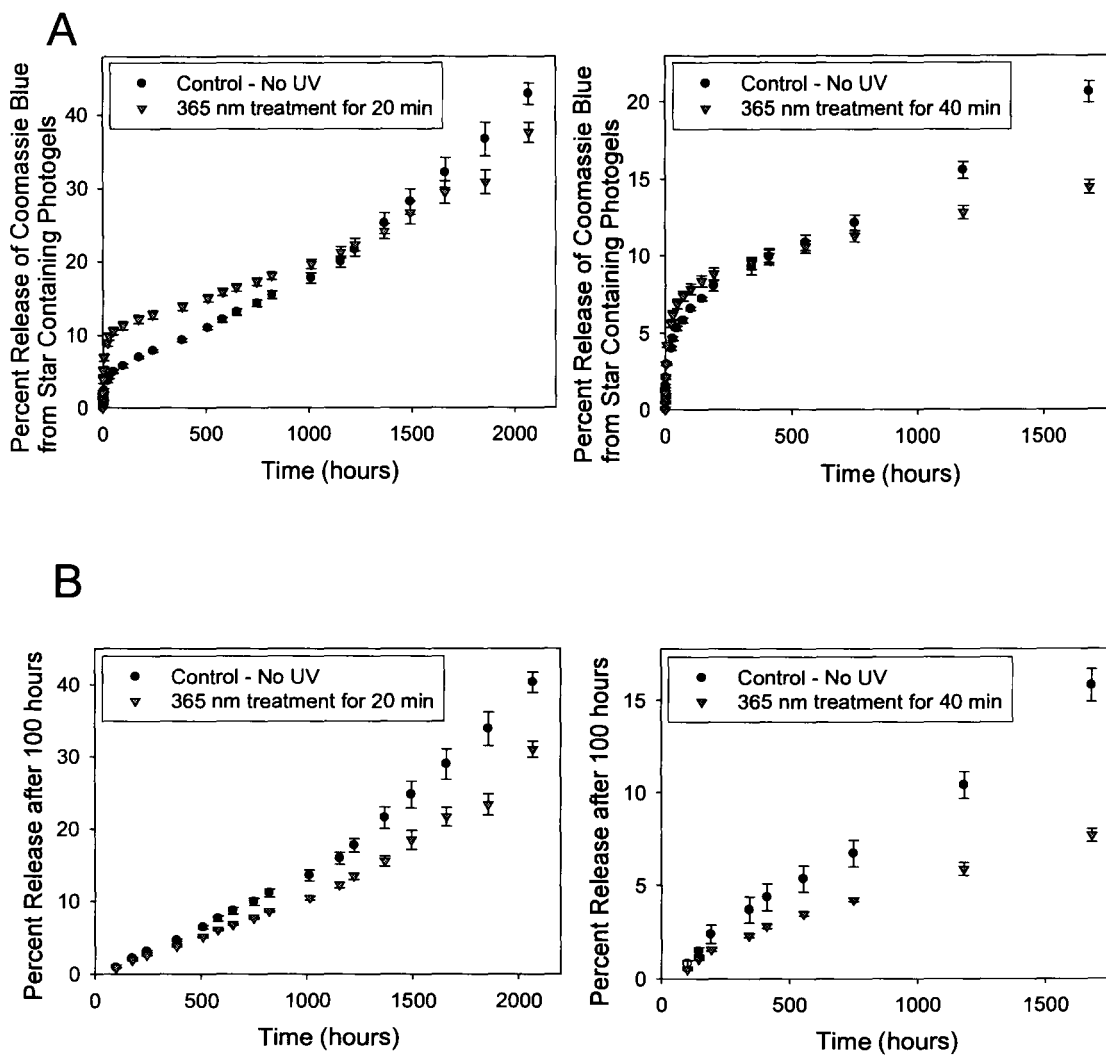


Figure 7.



Tables

Table 1.

| Gel type | Loading medium | Average estimated loading (mg/g gel) |
|--|----------------|--------------------------------------|
| Control PEG hydrogels (short) | PBS | 1.80 ± 0.69 |
| Control PEG hydrogels (long) | PBS | 10.50 ± 1.68 |
| Photogels | PBS | 28.50 ± 3.39 |
| High alginate concentration photogels | PBS | 9.37 ± 0.47 |
| Star-PEG-anthracene containing photogels | PBS | 18.40 ± 2.30 |
| Calcium alginate gels | TBS | 3.03 ± 1.65 |
| Calcium-reinforced photogels | TBS | 16.83 ± 2.84 |

Table 2.

| Gel type | UV treatment groups | Diffusion coefficient (cm ² /s x10 ⁻¹¹) | Diffusion exponent | Percent decrease with UV |
|---------------------------------------|---------------------|--|--------------------|--------------------------|
| Photogels | No UV | 1.23 ± 0.004 | 0.44 ± 0.02 | 54 % |
| | 10 min | 0.57 ± 0.003 | 0.30 ± 0.01 | |
| Photogels | No UV | 1.57 ± 0.011 | 0.42 ± 0.03 | 67 % |
| | 30 min | 0.51 ± 0.001 | 0.30 ± 0.02 | |
| High alginate concentration photogels | No UV | 31.49 ± 0.121 | 0.26 ± 0.01 | 29 % |
| | 30 min | 22.37 ± 0.267 | 0.16 ± 0.01 | |
| Calcium-reinforced photogels | No UV | 12.0 ± 0.093 | 0.57 ± 0.03 | 79 % |
| | 30 min | 2.47 ± 0.031 | 0.21 ± 0.01 | |
| Control PEG hydrogels | No UV | 1.57 ± 0.049 | 0.44 ± 0.04 | -44 % |
| | 40 min | 2.81 ± 0.076 | 0.44 ± 0.04 | |
| Calcium alginate hydrogels | No UV | 2186.6 ± 1.47 | 0.35 ± 0.03 | -59 % |
| | 30 min | 5429.1 ± 145.7 | 0.39 ± 0.04 | |

Table 3.

| Star-PEG-anthracene containing photogels | UV treatment groups | Diffusion coefficient ($\text{cm}^2/\text{s} \times 10^{-11}$) | Diffusion exponent | Percent decrease with UV |
|--|---------------------|--|--------------------|--------------------------|
| Total release time | No UV | 2.45 ± 0.014 | 0.44 ± 0.03 | 48 % |
| | 20 min | 1.28 ± 0.005 | 0.23 ± 0.02 | |
| Total release time | No UV | 0.92 ± 0.002 | 0.33 ± 0.01 | 57 % |
| | 40 min | 0.394 ± 0.002 | 0.19 ± 0.01 | |
| Release >100 hours | No UV | 3.54 ± 0.025 | 0.60 ± 0.04 | 53 % |
| | 20 min | 1.65 ± 0.011 | 0.33 ± 0.03 | |
| Release >100 hours | No UV | 0.981 ± 0.005 | 0.38 ± 0.03 | 72 % |
| | 40 min | 0.272 ± 0.00001 | 0.18 ± 0.01 | |

References

1. Gombotz WR, Wee SF. Protein release from alginate matrix. *Adv Drug Delivery Rev* 1998;31:267-285.
2. Tonnesen HH, Karlsen J. Alginate in drug delivery systems. *Drug Dev Ind Pharm* 2002;28:621-630.
3. Erstesvag H, Valla S. Biosynthesis and applications of alginates. *Polym Degrad Stab* 1998;59:85-91.
4. Augst AD, Kong HJ, Mooney DJ. Alginate hydrogels as biomaterials. *Macromol Biosci* 2006;6:623-633.
5. Lee KW, Yoon JJ, Lee JH, Kim SY, Jung HJ, Kim SJ, Joh JW, Lee HH, Lee DS, Lee SK. Sustained release of vascular endothelial growth factor from calcium-induced alginate hydrogels reinforced by heparin and chitosan. *Transplant Proc* 2004;36:2464-2465.
6. Quong D, Neufeld RJ. Electrophoretic extraction and analysis of DNA from chitosan or poly-L-lysine-coated alginate beads. *Appl Biochem Biotechnol* 1999;81:67-77.
7. Ferreiro MG, Tillman LG, Hardee G, Bodmeier R. Alginate/poly-L-lysine microparticles for the intestinal delivery of antisense oligonucleotides. *Pharm Res* 2002;19:755-764.
8. Monshipouri M, Rudolph AS. Liposome-encapsulated alginate: controlled hydrogel particle formation and release. *J Microencapsulation* 1995;12:117-127.
9. Cathell MD, Szewczyk JC, Schauer CL. Organic modification of the polysaccharide alginate. *Mini-Rev Org Chem* 2010;7:61-67.
10. Tada D, Tanabe T, Tachibana A, Yamauchi K. Albumin-crosslinked alginate hydrogels as sustained drug release carrier. *Mater Sci Eng C* 2007;27:870-874.
11. Eiselt P, Lee KY, Mooney DJ. Rigidity of two-component hydrogels prepared from alginate and poly(ethylene glycol)-diamines. *Macromolecules* 1999;32:5561-5566.
12. Lee KY, Rowley JA, Eiselt P, Moy EM, Bouhadir KH, Mooney DJ. Controlling mechanical and swelling properties of alginate hydrogels independently by cross-linker type and cross-linking density. *Macromolecules* 2000;33:4291-4294.

13. Kulkarni AR, Soppimath KS, Aralaguppi MI, Aminabhavi TM, Rudzinski WE. Preparation of cross-linked sodium alginate microparticles using glutaraldehyde in methanol. *Drug Dev Ind Pharm* 2000;26:1121-1124.
14. Drury JL, Boontheekul T, Mooney DJ. Cellular cross-linking of peptide modified hydrogels. *J Biomech Eng* 2005;127:220-228.
15. Yao B, Ni C, Xiong C, Zhu C, Huang B. Hydrophobic modification of sodium alginate and its application in drug controlled release. *Bioprocess Biosyst Eng* 2010;33:457-463.
16. Broderick E, Lyons H, Pembroke T, Byrne H, Murray B, Hall M. The characterisation of a novel, covalently modified, amphiphilic alginate derivative, which retains gelling and non-toxic properties. *J Colloid Interface Sci* 2006;298:154-161.
17. Rastello De Boissesson M, Leonard M, Hubert P, Marchal P, Stequert A, Castel C, Favre E, Dellacherie E. Physical alginate hydrogels based on hydrophobic or dual hydrophobic/ionic interactions: Bead formation, structure, and stability. *J Colloid Interface Sci* 2004;273:131-139.
18. Chanp LW, Heng WS, Wan LSC. Effect of cellulose derivatives on alginate microspheres prepared by emulsification. *J Microencapsulation* 1997;14:545-555.
19. Vasile C, Dumitriu RP, Cheaburu CN, Oprea AM. Architecture and composition influence on the properties of some smart polymeric materials designed as matrices in drug delivery systems. A comparative study. *Appl Surf Sci* 2009;2565:565-571.
20. Park H, Choi C, Kim J, Kim W. Effect of pH on drug release from polysaccharide tablets. *Drug Delivery* 1998;5:13-18.
21. deMoura MR, Aouada FA, Favaro SL, Radovanovic E, Rubira AF, Muniz EC. Release of BSA from porous matrices constituted of alginate-Ca²⁺ and PNIPAAm-interpenetrated networks. *Mater Sci Eng C* 2009;29:2319-2325.
22. Karemicz A, Zasada K, Szczubialka K, Zapotoczny S, Lach R, Nowakowska M. "Smart" alginate-hydroxypropylcellulose microbeads for controlled release of heparin. *Int J Pharm* 2010;385:163-169.
23. Wells LA, Brook MA, Sheardown H. Graftable PEG-anthracene to generate photoresponsive hydrogels for drug delivery. Submitted to the *J Biomed Mater Res, Part A*;2010.
24. Gilles MA, Hudson AQ, Borders CL, Jr. Stability of water-soluble carbodiimides in aqueous solution. *Anal Biochem* 1990;184:244-248.

25. Bray JC, Merrill EW. Poly (vinyl alcohol) hydrogels. Formation by electron beam irradiation of aqueous solutions and subsequent crystallization. *J Appl Polym Sci* 1973;17:3779-3794.
26. Flory PJ, Rehner J. Statistical mechanics of cross-linked polymer networks II. Swelling. *J Chem Phys* 1943;11:521-526.
27. de Jong SJ, van Eerdenbrugh B, van Nostrum CF, Kettenes-van den Bosch JJ, Hennink WE. Physically crosslinked dextran hydrogels by stereocomplex formation of lactic acid oligomers: degradation and protein release behavior. *J Controlled Release* 2001;71:261-275.
28. Amsden B, Turner N. Diffusion characteristics of calcium alginate gels. *Biotechnol Bioeng* 1999;65:605-610.
29. Li CY, Birnkrant MJ, Natarajan LV, Tondiglia VP, Lloyd PF, Sutherland RL, Bunning TJ. Polymer crystallization/melting induced thermal switching in a series of holographically patterned Bragg reflectors. *Soft Matter* 2005;1:238-242.
30. Leach JB, Bivens KA, Patrick CW, Schmidt CE. Photocrosslinked hyaluronic acid hydrogels: natural, biodegradable tissue engineering scaffolds. *Biotechnol Bioeng* 2003;82:578-589.
31. Ritger PL, Peppas NA. A simple equation for description of solute release I. Fickian and non-fickian release from non-swellable devices in the form of slabs, spheres, cylinders or discs. *J Controlled Release* 1987;5:23-36.
32. Leach JB, Schmidt CE. Characterization of protein release from photocrosslinkable hyaluronic acid-polyethylene glycol hydrogel tissue engineering scaffolds. *Biomaterials* 2005;26:125-135.
33. Islangulov RR, Castellano FN. Photochemical upconversion: anthracene dimerization sensitized to visible light by a Ru¹¹ chromophore. *Angew Chem* 2006;118:6103-6105.
34. Fu K, Klibanov AM, Langer R. Protein stability in controlled-release systems. *Nature Biotechnol* 2000;18:24-25.
35. Morris ER, Rees DA, Thom D. Chiroptical and stoichiometric evidence of a specific primary dimerisation process in alginate gelation. *Carbohydr Res* 1978;66:145-154.
36. Wells LA, Sheardown H. Extended release of high pI proteins from alginate microspheres via a novel encapsulation technique. *Eur J Pharm Biopharm* 2007;65:329-335.

37. Elnashar MM, Yassin MA, Moneim AEA, Bary EMA. Surprising performance of alginate beads for the release of low-molecular-weight drugs. *J Appl Polym Sci* 2010;116:3021-3026.
38. Bouhadir KH, Kruger GM, Lee KY, Mooney DJ. Sustained and controlled release of daunomycin from cross-linked poly(aldehyde guluronate) hydrogels. *J Pharm Sci* 2000;89:910-919.
39. Jeon O, Bouhadir KH, Mansour JM, Alsberg E. Photocrosslinked alginate hydrogels with tunable biodegradation rates and mechanical properties. *Biomaterials* 2009;30:2724-2734.
40. Xiao C, Zhou M, Lin X, Li R. Chemical modification of calcium alginate gel beads for controlling the release of insect repellent N,N-diethyl-3-methylbenzamide. *J Appl Polym Sci* 2006;102:4850-4855.
41. Leonard M, De Boisseson MR, Hubert P, Dalençon F, Dellacherie E. Hydrophobically modified alginate hydrogels as protein carriers with specific controlled release properties. *J Controlled Release* 2004;98:395-405.

6.0 Photoresponsive PEG-Anthracene Grafted Hyaluronate as a Smart Responsive Controlled-Delivery Biomaterial

Authors: Laura A. Wells, Stephanie Furukawa; Heather Sheardown

Publication Information: Submitted to *Biomacromolecules*.

Objectives: To optimize the synthesis of HA photogels and thoroughly investigate their release properties with various large and small model drugs, different UV exposure times and modified formulations. To determine the cytocompatibility of the HA photogels with retinal cell lines.

Main Scientific Contributions:

1. Investigation into the grafting of PEG anthracene onto HA with varying densities to determine grafting efficiencies and the properties of the resulting gels.
2. Thorough investigations into the release properties of HA photogels with loading and release of small and large model drugs. Effective crosslinking density, loading and release comparisons were performed to determine interactions occurring between the model drugs and the photogels. Formulations of photogels containing star-PEG anthracene are also investigated.
3. Diffusion coefficients were calculated to compare different systems. Photocrosslinked gels were exposed to excimer lasers as a proof-of-concept and to investigate the potential to increase release with exposures under 300 nm.
4. Cell studies were done through the supervision and instruction of Stephanie Furukawa. They evaluated populations of retinal pigment epithelial cells grown with solutions of PEG-anthracene, HA photogels and HA photogel degradation products.

Photoresponsive PEG-Anthracene Grafted Hyaluronate as a Smart Controlled-Delivery Biomaterial

Laura Anne Wells¹, Stephanie Furukawa², Heather Sheardown^{1,2*}

¹Department of Chemical Engineering and ²School of Biomedical Engineering
McMaster University
Hamilton ON
L8S 4L7

*to whom correspondence should be addressed sheadow@mcmaster.ca

Abstract

Ophthalmic drug delivery to the posterior segment of the eye could benefit from a responsive controlled drug delivery system with light or laser inducible changes. For example, the delivery of age-related macular degeneration drugs requires invasive monthly injections making long term photoresponsive drug delivery a desirable option. The feasibility of this may be facilitated by both the transparency of the eye and the advanced technology in ophthalmic lasers. Hyaluronic acid photogels that are compatible with retinal pigment epithelial cell lines are shown here to deliver a variety of small and large model drugs over the long-term (months). Varying UV exposures resulted in decreases/increases or the turning off and on of delivery potentially allowing the therapy to be tailored to suit the patient and the disease.

1. Introduction

The delivery rate of therapeutics can be adjusted using responsive controlled drug delivery devices to suit the natural progression of chronic diseases over years and to tailor delivery to the individual needs of the patients. The modification of polymer systems with molecules that respond to internal or external stimuli such as temperature, pH or light, can introduce controllable property changes [1] to alter drug releasing dosing profiles in pulsatile (on/off) or incremental (increase/decrease) fashions over the life-time of a delivery device.

The potential benefits of responsive controlled delivery systems are obvious in ophthalmic drug delivery for the treatment of posterior segment eye diseases such as wet age related macular degeneration (wet AMD) and diabetic retinopathy. Both diseases can result in significant vision loss. However, disease progression can potentially be arrested or reversed with new long-term treatment. Many new vascular endothelial growth factor (VEGF)-blocker drugs on the market have been shown to effectively suppress the disease pathology [2]. However, delivery to the retina remains a challenge. Topical eye-drop therapies deliver insufficient drug to the posterior segment with only 5 % drug penetration into the eye [3,4]. Systemic drug delivery can result in side effects to non-target organs and these drugs have very little capability to diffuse through the low permeability vessels of the blood-retinal barrier to reach the target site [5]. The most effective technique for retinal drug delivery are intravitreal injections which, while effective, must be repeated approximately monthly for the treatment of wet AMD. This injection frequency is associated with injection-related side-effects, low patient

compliance and high health care costs [6-8]. Controlled drug delivery devices for macular diseases that can deliver on the order of years have been well recognized to potentially alleviate these injection issues [9-11]. Furthermore, studies have suggested there are potential cost benefits with sustained visual improvements associated with altered AMD drug dose regimens based on monitoring with Optical Coherence Tomography [12,13]. Therefore, controlled release of drugs from smart materials that can alter released doses with stimuli over lengthy periods could optimize AMD treatments with VEGF-blocking agents.

Smart/responsive drug delivery systems made from polymers modified with photoisomerizing or photodimerizing groups have minimal side-products and require no photosensitizers, eliminating the toxicity risks associated with leachable molecules and producing potentially highly biocompatible biomaterials for *in vivo* applications [1]. Since individual photosensitive molecule in these systems must absorb light to isomerize or dimerize [14,15], in contrast to photopolymerization which is characterized by absorption of light by initiators followed by the propagation [16], incremental changes may be achieved with higher exposures leading to additional photoreactions and vice versa. In addition, the presence of more photosensitive molecules should increase the overall magnitude of these changes.

The vitreous humour, a clear gel that fills the back of the eye, consists largely of water (>98%) with collagen and hyaluronate (HA) [17]. Most retinal drug delivery devices would come into contact with and deliver drugs into the vitreous humour so gel devices synthesized with HA would presumably be highly compatible and would slowly

degrade through the action of low levels of native enzymes. Previous studies by Wells *et al.* (2010) focused on the synthesis of anthracene-containing hydrogels. These materials were synthesized via the grafting of polyethylene glycol (PEG) bound anthracene groups along the backbone of HA as illustrated in Figure 1 [18]. Anthracene dimerizes at ultraviolet (UV) wavelengths over 300 nm and de-dimerizes/dissociates at UV wavelengths under 300 nm [14] creating a switchable mechanism that crosslinks HA upon dimerization of anthracene due to the joining of grafted PEG chains and decrosslinks HA upon dedimerization of the anthracene groups.

Herein we explored HA photogel properties with the delivery of various compounds of high and low molecular weight with varying light exposures. Changes in release with light were consistently observed with both small and large model drug compounds that are representative of small anti-inflammatory steroids and larger anti-VEGF AMD drugs for retinal treatments. Altering the dose of 365 nm UV light was shown to cause incremental changes in release and the addition of anthracene-containing star-PEG can modify the sensitivity. Growth of retinal pigment epithelial cells with the photogels and degradation products showed high compatibility with similar cell viability as controls.

2. Methods

2.1 Materials

Sodium hyaluronate of 132.3 kDa was purchased from Life-Core Biomedical (Chaska, MN). PEG-diamine (*O,O'*-Bis(2-aminoethyl) octadecaethylene glycol), Boc-

PEG-amine (O-(2-Aminoethyl)-O'-[2-(Boc-amino)ethyl]decaethylene glycol), 1-ethyl-(dimethylaminopropyl) carbodiimide hydrochloride (EDC), N-hydroxysuccinimide (NHS), ninhydrin assay reagent, MTT reagent (3-[4,5-dimethylthiazol-2-yl]-2,5-diphenyl tetrazolium bromide), proteins (myoglobin, lysozyme and bovine serum albumin), small molecules (Coomassie Blue, Fast Green and dextran) and other reagents were purchased from Sigma-Aldrich (Oakville, ON). Anthracene-9-carboxylic acid was from Alfa Aesar (CA) and star-PEG-anthracene (four arm, with a pentaerythritol core, 9500 Da) was purchased from Polymer Source (Quebec). A 10 mW/cm² Curzone II lamp from CONTROL-CURE (Chicago, IL) (400 W, 120 VAC, 60Hz, 8 amps max) was used for 365 nm UV exposures and an excimer laser (krypton fluoride, at 58 mJ/cm² and 5 Hz) was used for 248 nm exposures. Human retinal pigment epithelial (RPE) cells were from ATCC (Manassas, VA) with media and supplements from Invitrogen (Burlington ON).

2.2 Photogel Synthesis

As previously described in detail in Wells *et al.* (2010) [18], amine terminated PEG-anthracene molecules were synthesized using carbodiimide chemistry between Boc-PEG-amine (n=11) and anthracene-9-carboxylic acid using EDC in dry dichloromethane under nitrogen. This was followed by removal of the Boc protecting group with trifluoroacetic acid and the scavenger triisopropylsilane then subsequent purification [18].

Photogels were then synthesized in MES buffer containing 0.1 M 4-morpholinoethanesulfonic acid and 0.5 M sodium chloride (pH=6) by mixing 6% HA with EDC/NHS solution and PEG-anthracene with varying HA/PEG-anthracene ratios at

4°C for 72 hours. The resulting photogels were then punched into disks and soak in de-ionized water to remove impurities [18]. To optimize the properties of the HA photogels and control PEG hydrogels, varying molar ratios of PEG-anthracene to HA carboxyl groups were reacted and monitored for grafting efficiency. The photocrosslinking ability of 0.8:1 versus 1:1 ratio gels (PEG anthracene:HA carboxylic acid) were used to test which photogels showed the highest photosensitivity.

To make 1:1 grafted photogels used in the release studies, 1mL of 6% HA was mixed with 0.353 mL of EDC/NHS solution (191.6mg/mL EDC and 57.5mg/mL NHS) and 0.443 mL PEG-anthracene solution (300 mg/mL with 1N NaOH to pH=6) [18]. The solution was allowed to react between glass plates with a 1 mm slide spacer and in the dark at 4°C overnight. Control-PEG-hydrogels had less PEG added (0.443 mL of 180 mg/mL PEG-diamine of n=20 plus HCl to pH=6) since both ends will react to the HA.

Star-PEG-anthracene was incorporated into some gels to increase the number of anthracene groups with a goal of increasing the photosensitivity of the gels. Star-PEG-anthracene was dissolved into the initial PEG-anthracene solution followed by mixing with EDC/NHS and 6% HA. Star-containing photogels had 40.6 mg of star-PEG-anthracene per mL of 6% HA in an anthracene molar ratio of grafted PEG-anthracene to star-PEG-anthracene of 10:1.

Ninhydrin Assay to Monitor Grafting

The ninhydrin assay detects primary amine groups on unbound PEG-diamine and PEG-anthracene through the conversion of ninhydrin to Ruhemann's purple. By testing

the gel soaking solutions and gels, unbound PEG can be detected and concentrations determined by a calibration curve of glycine. Gels soaked in 1 mL of water and 1 mL soaking solutions from their purification were mixed with 0.5 mL of reagent and heated in an oil bath at 100°C for 10 minutes. After cooling at room temperature, 2.5 mL of 95% ethanol were added to dilute the samples followed by detection of Ruhemann's purple by spectrophotometric measurements of solution adsorption at 595 nm in a microplate reader. The unbound PEG-anthracene or PEG-diamine was compared to the amounts added during synthesis to determine the efficiency of the reaction (unbound-bound/bound) and the actual grafting ratios of the resulting gels (moles of PEG-anthracene per mole of HA polymer carboxyl groups).

2.3 Release Studies

To investigate drug release from and diffusion properties of the gels, model drug compounds were loaded and released from photogels with and without UV treatment. Air-dried gel disks were loaded by soaking in 0.5 mg/mL solutions of the model compounds in PBS for 24 hours. The photogel disks were then rinsed and placed in PBS at 37°C in a shaking waterbath with periodic changes in the soaking medium. This medium was sampled and tested over time to obtain release profiles. At 1.5 hours, certain sets of gels were irradiated with 365 nm light and compared to controls with no UV light exposure. Some photocrosslinked gels in protein release studies were also exposed to a 248 nm excimer laser after approximately 1000 hours of release and release results were compared to controls with no UV light and gels that were exposed to exclusively 365 nm

light. Statistical differences in release points from gels exposed to UV versus controls were assessed using t-tests.

Three different small molecules, Coomassie Blue (854 Da), Fast Green (765.9 Da) and dextran (1000 Da), were loaded into and released from the HA photogels. These molecules were chosen to represent small steroidal drugs and because of their different structures. As illustrated in Table 1, Coomassie Blue and Fast Green are globular and dextran is chain-like. Coomassie blue and Fast Green were detected spectrophotometrically at 595 nm and 630 nm respectively. Dextran was detected spectrophotometrically at 405 nm after precipitation for 5 minutes with ethanol in a sample:ethanol volumetric ratio of 1:2. Loading of the small molecules was determined by measuring the amounts of unloaded compounds remaining in the soaking solution.

Three proteins of varying molecular weight and isoelectric points (pI) were used in the release studies were also examined as model compounds. These large proteins were chosen to represent large VEGF-blocker drugs because they are of varying large molecule weights and varying charges at 7.4 due to their different isoelectric points (Table 1). Molecules with isoelectric points above 7.4 are positive in PBS and those with isoelectric points below 7.4 are negative in PBS. Release of lysozyme (14,400 Da, pI = 9.3), bovine serum albumin (BSA) (67,000 Da, pI = 4.9) and myoglobin (17,600 Da, pI= 7.3, minor 6.8) was detected using the Bradford assay. Loading was defined as the average amount of protein completely released by the control (no UV) photogels that release and degrade quickly.

2.4 Effective Crosslinking Density

Effective crosslinking densities were used to assess possible crosslinking from interactions of the model compounds with the photogel bulk materials or the anthracene. The effective crosslinking density (ν_e) was determined by dividing the polymer density (ρ_p) of the average molecular weight between crosslinks (M_c) as per equation 1.

$$\nu_e = \frac{\rho_p}{M_c} \quad (1)$$

M_c is determined using an adapted version of the Flory-Rehner equation by Bray and Merrill (equation 2) for hydrogels crosslinked in solution [19-21]. In equation 2, ν is the specific volume of dry polymer (HA = 0.814 cm³/g [22] and PEG = 0.89 cm³/g for PEG [23]), $\nu_{2,s}$ is the volumetric polymer fraction at maximum swelling calculated from swelling in PBS, $\nu_{2,r}$ is the volumetric polymer fraction in a relaxed state calculated from synthesis masses, V_1 is the molar volume of solvent (18 mol/cm³), χ is the Flory polymer-solvent interaction parameter (approximately 0.473 for HA [22] and PEG [23]) and M_n is the number average molecular weight of the polymer.

$$\frac{1}{M_c} = \frac{2}{M_n} - \frac{(\bar{\nu}/V_1) \left[\ln(1 - \nu_{2,s}) + \nu_{2,s} + \chi_1(\nu_{2,s})^2 \right]}{\nu_{2,r} \left[(\nu_{2,s}/\nu_{2,r})^{1/3} - 0.5(\nu_{2,s}/\nu_{2,r}) \right]} \quad (2)$$

2.5 Diffusion calculations

Diffusion exponents describe the diffusion mechanism of molecules and diffusion coefficients the speed of the molecules and are a method of directly comparing the effect of different molecules and exposures on the photogel systems. The release mechanisms were determined by calculating diffusion exponents using the relationship in Equation (3) by linear regression of the natural logarithms of release data from 20 hours after UV treatments until 500 hours. M_t and M_∞ are the amount of drug released at time t and at infinite time, k is a constant dependent on the system and n is the diffusion exponent. The diffusion exponent is indicative of the type of release. The gel disks were treated as slabs since their diameters are over 4 times their thickness [24,25]. For Fickian release ($n \leq 0.5$), during early time when $M_t/M_\infty \leq 0.6$, diffusion coefficients can be calculated using the Ritger and Peppas model shown in Equation (4) for controlled release of polymeric devices [26] where l is the thickness of the slab and D is the diffusion coefficient. Regression on the natural logarithms of release data from various photogels were used to determine their diffusion coefficients.

$$\frac{M_t}{M_\infty} = kt^n \quad (3)$$

$$\frac{M_t}{M_\infty} = 4 \left[\frac{Dt}{\pi l^2} \right]^{1/2} \quad (4)$$

2.6 Degradation Studies

Hydrolytic and decrosslinking driven degradation of the gels was monitored by soaking disks in 1 mL of phosphate buffered saline (PBS) at 37°C with regular changes of the buffer until disks were no longer visible. Enzymatic degradation of HA by hyaluronidase (bovine testes) was monitored by placing the disks in 0.5 mL buffer containing 100 Units of hyaluronidase per mL at 37°C with regular solution changes to ensure maintenance of the enzyme activity. The buffer was prepared using 3.871 g of sodium citrate, 10.647g of disodium hydrogen phosphate and 4.383 g of sodium chloride in 500 mL of water with pH adjusted to 6.3 with 1N NaOH/1N HCl to promote enzyme function.

2.7 Photogel Cytocompatibility with Retinal Cells

Human retinal pigment epithelial (RPE) cells were grown in Dulbecco's modified Eagle's medium F12 (DMEM-F12) containing 5% fetal bovine serum, 1% L-glutamine and 0.8% sodium bicarbonate and incubated at 37°C with 5% carbon dioxide and 95% air. After growth with PEG-anthracene, HA, photogels, or degradation products, the cell populations were assessed using the MTT assay (Sigma-Aldrich), which monitors mitochondrial function by conversion of MTT to purple formazan by enzymes. 0.4 mg/mL solution of MTT in medium was added to cells and they were incubated for 4 hours followed by the dissolution of formazan precipitate into DMSO which was measured spectrophotometrically at 595 and 700 nm. PEG-anthracene solutions were

sterile filtered and gels were sterilized with ethanol after synthesis to avoid UV sterilization which would induce premature dimerization.

Solutions of PEG-anthracene in medium were used to evaluate direct effects of the molecules on cell viability and growth. Varying densities of cells (17,000-68,000 cells/well) were grown for 24 hours on a 48 well plate at which time varying concentrations of PEG-anthracene were added. The MTT assay was used to evaluate cell viability 3 days or 7 days after the addition of PEG-anthracene to the cell media. Solutions of HA (0-0.1mg/mL in medium) were added to RPE cells 24 hours after seeding at 120,000 cells/well in a 48 well plate and tested with the MTT assay to assess the effect HA may have on cell growth.

Cells were grown with gels separated by an insert to test for the effect by-products may have on RPE cell growth and respiration. Gels were sterilized with a 2 hour ethanol soak followed by sterile air drying for 16 hours and a medium soak for 2 hours. 24 hours after seeding of 300,000 cells/well in a 24 well plate, cell inserts (low density, 1.0 micron pore-size) with gels were introduced and cells were grown for an additional 3 days or 7 days then tested with the MTT assay.

Long term degradation products were grown with cells to test the long term effects the gels may have as they degrade. Sterilized gels in 2 mL of medium and medium alone (with no gels) were put in an incubator for 45 days. Low concentrations of degradation products (0.2 mL of the soaking medium with 0.4 mL of fresh medium) or high concentrations of degradation products (0.6 mL of soaking medium) were added to cells that were previously seeded at 120, 000 cells/well (48 well plate) and grown for 24

hours. Controls of 0.6 mL of fresh medium were used to verify the technique. Cell growth and viability 3 days later was then assessed with the MTT assay.

3. Results and Discussion

3.1 Gel Synthesis

The grafting of PEG-anthracene to HA provides a photo-induced crosslinking mechanism with anthracene dimerization causing the grafted PEG groups to join effectively causing crosslinking of the HA chains. Varying ratios of PEG-anthracene and HA (available carboxyl groups) were added into the reaction mixture to observe the resulting gel properties and grafting efficiencies (Table 2). Increases in the amount of grafted PEG-anthracene groups was noted to increase the degree of photocrosslinking upon UV exposure with 60 minutes of 365 nm light ($10\text{mW}/\text{cm}^2$) exposure on 80% grafted photogels resulting in an increase of effective crosslinking density of 39% whereas 100% grafted photogels resulted in an increase in effective crosslinking density of 105% (data not shown). In addition to having more bound groups to create more crosslinking connections, increases in the amount of PEG-anthracene groups from 80 to 100 % likely increases the chance of dimerization to occur since the reaction is dependent on the concentration and density of anthracene groups [27]. Due to their higher sensitivity the 100% (1:1 ratio) grafted gels were used in the loading and release studies.

3.2 Loading and Effective Crosslinking Density

As described in Table 3, loading into uncrosslinked photogels is higher than loading into the tighter, more highly crosslinked control PEG hydrogels. Protein loading appears to be dependent on the individual protein properties. For example, less BSA is absorbed versus smaller lysozyme over 24 hours likely due to inhibition of absorption of larger BSA. In addition, protein loading may also be somewhat dependent on ionic interactions since BSA is electronegative at the neutral pH of the PBS buffer. Any remaining negative HA carboxyl groups may inhibit absorption resulting in the observed low loadings. Lysozyme is electropositive at neutral pHs so its high loading may be partially due to attraction to any remaining HA carboxyl groups. Myoglobin is neutral therefore minimal interactions are expected to occur and it loads at amounts between the BSA and lysozyme loadings as expected. Due to detection limits, the loading of dextran could not be determined.

Interactions between HA and loaded compounds could lead to increases in crosslinking. This may be monitored by calculating the effective crosslinking density of loaded versus unloaded photogels and control PEG hydrogels. As illustrated in Figure 2, there were statistically significant increases in effective crosslinking density noted upon the loading of Coomassie Blue into photogels ($p=0.0095$). Insignificant changes were noted with protein loading (myoglobin $p=0.8609$, lysozyme $p=0.0889$ and BSA $p=0.7214$) or dextran loading ($p=0.8141$) (single factor Anova) versus unloaded photogels. Therefore the interactions between Coomassie Blue and the photogels but not the proteins or dextran and the photogels caused physical crosslinking to occur. Control

PEG gels are not significantly different upon loading with Coomassie Blue ($p=0.0544$, single factor Anova). Overall it appears that Coomassie Blue may be interacting with the bound anthracene groups on the HA likely by physical interactions between the aromatic groups present in both molecules. Past studies with alginate photogels by Wells and Sheardown (2010) also noted potential interactions of Coomassie Blue with both alginate and the anthracene but not in a crosslinking fashion [28]. HA photogels have a PEG-anthracene grafting density that is over 2 times higher than previous alginate photogels. Therefore interactions between the Coomassie blue and the anthracene are more prevalent and affect crosslinking. This will ultimately affect release since the strong interactions will allow for rapid and high loading of Coomassie Blue into the HA photogels but the strong attractions will slow Coomassie Blue diffusion through the gels to allow for controlled release over lengthy periods of time.

3.3 Release of different small model compounds

Small model compounds are representative of small drugs such as ophthalmic anti-inflammatory corticosteroids which are around 500 Da in size [29]. Coomassie Brilliant blue (854 Da), Fast Green (765.89 Da) and dextran (1000 Da) were loaded and released into PBS with either no UV or with UV exposure at 365 nm at 1.5 hours for 30 minutes ($10\text{mW}/\text{cm}^2$) (Figure 3). Dextran, likely due to its linear chain structure and resulting entanglement within the photogel matrix, showed small changes in release after UV treatment ($p=0.09$ at 93 hours) whereas globular Coomassie Blue and Fast Green would not entangle and their release was more affected with UV treatment of the

photogels ($p=0.08$ at 968 minutes for Coomassie blue and $p=0.028$ at 936 minutes for Fast Green).

Early time diffusion coefficients were calculated to observe the influence of the different model compounds on release following UV treatment. Coomassie Blue and Fast Green are quite similar in size and structure with both containing similar numbers of aromatic groups, Coomassie blue with 6 and Fast Green with 5, which may interact with the anthracene aromatic groups. As shown in Table 4, the percent decrease in the diffusion coefficient upon treatment with 30 minutes of 365 nm light ($10\text{mw}/\text{cm}^2$) varied from 62 to 82% between the two molecules. Since there was an undetermined amount of loaded dextran, diffusion coefficients could not be accurately calculated. Both Coomassie Blue and Fast Green interacted with the HA photogels to extend their release although the results suggest that Coomassie Blue was likely more attracted to the HA photogel matrix, indicated by its high loading. Quick loading followed by extended release due to both attractions between the small model drugs and photocrosslinking presents a complex system that provides extended release in a smart stimuli-responsive matrix. Upon close examination, there are two phases of Coomassie Blue release from photocrosslinked photogels; there is a burst followed by controlled release then a slight second burst followed by controlled release. After 5 mg/g gel has been released a second burst is noted at 800 hours. This is thought to be due to a critical concentration of Coomassie Blue being released which lowers the overall crosslinking density of the gels, allowing more dye to escape. Loading at a level below this concentration would prevent

a second burst or loadings with compounds that interact in a non-crosslinking fashion would eliminate it entirely.

Early time diffusion coefficients of photogels releasing Coomassie Blue with different UV exposures were compared to determine the effect of different UV treatment times on changes in release rate. Also shown in Table 3, increases in 365 nm UV treatment time (exposure) resulted in greater decreases in the diffusion coefficient versus controls. Note that the diffusion coefficients are slightly different due to batch-to-batch variability likely caused by baseline ambient light exposure during synthesis and processing. Since the photocrosslinking reaction requires individual absorption of light by anthracene groups, increases in UV time increases the amount of dimerization and therefore crosslinking of the HA photogel matrix. The photogels are therefore a unique system with the ability to fine-tune crosslinking and delivery of drug molecules with specified UV treatments. This could have a huge impact in drug delivery technology where current systems are fixed devices assumed to work similarly in different patients. Incremental alterations to fine-tune drug delivery present the opportunity to provide individualized treatments based on the patient and etiology of disease. For retinal drug delivery this is especially important in older populations and diseased eyes. Externally light controlled incremental changes of drug delivery from a device may account for and counterbalance changes that occur in the aging vitreous humour which undergoes liquefaction and contraction ultimately altering drug diffusion and distribution in unpredictable manners [30].

The addition of star-PEG-anthracene into the HA photogel matrices introduces more anthracene groups for dimerization. As shown in Figure 4, at 400 hours there were changes in release of Coomassie Blue from photogels exposed to 20 minutes of 365 nm light versus controls with no UV light exposures with significant decreases occurring at 892 hours ($p=0.005$). Changes in release were obvious by 350 hours. However upon close examination it is apparent that the release rate (slope in Figure 4) decreases in 365 nm treated photogels at 100 hours. There was a burst shortly after UV treatments likely since loosely entangled star-PEG-anthracene may cause contraction to temporarily increase release while increasing crosslinking density. This phenomenon was also noted in alginate photogels containing the same star-PEG-anthracene molecule [28]. Overall the sensitivity of the photogels containing star-PEG-anthracene is higher since large changes in release occurred with 20 minute 365 nm UV treatment times, but there is a burst after UV treatment that initially masks this observation.

3.4 Release of different large model compounds

Large model compounds are representative of anti-VEGF AMD drug molecules which vary from 48-148 kDa in size [31-34]. Lysozyme (14.4 kDa, $pI = 9.3$) and bovine serum albumin (BSA) (67 kDa, $pI = 4.9$) release show an “off effect” when the photogels are irradiated with 365 nm light for 30 minutes (10 mW/cm^2 , total fluence of $18\,000 \text{ mJ/cm}^2$) (Figure 5). Significant decreases following UV light occurred at 5.5 hours for lysozyme ($p=0.001$) and 49 hours for BSA ($p=0.001$). This is consistent with previously studies by Wells *et al.* 2010 which demonstrated myoglobin (17.6 kDa $pI=7.3$, minor 6.8)

release from HA photogels that could be turned off with similar exposures [18]. The effect is attributed to the increased crosslinking density greatly inhibiting the diffusion of the large proteins. Despite differences in molecular weight and charge of BSA, lysozyme and myoglobin, 365 nm treatment of the HA photogels sufficiently shut release down suggesting a size rather than a charge effect and indicating that the system is versatile and will work with a multitude of different large molecular weight drugs. The “off effect” noted with 365 nm exposures was found to occur even with low 365 nm exposures. Specifically 10 minutes of 365 nm light (10 mW/cm^2) was sufficient to stop the release of myoglobin from the photogels (data not shown).

The initial burst from photogels releasing BSA and lysozyme is 44 and 42% of their loaded protein before 365 nm UV exposure shuts down release. However, less BSA is loaded into the gels so a lower release would be expected. The pI of BSA makes it negatively charged at pH 7.4 and it therefore may be less attracted to the small residual negative charge on the carboxyl groups of the HA photogels. Therefore, there is a lower loading of BSA but it releases over a relatively lengthy time extending past 2.5 months. Interestingly, past studies have shown some interaction exists between anthracene derivatives and human serum albumin [35]. Therefore, it is possible that these interactions contribute to the lengthy release time of BSA from the photogels despite its low loading and attraction. Lysozyme, which is slightly positive at pH 7.4 due to its high pI, should show a small attraction to the HA photogels. Therefore, more lysozyme loaded into the gels but showed slower release than BSA from laser treated photocrosslinked photogels.

When photogels were exposed to a 248 nm excimer laser for 18,000 mJ/cm² (310 pulses of 58 mJ/cm² at 5 Hz) the protein release turned back on (Figure 5). There was a slight burst followed by little to no protein release resulting in slight increases in the release curve for lysozyme (p=0.229) and BSA (p=0.370). Decrosslinking from 248 nm is caused by anthracene de-dimerization/dissociation at the surface of the photogels to increase release and the laser exposure was matched to be equivalent to the 365 nm light that previously shut release off. The small increase in protein release with 248nm laser exposure is thought to occur because the surface and not the bulk, of the photogels were decrosslinked since HA effectively absorbs UV at 248nm to prevent its penetration into the photogels as illustrate in previous studies by Wells *et al.* [18].

Diffusion coefficients were used to compare and assess the recovery in release that occurred when the release of protein from photogels was shut down by 365 nm light then turned back on by 248 nm laser treatments. Table 5 shows the diffusion coefficients before and after 365 nm light and 248 nm laser treatments. Following laser exposure, lysozyme release turned on and had continual release for 146 hours with a 2.6% recovery in the diffusion coefficient. With the laser treatments, BSA release from photogels had an 18.4 % recovery of the diffusion coefficient for 146 minutes then release stopped. The negative charge of BSA at pH 7.4 may cause a quick release of protein at the surface that escapes after laser exposure, an effect presumably overcome in the lysozyme containing gels which are likely attracted to the HA matrix.

The use of the 248 nm excimer laser demonstrates the proof of concept for the photogels as an ophthalmic device that may be stimulated with lasers. High wavelengths

are well-used and known to penetrate the eye and low wavelengths are known to penetrate when above 600mW/cm^2 [36]. However, two-photon absorption (TPA) may offer a safer opportunity to cause effective dimerization and de-dimerization at the back of the eye. Ocular tissues at the front of the eye may absorb UV [37]. TPA uses high wavelength visible light that can penetrate through the cornea and lens to absorb and accumulate at the required UV wavelengths with high dimensional and spatial selectivity [38]. Importantly, TPA has been demonstrated to deliver low UV wavelengths and for example has effectively caused the dissociation of the photodimerizing molecule coumarin [39]. TPA may also allow deeper penetration of UV $< 300\text{ nm}$ into the HA photogels. 248 nm excimer laser exposure could not penetrate the HA photogels resulting decrosslinking at the surface to produce small increases in release seen at 1000 hours in Figure 5. Exposures using TPA may result in deeper penetration into the photogels to cause bulk decrosslinking and therefore greater changes in release.

The trends between the different types of proteins show the ability for the photogels to control their release and increase or decrease their release under specific conditions of UV exposure. Wet AMD anti-VEGF drugs have various properties and are around 48-148 kDa in size. Therefore these HA photogels provide a workable platform for their long term, photocontrollable delivery. By lowering the 365 nm photocrosslinking UV exposures, tuneable release profiles similar to those seen with Coomassie Blue release, should be obtainable to allow continuous large molecule release. In addition, the ability to turn off release is a critical asset to for patients with adverse side effects to drugs being delivered by intravitreal drug delivery devices and could be

incorporated into existing devices as a new safety mechanism to allow quick and easy shutdown of drug release when adverse reactions occur.

3.5 Gel Degradation

When placed *in vivo* HA gels may degrade by the enzyme hyaluronidase (HAase) which is present in the posterior segment of the eye at 20 turbidity reducing units (TRU) per mL in human vitreous humour [40]. Both hydrolytic/decrosslinking degradation that may occur in aqueous solutions such as PBS and enzymatic degradation in solutions of HAase were determined to be related to covalent modifications of HA with PEG and to UV crosslinking. HAase concentrations of 100 Units/mL were used to speed up observed effects. Photogel degradation rates in were decreased after UV crosslinking treatments of 30 minutes at 365 nm (10 mw/cm^2) from approximately 400 hours to over 3000 hours in PBS and from 48 hours to past 440 hours in 50 Units solutions of hyaluronidase. While control PEG hydrogels were found to last over 800 hours in PBS, HAase caused degradation times to decrease to ~220 hours both with and without UV exposure, consistent with literature [41] illustrating the lack of UV effect on the HA control hydrogels. As expected, the increased degradation times of the HA photogels in PBS and with HAase was dependent on their crosslinking density from 365 nm UV exposure. HAase is a relatively large enzyme composed of 4 units of 14 kDa [42] which must diffuse into the gels to effectively cause degradation. Therefore photocrosslinking slows influx of the enzyme thereby inhibiting enzymatic biodegradation.

Of note are the long hydrolytic/decrosslinking degradation times associated upon the loading and release of Coomassie Blue and Fast Green into PBS from photogels that have no 365 nm photocrosslinking UV. Loading of Coomassie Blue increased control photogel (no UV) degradation from approximately 400 hours to over 1000 hours in PBS and is attributed to interactions between the dye and the photogels. Fast Green loading had a similar effect increasing degradation past 800 hours with control photogels (no UV). This observation is not noted with photogels loaded with proteins (myoglobin, lysozyme and BSA) further suggesting some crosslinking interactions between the Coomassie Blue and the photogels but not between the proteins and the photogels. Since spectrophotometric studies did not indicate that that UV treatment resulted in covalent interactions between Coomassie Blue and anthracene, it is likely that the interactions are physical, allowing for a slowed and lengthy release and reduced photogel degradation. This is consistent with the observations that Coomassie Blue increased the effective crosslinking density of the photogels (Figure 2) and together they prove there is physical crosslinking occurring. HAase present *in vivo* will ultimately influence release of drugs from the photogels but minimally when they are photocrosslinked. The amounts will be lower than 100 Unit/mL and will likely vary between different patients but this degradation can be accounted for by fine-tuning photogel properties by appropriate UV light treatment of the gel to dial in specific drug release rates.

3.6 Cytocompatibility Studies

Preliminary studies have shown that human corneal epithelial cells are viable with HA and alginate photogels [18]. However, human RPE cells better represent the posterior segment of the eye so were used for a thorough investigation into HA photogel cytocompatibility.

Cells were grown with solutions of PEG-anthracene crosslinker to evaluate its direct effect on cells. Initial screening assays demonstrated that concentrations around 0.1 mg/mL negatively impacted cell growth. Therefore, cells at different densities were grown at concentrations between 0-0.7 mg/mL over 3 and 7 days. As shown in Figure 6, higher cell concentrations were least affected by PEG-anthracene with seeding densities over 34000 cells/well having normal growth up to concentrations of 0.1 mg/mL. Lower cell seeding concentrations of 17,000 cells/well with PEG-anthracene concentrations over 0.05 mg/mL had negatively impacted growth. *In vivo*, it is expected that very little unbound PEG-anthracene will be present since very little is detected after the gels are soaked in water for 24 hours after synthesis. A 1 mm thick and 0.5 cm diameter gel, such as those that were used for drug release studies, contains 5.86 ± 0.02 μg unbound anthracene per disk. In addition there is approximately 1.32 mg of bound PEG-anthracene per disk that is not likely to be released because covalently bound. The gel sizes are much larger than those that would be used *in vivo* as compared to other release devices on the market so once sized appropriately for *in vivo* applications, even less PEG-anthracene would be present [43].

Also important is the potential effect solutions of HA have on cell growth. HA is well known to affect cell behaviour including adhesion, migration and proliferation. RPE cells have been shown to produce HA and maybe be affected by HA via binding to CD44 receptors [44]. Minimal changes in growth were noted when found RPE cells were grown in 0.01 and 0.1 mg/mL HA in medium versus controls grown in medium (data not shown). Therefore the bulk HA of the photogels is not expected to significantly increase cell growth. Since present PEG-anthracene will be bound to HA polymer chains, RPE cells grown with gels and degradation products were also investigated since they are more representative of *in vivo* systems.

3.6.1 Cell Grown in Indirect Contact

Cells grown in the presence of gels evaluate the effect of any released short term degradation and side products on cell viability. In all cases, both the control PEG hydrogels (3 days $p=0.696$, 7days $p=0.148$) and the photogels (3 days $p=0.998$, 7 days $p=0.414$) did not cause significant changes in growth in RPE cells versus controls as illustrated in Figure 7. RPE cells grown with control PEG gels and photogels had similar growth and respiration over 3 and 7 days showing the relative cytocompatibility of the photogels. Any leftover by-products do not significantly effect growth and binding of PEG-anthracene to HA protects cells from its effects. Future studies will check the effects of UV since gels should provide a protective barrier if grown between the UV source and the cells.

3.6.2 Long Term Degradation Product Study

With long term implantations, released degradation products are a concern for cell toxicity. Therefore, medium used to soak gels for 45 days was grown with cells to evaluate the possible effect of long term degradation products on cell cytocompatibility. This was compared to medium that was under the same conditions for 45 days as well as a control of fresh medium. There were no significant changes in growth with RPE cells grown with low ($p=0.343$) or high ($p=0.896$) concentrations of degradation products versus medium as shown in Figure 8.

As the photogels degrades, the risk that PEG-anthracene might leach out increases. However after 45 days this risk appears minimal demonstrated from the lack of changes in cell growth. Degradation products are not expected to build up to high concentrations *in vivo* due to their local transport and removal. Even so, high concentrations were not shown to significantly impact RPE cell viability and even less effects were noted with the more representative low concentrations of degradation products. While showing high compatibility with RPE cells, further cytocompatibility studies and ultimately *in vivo* studies will be required in the future.

4. Conclusions

The HA photogels have the potential to act as controlled long term delivery materials, showing photoresponsive changes in the release of small and large molecule model drug compounds that represent steroidal and wet-AMD drugs. Release can be slowed in an incremental fashion or turned off completely dependent on UV exposures

and the size of the model drugs. HA photogels show high compatibility with human retinal cell lines demonstrating their potential capability for drug delivery *in vivo*. Once put into an appropriate platform, these materials can be used to control release rates, to shut-down the release of drugs if adverse reactions occur and to tailor drug delivery to the patient and disease over the long-term.

Acknowledgements

Funding support from NSERC and 20/20 NSERC Ophthalmic Materials Network is gratefully acknowledged. John Preston and Gabriel Devenyi are acknowledged for excimer laser expertise.

Captions

Table Captions

Table 1. The properties of the different small and large model compounds used in the release studies.

Table 2. The grafting efficiency and resulting molar ratios of PEG-anthracene to HA carboxyl groups in the synthesis of photogels and control PEG hydrogels.

Table 3. The loading of model compounds into the various type of HA gels.

Table 4. The diffusion coefficients and exponents for the release of Fast Green and Coomassie Blue from HA photogels with different UV treatment times.

Table 5. The diffusion coefficients and exponents for the release of proteins from HA photogels before and after 365 nm light and 248 nm laser treatments.

Figure Captions

Figure 1. PEG-anthracene grafted onto HA.

Figure 2. The effective crosslinking of unloaded versus loaded photogels and control PEG hydrogels.

Figure 3. Cumulative release of Coomassie Blue, Fast Green and dextran from HA photogels into PBS at 37°C. At 1.5 hours one set of gels in each study was treated with 365 nm exposures of 10mW/cm² for 30 minutes. Loading of Coomassie Blue was 22.6 ± 0.35 mg/g gel, of Fast Green was 1.3 ± 0.65 mg/g gel and of Dextran was undetermined.

Figure 4. Cumulative release of Coomassie Blue from star-PEG-anthracene containing HA photogels into PBS at 37°C. At 1.5 hours one set of gels was treated with 365 nm exposures of 10mW/cm² for 20 minutes. Loading of Coomassie Blue was 21.9 ± 1.9 mg/g gel.

Figure 5. Lysozyme and BSA release from photogels. At 1.5 hours two sets of gels were irradiated with 365 nm at 10mW/cm² for 30 minutes (18,000 mJ/cm²). At 1038 hours one set of gels was then exposed to a 248 nm excimer laser for 18,000 mJ/cm² (310 pulses of 58 mJ/cm² at 5 Hz). Loading of lysozyme was 0.512 ± 0.14 mg/g gel and of BSA was 0.097 ± 0.01 mg/g gel.

Figure 6. MTT assay results of RPE cells growth with varying PEG-anthracene concentrations over 3 and 7 days.

Figure 7. Gels were added to a confluent layer of RPE cells after 24 hours of growth. After 3 and 7 days there were no significant changes in growth between the PEG gels and the controls (3 days p=0.696, 7days p=0.148) and between the photogels and the controls (3 days p=0.998, 7 days p=0.414) when evaluated using the MTT assay and single factor anova.

Figure 8. Confluent layers of RPE cells had no changes in growth when exposed to media containing low concentrations of degradation products versus controls of medium (n=4, p=0.343) or high concentrations of degradation products versus medium (n=4, p=0.896) when evaluated using the MTT assay and single factor anova.

Tables

Table 1.

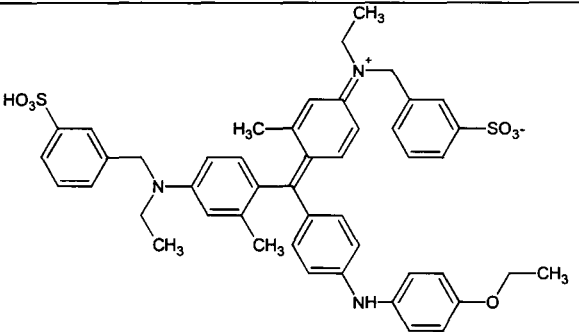
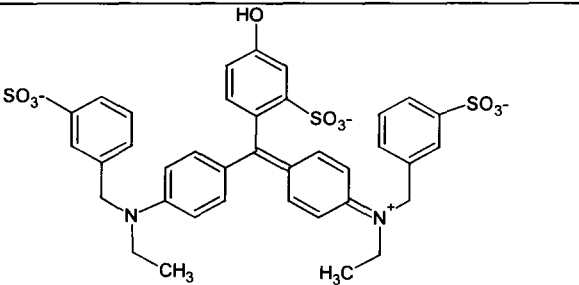
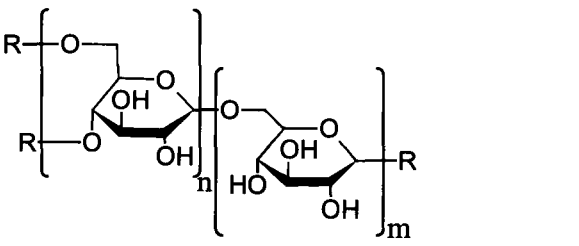
| Small Model Compounds | Name | Molecular Weight | Structure |
|-----------------------|----------------|------------------|--|
| | Coomassie Blue | 833 Da |  |
| | Fast Green | 766 Da |  |
| | Dextran | 1000 Da |  |
| Large Model Compounds | Name | Molecular Weight | Isoelectric Point |
| | Myoglobin | 17,600 Da | 7.3, minor 6.8 |
| | Lysozyme | 14,400 Da | 9.3 |
| | BSA | 67,000 Da | 4.9 |

Table 2.

| Procedural ratio of NH ₂ :COOH | Photogels (grafting of NH ₂ -PEG-anthracene) | | Control PEG Hydrogels (grafting of PEG-diamine) | |
|---|---|--------------------------------|---|----------------------------------|
| | Grafting efficiency | Ratio grafted/percent grafting | Grafting efficiency | Ratio grafted / Percent grafting |
| 1.2:1 | 96% | 1:1 / 100% | 86% | 1:1 / 100% |
| 1.1:1 | 87% | 0.94:1 / 94% | 83% | 0.9:1 / 90% |
| 0.95:1 | 83% | 0.8:1 / 80% | 87% | 0.83:1 / 83% |
| 0.9:1 | 86% | 0.76:1 / 76% | 83% | 0.74:1 / 74% |
| 0.83:1 | 87% | 0.72:1 / 72% | 81% | 0.68:1 / 68% |

Table 3.

| Gel Type | Model Compound | Average estimate loading (mg/g gel) |
|---------------------------|----------------|-------------------------------------|
| Photogels | Coomassie Blue | 22.57 ± 2.06 |
| | Fast Green | 1.30 ± 0.65 |
| | Myoglobin | 0.267 ± 0.055** |
| | Lysozyme | 0.512 ± 0.138* |
| | BSA | 0.097 ± 0.012* |
| Star-containing Photogels | Coomassie Blue | 21.92 ± 1.97 |
| Control-PEG-hydrogels | Coomassie Blue | 1.92 ± 0.11 |
| | Myoglobin | 0.187 ± 0.043 |

*Loading determined by total release when gel degraded.

** From Wells *et al.* 2010 [18].

Table 4.

| Model Compound | UV time (min) | Diffusion coefficient ⁺¹¹ (cm ² /s) x10 | Diffusion exponents | Percent decrease in diffusion coefficient with UV treatment |
|----------------|---------------|---|---------------------|---|
| Fast Green | 0 | 2.87 ± 0.208 | 0.21 ± 0.07 | 62% |
| | 30 | 1.78 ± 0.001 | 0.09 ± 0.01 | |
| Coomassie Blue | 0 | 5.82 ± 0.028 | 0.46 ± 0.03 | 82% |
| | 30 | 1.06 ± 0.002 | 0.20 ± 0.01 | |
| Coomassie Blue | 0 | 8.83 ± 0.017 | 0.51 ± 0.02 | 66% * |
| | 20 | 2.98 ± 0.011 | 0.27 ± 0.02 | |
| Coomassie Blue | 0 | 0.49 ± 0.002 | 0.46 ± 0.03 | 46% |
| | 7 | 0.27 ± 0.0003 | 0.36 ± 0.02 | |

*Calculated from release study in Wells *et al.* 2010 [18].

Table 5.

| Protein | Treatment | Diffusion Coefficient (cm ² /s) | Diffusional Exponent | Percent Recovery of the Diffusion Coefficient after 365 nm then laser exposure |
|----------|---------------------|--|----------------------|--|
| Lysozyme | No UV (control) | 7.15×10^{-10} | 0.15 | 2.6 % |
| | After 365 | 0 | 0 | |
| | After 365 and laser | 1.84×10^{-11} | 0.22 | |
| | After 146 minutes | 4.63×10^{-13} | 0.01 | |
| BSA | No UV (control) | 5.88×10^{-10} | 0.12 | 18.4 % |
| | After 365 | 0 | 0.003 | |
| | After 365 and laser | 1.08×10^{-10} | 0.5 | |
| | After 146 minutes | 0 | 0 | |

Figures

Figure 1.

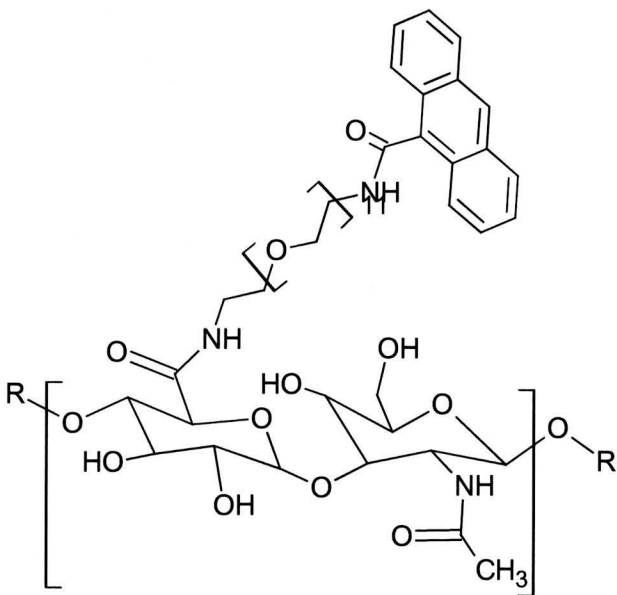


Figure 2.

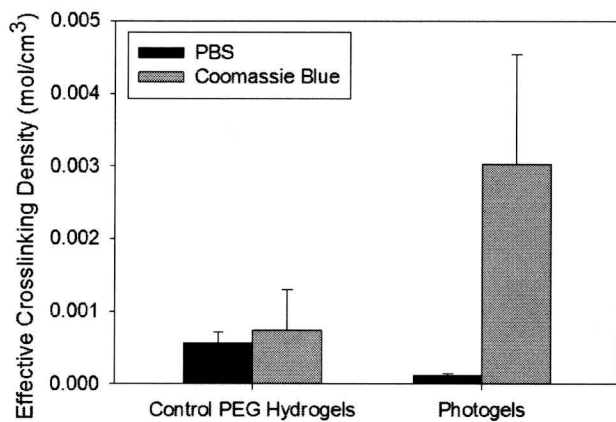


Figure 3.

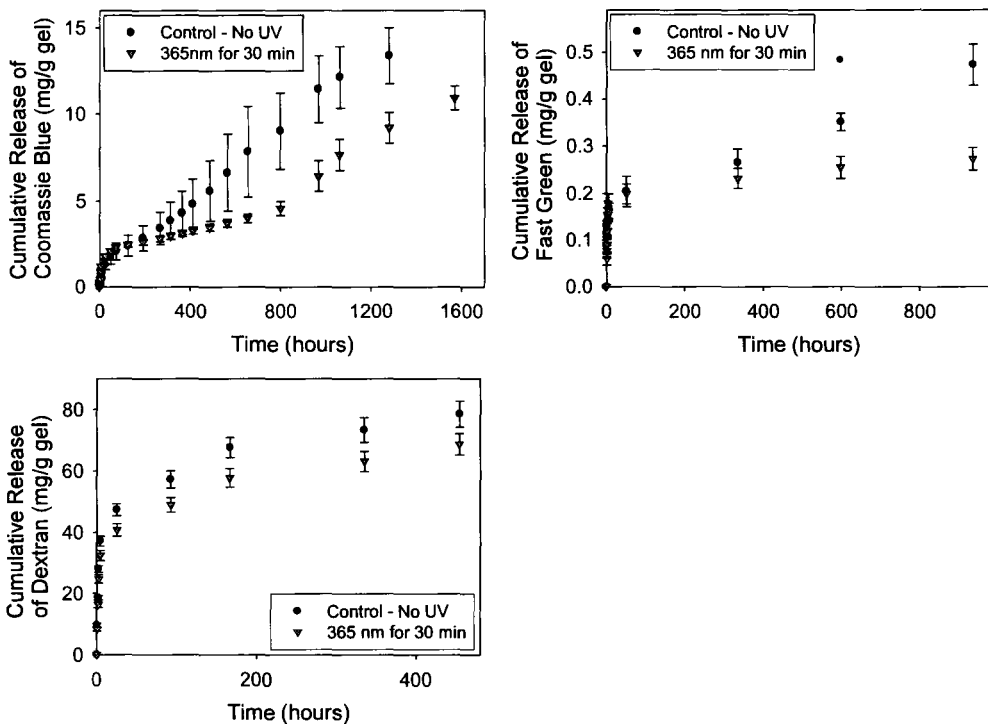


Figure 4.

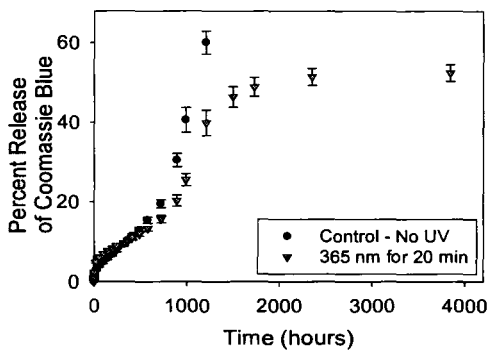


Figure 5.

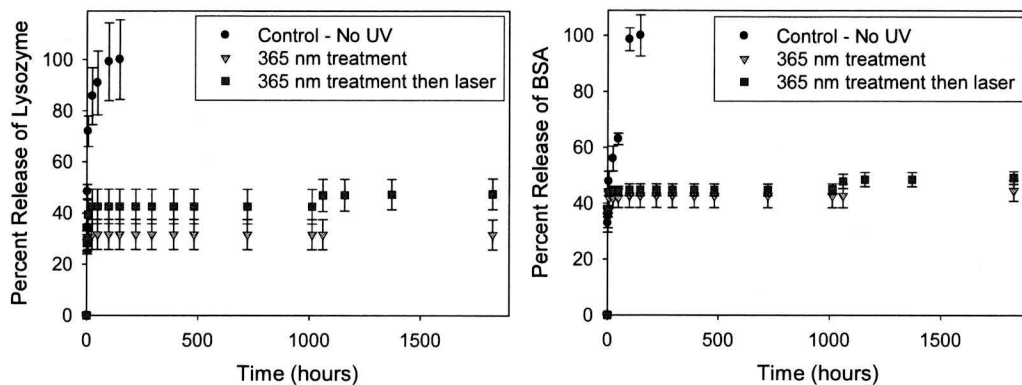


Figure 6.

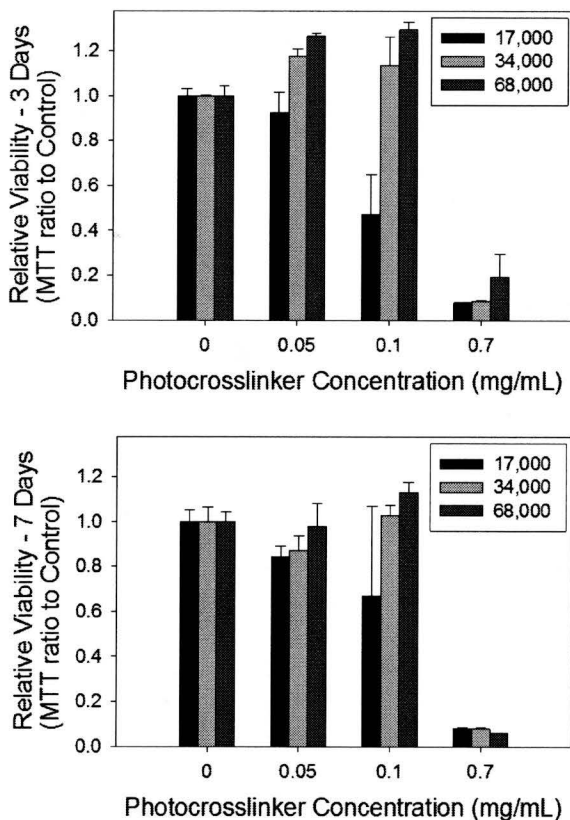


Figure 7.

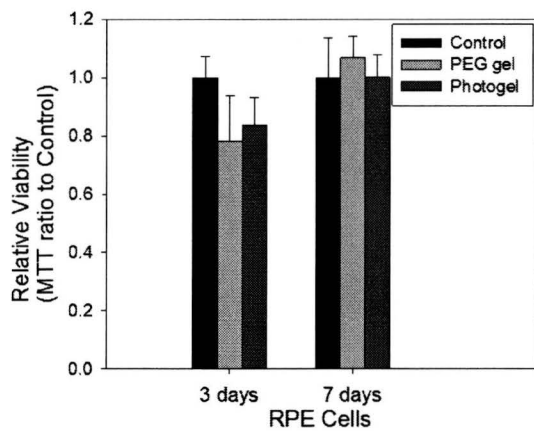
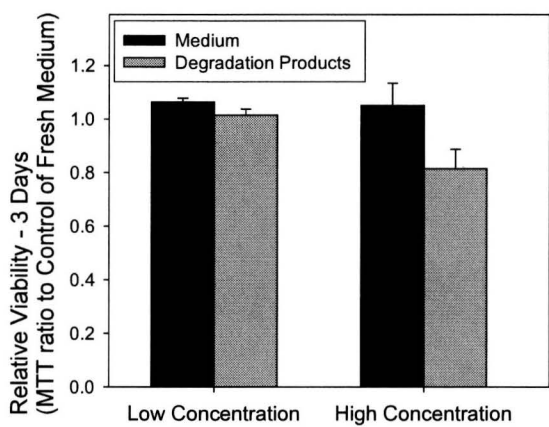


Figure 8.



References

1. Qiu Y, Park K. Environment-sensitive hydrogels for drug delivery. *Adv Drug Delivery Rev* 2001;53:321-339.
2. Molokhia SA, Sant H, Simonis J, Bishop CJ, Burr RM, Gale BK, Ambati BK. The capsule drug device: Novel approach for drug delivery to the eye. *Vision Res* 2010;50:680-685.
3. Lang JC. Ocular drug delivery conventional ocular formulations. *Adv Drug Delivery Rev* 1995;16:39-43.
4. Urtti A. Challenges and obstacles of ocular pharmacokinetics and drug delivery. *Adv Drug Delivery Rev* 2006;58:1131-1135.
5. del Amo EM, Urtti A. Current and future ophthalmic drug delivery systems. A shift to the posterior segment. *Drug discovery today* 2008;13:135-143.
6. Kurz D, Ciulla TA. Novel approaches for retinal drug delivery. *Ophthalmol Clin N Am* 2002;15:405-410.
7. Fletcher EC, Lade RJ, Adewoyin T, Chong NV. Computerized Model of Cost-Utility Analysis for Treatment of Age-Related Macular Degeneration. *Ophthalmology* 2008;115:2192-2198.
8. Yasukawa T, Ogura Y, Tabata Y, Kimura H, Wiedemann P, Honda Y. Drug delivery systems for vitreoretinal diseases. *Prog Ret Eye Res* 2004;23:253-281.
9. Booth BA, Denham LV, Bouhanik S, Jacob JT, Hill JM. Sustained-release ophthalmic drug delivery systems for treatment of macular disorders. Present and future applications. *Drugs Aging* 2007;24:581-602.
10. Yasukawa T, Ogura Y, Sakurai E, Tabata Y, Kimura H. Intraocular sustained drug delivery using implantable polymeric devices. *Adv Drug Delivery Rev* 2005;57:2033-2046.
11. Choonara YE, Pillay V, Danckwerts MP, Carmichael TRd,L.C. A review of implantable intravitreal drug delivery technologies for the treatment of posterior segment eye diseases. *J Pharm Sci* 2010;99:2219-2239.
12. Holz FG, Korobelnik J, Lanzetta P, Mitchell P, Schmidt-Erfurth U, Wolf S, Markabi S, Schmidli H, Weichselberger A. The Effects of a Flexible Visual Acuity-Driven Ranibizumab Treatment Regimen in Age-Related Macular Degeneration: Outcomes of a Drug and Disease Model. *Invest Ophthalmol Vis Sci* 2010;51:405-412.

13. Lalwani GA, Rosenfeld PJ, Fung AE, Dubovy SR, Michels S, Feuer W, Davis JL, Flynn Jr HW, Esquiabro M. A variable-dosing regimen with intravitreal ranibizumab for neovascular age-related macular degeneration: year 2 of the PrONTO Study. *Am J Ophthalmol* 2009;148:43-58.
14. Bouas-Laurent H, Castellan A, Desvergne J-, Lapouyade R. Photodimerization of anthracenes in fluid solutions: (part 2) mechanistic aspects of the photocycloaddition and of the photochemical and thermal cleavage. *Chem Soc Rev* 2001;30:248-263.
15. Kumar GS, Neckers DC. Photochemistry of azobenzene-containing polymers. *Chem Rev* 1989;89:1915-1925.
16. Kaur M, Srivastava AK. Photopolymerization: a review. *J Macromol Sci Poly Rev* 2002;C42:481-512.
17. Bishop PN. Structural macromolecules and supramolecular organisation of the vitreous gel. *Prog Ret Eye Res* 2000;19:323-344.
18. Wells LA, Brook MA, Sheardown H. Graftable PEG-anthracene to generate photoresponsive hydrogels for drug delivery . Submitted to the *J Biomed Mater Res Part A*;2010.
19. Bray JC, Merrill EW. Poly (vinyl alcohol) hydrogels. Formation by electron beam irradiation of aqueous solutions and subsequent crystallization. *J Apply Poly Sci* 1973;17:3779-3794.
20. Flory PJ, Rehner J. Statistical mechanics of cross-linked polymer networks II. Swelling. *J Chem Phys* 1943;11:521-526.
21. de Jong SJ, van Eerdenbrugh B, van Nostrum CF, Kettenes-van den Bosch JJ, Hennink WE. Physically crosslinked dextran hydrogels by stereocomplex formation of lactic acid oligomers: degradation and protein release behavior. *J Controll Rel* 2001;71:261-275.
22. Leach JB, Bivens KA, Patrick CW, Schmidt CE. Photocrosslinked hyaluronic acid hydrogels: natural, biodegradable tissue engineering scaffolds. *Biotechnol Bioeng* 2003;82:578-589.
23. Li CY, Birnkrant MJ, Natarajan LV, Tondiglia VP, Lloyd PF, Sutherland RL, Bunning TJ. Polymer crystallization/melting induced thermal switching in a series of holographically patterned Bragg reflectors. *Soft Mat* 2005;1:238-242.

24. Leach JB, Schmidt CE. Characterization of protein release from photocrosslinkable hyaluronic acid-polyethylene glycol hydrogel tissue engineering scaffolds. *Biomaterials* 2005;26:125-135.
25. Chorny RC, Krasuk JH. Extraction for different geometries. Constant diffusivity. *Ind Eng Chem Process Des Dev* 1966;5:206-208.
26. Ritger PL, Peppas NA. A simple equation for description of solute release. 1. Fickian and non-fickian release from non-swellable devices in the form of slabs, spheres, cylinders or discs. *J Controlled Release* 1987;5:23-36.
27. Bratschkov C, Karpuzova P, Mullen K, Klapper M. Synthesis and photochemical transformations of an anthracene containing methacrylic copolymer. *Polymer Bulletin* 2001;46:345-349.
28. Wells LA, Sheardown H. Controlled release with polyethylene glycol - anthracene modified alginate. Submitted to *Acta Biomaterialia* 2010.
29. Jaffe GJ, Ashton P, Pearson PA. *Intraocular drug delivery*. NY: Taylor & Francis, 2006.
30. Laude A, Tan LE, Wilson CG, Lascaratos G, Elashry M, Aslam T, Patton N, Dhillon B. Intravitreal therapy for neovascular age-related macular degeneration and inter-individual variations in vitreous pharmacokinetics. *Prog Ret Eye Res* 2010;XXX:1-10. In press.
31. Blick SKA, Keating GM, Wagstaff AJ. Ranibizumab. *Drugs* 2007;67:1199-1206.
32. Ahmadi MA, Lim JJ. Pharmacotherapy of age-related macular degeneration. *Expert Opin Pharmacother* 2008;9:3045-3052.
33. Landa G, Amde W, Doshi V, Ali A, McGevna L, Gentile RC, Muldoon TO, Walsh JB, Rosen RB. Comparative study of intravitreal bevacizumab (Avastin) versus ranibizumab (Lucentis) in the treatment of neovascular age-related macular degeneration. *Ophthalmologica* 2008;223:370-375.
34. Anderson OA, Bainbridge JWB, Shima DT. Delivery of anti-angiogenic molecular therapies for retinal diseases. *Drug Discovery Today* 2010;15:272-282.
35. Skupinska K, Zylm M, Misiewicz I, Kasprzycka-Guttman T. Interaction of anthracene and its oxidative derivatives with human serum albumin. *Acta Biochim Pol* 2006;53:101-112.

36. Schmidt-Erfurth U, Hasan T. Mechanisms of action of photodynamic therapy with verteporfin for the treatment of age-related macular degeneration. *Surv Ophthalmol* 2000;45:195-213.
37. Thompson KP, Ren QS, Parel JM. Therapeutic and diagnostic application of lasers in ophthalmology. *Proc IEEE* 1992;80:838-860.
38. Bhawalkar JD, He GS, Prasad PN. Nonlinear multiphoton processes in organic and polymeric materials. *Rep Prog Phys* 1996;59:1041-1070.
39. Hartner S, Kim HC, Hampp N. Phototriggered release of photolabile drugs via two-photon absorption-induced cleavage of polymer-bound dicoumarin. *J Polym Sci Part A: Polym Chem* 2007;45:2443-2452.
40. Schwartz DM, Shuster S, Jumper MD, Chang A, Stern R. Human vitreous hyaluronidase: isolation and characterization. *Curr Eye Res* 1996;15:1156-1162.
41. Jeon O, Song SJ, Lee K-, Park MH, Lee SH, Hahn SK, Kim S, Kim B-. Mechanical properties and degradation behaviors of hyaluronic acid hydrogels cross-linked at various cross-linking densities. *Carbohydrate Polymers* 2007;70:251-257.
42. Khorlin AY, Vikha IV, Milishnikov AN. Subunit structure of testicular hyaluronidase. *FEBS Lett* 1973;31:107-110.
43. Weiner A. Drug delivery systems in ophthalmic applications. In: Yorio T, Clark AF, Wax MB, editors. *Ocular therapeutics: eye on new discoveries* New York: Academic Press, 2008. p. 7-30.
44. Garg HG, Hales CA. *Chemistry and biology of hyaluronan*. Oxford UK: Elsevier Ltd., 2004.

7.0 Conclusions and Future Work

In this thesis, anthracene, as a model photoactive linker, was incorporated into hydrogel polymers via a versatile grafting technology that successfully introduced photoresponsive properties of sufficient influence to modify diffusion and release of various model drug compounds. Reversibly photodimerizing amine-terminated PEG-anthracene molecules were synthesized and grafted onto different hydrogel polymer backbones via carbodiimide chemistry at varying grafting densities. PEG-anthracene dimerizes at UV wavelengths above 300 nm resulting in the formation of PEG based crosslinks in these materials. Exposure to light below 300 nm resulted in decrosslinking. Low PEG-anthracene grafting densities produced viscous liquids that became more viscous or gelled upon 365 nm UV exposure. Higher grafting densities led to the production of loose gels that had increased crosslinking upon 365 nm UV exposures. Both alginate and hyaluronate (HA) based “photogels” were created by grafting PEG-anthracene to their carboxyl groups. Linking and dimerization were verified by either carbon NMR or UV/vis spectroscopy. Alginate was selected because it is a non-toxic hydrophilic polymer from a renewable resource (kelp) making it both cheap and readily available. HA was used because it is a hydrophilic polymer that already exists in the vitreous humour of eyes, a potential target application of these gels. As a result, HA gels should be relatively biocompatible and possibly biodegradable via native enzymes. Determination of the effective crosslinking density of photogels before and after UV exposure versus controls demonstrated the ability for 365 nm light to cause increases in crosslinking. The release of loaded small and large model drug compounds from

photogels was found to be photoreversible with decreased release with 365 nm UV treatment that could be briefly increased with 248 nm excimer laser exposures.

There appears to be a clear relationship between both grafting density and hydrogel molecular weight in the synthesis of gels versus liquids. High density grafting of PEG-anthracene to HA resulted in loose gels where low density grafting to HA resulted in viscous liquids. In addition, it was also found that with matched grafting densities, high molecular weight HA of 132 kDa produced gels while a lower molecular weight HA of 31 kDa produced liquids. This was thought to be due to varying degrees of entanglement which would introduce more physical crosslinks in higher molecular weight HA. Discovering the nature of this relationship would be valuable in the exploration to use photostimuli to modify the viscosity of fluids and potentially lead to the development of injectable, *in situ* gelable materials. For example, molecular weights of HA above 1000 kDa may require lower PEG anthracene grafting to produce photogels of a similar nature to the 132 kDa photogels used in this study. A variety of molecular weights of HA prepared with similar grafting would likely produce an array of gels and liquids. They could prove to be useful to allow the easy delivery of fluids followed by viscosity adjustments for joint friction applications or as aqueous or vitreous humour substitutes.

Since the lower molecular weight 31 kDa HA produced viscous liquids when grafted with PEG-anthracene which could be gelled with the application of 365 nm light, it is possible that this may be extended to the development of *in situ* gelling devices. The widespread use of lasers in medicine may facilitate rapid anthracene photodimerization and therefore quick gelation. High viscosity fluids could be injected and would not

significantly diffuse after injection. Therefore, the location would likely be contained in a small area to allow for subsequent laser treatment for gelation. Alternatively the photocrosslinkers could be grafted to or the photogels combined with thermosensitive materials. The resulting material would likely gel shortly after injection due to temperature changes, followed by precise fine-tuning of crosslinking to allow strict control of the biomaterial properties for drug delivery.

High loading of model drug compounds into photogels followed by their slow release was possible by soaking loosely crosslinked dried gels with low concentration solutions of model drug compounds followed by their photocrosslinking to “lock” the model drug compounds within the matrix. These high loaded materials showed controlled release since the new crosslinks impede the diffusion of drugs out of the matrix. In addition, interactions of small molecules with the anthracene groups provided a mechanism to slow diffusion of aromatic-containing compounds out of the photogels. Alginate photogels were particularly interesting as they showed the potential for interaction with both the alginate and anthracene components. In the case of the model compound Coomassie Blue, a release duration of more than 2000 hours was observed in non-photocrosslinked gels. HA photogels with higher grafting also showed delayed release and with Coomassie Blue-anthracene interactions sufficiently strong to cause increases in effective crosslinking density with Coomassie Blue loading. Release of large proteins was more inhibited by photogels exposed to 365 nm light treatments with an on/off release profile observed. While not surprising that release rates of larger molecules were more inhibited than those of smaller molecules, this does lead to the potential for

tailoring of drug release rates between high and extremely low or off levels, allowing for the devices to be tuned with disease progression.

UV exposure to HA and alginate photogels altered the diffusion and release of small and large model compounds versus control with no UV. The changes in release of small molecules were found to be incremental with larger decreases in release rates occurring with increases in exposure to 365 nm light. For example, 365 nm treatment times from 7, 20 and 30 minutes resulted in percent decreases in diffusion of 46% 66% and 82%. A release system that has alterable rates is a significant accomplishment in a smart-drug-delivery research era mostly consisting of pulsatile on/off systems. The ability to fine-tune release would allow for the optimization of treatment for individuals. The results from these types of treatments would provide data to further the understanding of diseases and their variation between individuals.

The small model drugs used in release studies were representative of anti-inflammatory steroids (500 kDa) [1] and larger proteins used were representative of AMD drugs (48-148 kDa) [2-5] with varying charge properties to explore interactions. Future studies looking at the release of more relevant drug molecules including Lucentis or Avastin from photogels followed by activity studies using ELISAs would further evaluate their use for AMD drug delivery. Many systems are unable to deliver active forms of Lucentis; however, most of these systems were made of hydrophobic polymers. Therefore, there is the possibility that the high hydrophilicity of alginate and HA photogels may be key in the maintenance AMD drug activity from controlled release devices.

Control hydrogels that were crosslinked PEG-diamine provided a comparison to confirm decreases in release from photogels exposed to 365 nm light were due to incorporated anthracene and not other polymer-related phenomena. 365 nm UV exposure to Coomassie Blue loaded control PEG hydrogels had an opposing effect, slightly increasing release of Coomassie Blue after UV treatment presumably due to slight chain scission since anthracene was not present to absorb the light energy. Both HA and alginate control PEG hydrogels turned out to be valuable control delivery materials. HA would degrade *in vivo* and making it valuable in a variety of applications where surgical removal of delivery materials is invasive and undesired.

Alterations in the formulation of the photogels altered their photosensitivity resulting in variations in the magnitude of the change in release of Coomassie Blue after 365 nm UV treatment. There were variations between alginate and HA thought to be due to light scattering with alginate, reducing the transmission of UV; HA was found to allow complete transmission of UVA but not the lower UV wavelengths under 300 nm. Alginate photogels and control gels had decreased degradation rates compared to physically crosslinked calcium alginate gels. Calcium-reinforced alginate photogels are tighter and have more efficient photocrosslinking with 365 nm UV exposures. The addition of 4 arm star-PEG-anthracene into HA and alginate photogels created a system with a large burst followed by controlled release. The nature of the different release kinetics in this system should be investigated through the creation of gels with varying star-PEG-anthracene contents and may be useful to optimizing the delivery properties for specific drug molecules.

Amine-terminated PEG-anthracene was synthesized using simple chemistry that may be modified to alter the end groups to include different chromophores or different terminal groups for polymer grafting. Binding of anthracene to hydrophilic PEG allowed hydrophobic anthracene to become soluble in aqueous solutions and allowed it to maintain its dimerization/dedimerization capabilities. The simple, versatile chemistry used to make the PEG-anthracene opens the possibility for investigating the incorporation of other chromophores into the hydrogel systems. Nitrocinnamate [6], cinnamylidene acetate [7] and coumarin [8,9] are popular photodimerizers for polymer modifications. Carboxyl terminated forms, such as readily available *trans*-4-nitrocinnamic acid (Sigma Aldrich) could easily be substituted for anthracene-9-carboxylic acid to produce a PEG-nitrocinnamate molecule that could form photogels with different sensitivities and interactions with loaded drug molecules. By using different end-terminated PEG, different chromophores may be bound using different chemistries.

In chapter 4, two different sized PEG chains ($n=3$ or 11) were used to synthesize PEG-anthracene. For the majority of the subsequent studies, the 11 unit PEG was chosen since it had higher yields likely due to solubility. When grafted, the length of the PEG must be adequate to give mobility to anthracene to allow it to align for dimerization to occur. The creation of PEG-anthracene with different sized PEG ranging from 11 to 100 units could ultimately be used to create gels with different pore structures and photosensitivity. Studies investigating different lengths to optimize dimerization would both create the most effective photogels and also provide valuable insight into what length of PEG would allow for most efficient photocrosslinking.

Light effectively caused dimerization of anthracene and crosslinking of the photogels, however, due to the low powers of the lamps, long exposure times of 10-40 minutes were required. Excimer lasers for 248 nm exposures on the other hand, led to a relatively quick response due to the high power of the laser. While increases in Coomassie Blue and protein release were noted from photocrosslinked HA photogels that were treated with the 248 nm laser, future studies should investigate this further. It is thought that the 248 nm wavelengths do not penetrate the entire HA photogel since HA does not allow its transmission. SEM on the top versus bottom surface of laser treated gels may provide insight into this theory since the roughness of the laser exposed surface is likely higher than its opposing surface due to one-sided de-crosslinking. Optimization of the laser treatments must also be performed to further validate their ability to increase release and to determine the required exposures.

Due to their high power and low required exposure times, it is envisioned that lasers will be used for UV treatments for *in vivo* applications. However, excimer lasers for *in vivo* UV treatments are not a viable UV source since the UV light may not effectively penetrate the front layers of the eye potentially causing damage to the cornea and lens. Two-photon absorption (TPA) uses two wavelengths (equal or different) that are both absorbed by molecules (within nanoseconds) and accumulate to an equivalent absorption of higher energy/lower wavelengths. For example, anthracene dimers have been shown to dissociate using TPA with two 532 nm photons; which was equivalent to 266 nm [10]. Using TPA for the de-dimerization of anthracene within the photogels may therefore resolve any inhibition in photogel absorption allowing full penetration into the

gels, as opposed to the surface decrosslinking observed by 248 nm treatments in chapters 3 and 6. One further advantage of these systems is their relatively widespread availability due to the development of light responsive drugs for treatment of AMD. Ultimately, TPA will be an important tool for *in vivo* applications to allow for UV treatments to effectively and safely penetrate the cornea and lens to reach photogel drug delivery platforms. Therefore, experiments into its implementation are an important next step in photogel investigations and development.

Initial degradation studies show that hyaluronidase (50 units) degraded uncrosslinked photogels in 48 hours while photocrosslinked photogels remained intact past 440 hours. The photocrosslinking of the photogels likely inhibits the migration of the enzymes into the gels to slow degradation. The carbazole assay should be used in future degradation studies to assess the amount of HA that degrades and is released from the gels over time [11]. This may provide further insight into the rates of degradation of photocrosslinked photogels. In addition, native hyaluronidase found in vitreous humour could influence the delivery rates from HA photogels. Therefore, release studies with hyaluronidase-containing PBS should be performed to determine its effect on release from photogels exposed to 365 nm light versus controls (no UV).

The cytocompatibility of the photogels was found to be relatively high even though anthracene is a known toxin. The high compatibility of the photogels is thought to be due to the altered properties of anthracene as a result of PEG modification and protection via grafting into the polymer hydrogels. Both human corneal epithelial and human retinal pigment epithelial cell lines showed similar growth to controls when grown

with photogels. Long term degradation products had insignificant effects on RPE cell lines and only high concentrations of PEG-anthracene impacted the growth of low density cell populations; this is not expected to be an issue once PEG-anthracene is bound to polymer gels. Since photogels absorb UV light during dimerization, there is the likelihood that their reduced UV transmission will have a protective effect when placed between UV sources and tissues or cells. Ultimately the UV protective effects of these materials should be investigated.

Despite the promising cytocompatibility study results that showed normal cell growth and viability with human retinal and corneal cell lines, anthracene may have a negative stigma in the health community since it is a polycyclic aromatic hydrocarbon. Therefore, studies looking into coatings that would encapsulate disks or microparticle photogels while still allowing UV transmission would be beneficial in the development of workable platforms. This may also provide a barrier to protect HA photogels from hyaluronidase degradation if desired.

Overall, the results of this study suggest that PEG-anthracene is a generic, graftable photocrosslinker that introduces photosensitive properties into hydrogels sufficient to cause changes in crosslinking and diffusion of model drug compounds. The chemistry to synthesise PEG-anthracene is versatile and can be easily modified to incorporate different chromophores or allow for its grafting to different polymers making it a generic system and a potentially valuable tool in the synthesis, development and scientific exploration of photoreversible polymers. Both alginate and HA photogels were synthesized by grafting of PEG anthracene onto the carboxyl groups via carbodiimide

chemistry. Dimerization of anthracene within the gels by 365 nm UV light, verified by spectrophotometry or carbon NMR, causes increases in their crosslinking density and slows the release of small and large model drug compounds. Exposure to 248 nm laser light was found to increase release for periods of time. The ability for these photoresponsive materials to fine-tune release of molecules due to photo-stimuli could allow for drug delivery to be adjusted according to disease progression and individualized patients make it a potentially important discovery in drug delivery technology.

7.1 References

1. Jaffe GJ, Ashton P, Pearson PA. Intraocular drug delivery. NY: Taylor & Francis, 2006.
2. Blick SKA, Keating GM, Wagstaff AJ. Ranibizumab. *Drugs* 2007;67:1199-1206.
3. Ahmadi MA, Lim JI. Pharmacotherapy of age-related macular degeneration. *Expert Opin Pharmacother* 2008;9:3045-3052.
4. Landa G, Amde W, Doshi V, Ali A, McGevna L, Gentile RC, Muldoon TO, Walsh JB, Rosen RB. Comparative study of intravitreal bevacizumab (Avastin) versus ranibizumab (Lucentis) in the treatment of neovascular age-related macular degeneration. *Ophthalmologica* 2008;223:370-375.
5. Anderson OA, Bainbridge JWB, Shima DT. Delivery of anti-angiogenic molecular therapies for retinal diseases. *Drug Discovery Today* 2010;15:272-282.
6. Zheng Y, Andreopoulos FM, Micic M, Huo Q, Pham SM, Leblanc RM. A novel photoscissile poly(ethylene glycol)-based hydrogel. *Adv Funct Mater* 2001;11:37-40.
7. Andreopoulos FM, Beckman EJ, Russell AJ. Light-induced tailoring of PEG-hydrogel properties. *Biomaterials* 1998;19:1343-1352.
8. Trenor SR, Long TE, Love BJ. Photoreversible chain extension of poly(ethylene glycol). *Macromol Chem Phys* 2004;205:715-723.

9. Trenor SR, Shultz AR, Love BJ, Long TE. Coumarins in polymers: From light harvesting to photo-cross-linkable tissue scaffolds. *Chem Rev* 2004;104:3059-3077.
10. Dvornikov AS, Rentzepis PM. Anthracene monomer-dimer photochemistry: high density 3D optical storage memory. *Res Chem Intermed* 1996;22:115-128.
11. Song JM, Im JH, Kang JH, Kang DJ. A simple method for hyaluronic acid quantification in culture broth. *Carbohydr Polymer* 2009;78:633.634.

APPENDIX 1

PEG-anthracene Synthesis

Purpose

To synthesis amine terminated PEG-anthracene

Materials

- O-(2-Aminoethyl)-O'-[2-(Boc-amino)ethyl]decaethylene glycol (Boc-PEG-amine)
- Anthracene-9-carboxylic acid
- Dichloromethane (DCM) (dried over molecular sieves), ethyl acetate, methanol and hexane
- 1-ethyl-(dimethylaminopropyl) carbodiimide hydrochloride (EDC)
- Trifluoroacetic acid (TFA)
- Triisopropylsilane (TIPS)

Methods

*Prepare under dark conditions.

1. Reaction 1

1. In a round bottom flask under stirring, dissolve 40 drops (≈ 200 mg) of Boc-PEG-amine into 20 mL of dry DCM.
2. Add 288 mg of anthracene-9-carboxylic acid then 268 mg of EDC.
3. Seal under nitrogen and cover in tinfoil. Stir for 24 hours at room temperature.

2. Purification

1. Dry in a rotating evaporator under vacuum at 40°C then dry with a stream of nitrogen if slight DCM remains.
2. Dissolve/disperse in water (30 mL) and using a separatory funnel to extract with 2 x 20 mL of ethyl acetate.
3. Dry ethyl acetate layer in a rotating evaporator under vacuum at 60°C then dry with a stream of nitrogen.

3. Reaction 2

1. Dissolve in 16 mL of DCM.
2. Add 4 mL of TIPS then slowly add 2 mL of TFA (dropwise).
3. Leave stirring in tinfoil for 4-24 hours (4 hours is adequate).

4. Purification

1. Can remove lid in fumehood to allow high volatiles to escape, then dry in a rotavap under vacuum at 40°C. Then use a stream of nitrogen to completely dry.
2. Dissolve in 16 mL of water. Centrifuge in 2 tubes at 3000 rpm for 10 minutes.
3. Remove and filter top liquid layer through a syringe filter at 0.2 microns (other layer will be solid pellet).
4. Freeze dry.

Further purification

1. Once have several batches combine.
 2. Load the top of a silica column with hexane/DCM (1:1 ratio) and run with methanol/DCM (7:3 ratio). Dry.
5. Storage
1. PEG-anthracene will be highly viscous, clear, orange liquid.
 2. Store in sealed dry vials, under nitrogen. Cover with tinfoil to prevent premature dimerization.

APPENDIX 2**Grafting of PEG-anthracene onto Hyaluronic Acid*****Purpose***

To graft PEG-anthracene onto HA to create HA photogels.

Materials

- Hyaluronic acid (132 or 31 kDa)
- 4-morpholinoethanesulfonic acid (MES) buffer
- 1-ethyl-(dimethylaminopropyl) carbodiimide hydrochloride (EDC)
- N-hydroxysuccinimide (NHS)
- NH₂-PEG-Anthracene

Methods

1. Preparation of MES buffer containing 0.1M MES and 0.5M NaCl
Dissolve 9.762g of MES and 14.611g of NaCl into 500mL of deionized water.
Adjust pH to 6 with NaOH/HCl
2. Solution preparation
 1. Make a 6% solution of HA in MES buffer.
 2. Make 191.6mg/mL EDC and 57.5mg/mL NHS in MES buffer.
 3. Make 300 mg/mL solution of PEG-anthracene in MES buffer, add approximately 0.00158 mL of 1N NaOH per mg of PEG-anthracene to bring the final pH to 6.
3. Synthesis
 1. Add 0.353 mL of EDC/NHS solution to 0.443 mL of PEG-anthracene solution (important: do not want to add EDC/NHS directly to HA because may form ester bonds)
 2. Add this solution to 1 mL of 6% HA and mix well (doing this in a 50mL falcon tube helps).
 3. Mix and transfer with a glass Pasteur pipette to a glass plate with slides as spacers. This setup should be in a container to it can be covered with tinfoil and placed inside a fridge.
 4. Leave in fridge (4°C) for 72 hours.
4. Purification
 1. Punch gels to 0.5 cm diameters and soak each 1 mL deionized water (in a 48 well plate) for 24 hours.
 2. Weigh labeled, empty vials. Dab dry gels with kimwipe and add each to a vial. Weigh the vial again to obtain mass.
 3. Dry in open for 72 hours in dark area (box). Do not freeze dry.
 4. Seal and store protected in tinfoil.

APPENDIX 3

Model Drug Assays

3.1 Small Molecule Detection

Materials

- Samples and calibration samples of known concentrations
- 96 well plate
- Microplate reader

Methods

1. Coomassie Blue and Fast Green <1mg/mL

Low concentration samples (for release studies ≤ 0.1 mg/mL)

1. Pipette 300 μ L of each sample/standard (with repeats) into different wells in a 96 well plate.
2. Read adsorbance using a microplate reader at 595 nm for Coomassie Blue and 630 nm for Fast Green.
3. Run unknown samples against a calibration curve to determine their concentration.

High concentration samples (for loading, 0.1-0.5 mg/mL)

1. Preload 96 well plate wells with 130 μ L of PBS
2. Add 20 μ L of each solution into each well (remember the blank of PBS)
3. Measure with microplate reader (595nm filter or 630 nm filter)

2. Dextran Detection

1. Pipette 100 μ L of each sample/standard and add 200 μ L of ethanol into a 96 well plate.
2. Wait 5 minutes.
3. Read adsorbance using a microplate reader at 405 nm.
4. Run unknown samples against a calibration curve to determine their concentration.

3.2 Protein Detection

A microplate version of the Bradford assay can detect protein amounts of 0.001-0.1 mg/mL.

Materials

- Samples and calibration samples of known concentrations
- 96 well plate
- Bradford Reagent
- Microplate reader

Methods

1. Preparation of Bradford reagent:

- Prepare in a 1 L volumetric flask
- Dissolve 100 mg of Coomassie brilliant blue 250 into 50 mL of 95% ethanol
- Add 100 mL of 85% (w/v) phosphoric acid to the above solution

Dilute this solution to 1 L using milli Q water.

Note: always add the Coomassie blue dye reagent last and pipette each sample-mixture up and down a couple times to ensure they are well mixed

2. For Myoglobin and Lysozyme

0.01-0.1 mg/mL

Assay: 50 μ L of sample in each well then add 200 μ L of dye reagent. Allow to stand for 5 minutes before running through the platereader using the 595 nm filter. Each well should be repeated 2-3 times and a blank of PBS should be run through to normalize the samples.

0.001-0.01 mg/mL

Assay: 200 μ L of sample in each well then add 100 μ L of dye reagent. Allow to stand for 5 minutes before running through the platereader using the 595 nm filter. Each well should be repeated 2-3 times and a blank of PBS should be run through to normalize the samples.

3. For Bovine Serum Albumin (BSA)

0.01-0.1 mg/mL

Assay: 50 μ L of sample in each well then add 200 μ L of dye reagent. Allow to stand for 5 minutes before running through the platereader using the 595 nm filter. Each well should be repeated 2-3 times and a blank of PBS should be run through to normalize the samples.

0.001-0.01 mg/mL

Assay: 150 μ L of sample in each well then add 150 μ L of dye reagent. Allow to stand for 5 minutes before running through the platereader using the 595 nm filter. Each well should be repeated 2-3 times and a blank of PBS should be run through to normalize the samples.

APPENDIX 4

Release Study Protocol

Materials

- Gel disks
- PBS
- Coomassie Brilliant Blue/Fast Green/Protein/Dextran
- UV lamp/excimer laser

Methods

1. PBS preparation

Na₂HPO₄: 1.32 g

NaH₂PO₄ H₂O: 0.345 g

NaCl: 8.5 g

Into a volumetric flask, fill 1 L with H₂O (milliQ)

Transfer to large beaker. Using pH meter (stir!) adjust pH to 7.4 with NaOH/HCl.

2. Glassware Preparation Equipment blocking with Milk Protein

Small concentrations of protein can adsorb to glassware. Pre-soaking of the glassware in skim milk powder solutions assure the released protein does not adsorb to allow for accurate measurements.

1. Make a 1mg/mL solution of skim milk powder in deionized water.
2. Put into vials/plates or soak glassware, let sit for 10 minutes.
3. Rinse x3 with fresh deionized water.
4. Dab to dry.

3. Loading solution

0.5 mg/mL of Coomassie Blue/Fast Green/Protein/Dextran (50 mg into 100 mL PBS)

4. Loading Procedure

1. The disks will have been air dried in the dark for 2 days (minimum) (tube mass known).
2. Mass closed tubes containing dried gel disks.
3. Add 1.9 mL of 0.5 mg/mL loading solution into each tube, place in the oven at 37°C
4. Allow to soak for 24 hours.

5. Release Study

1. One at a time, remove each disk, rinse with PBS, dab dry and mass on scale.
2. Put each disk into fresh, labeled tube. Continue massing until complete.
3. Add PBS to all the tubes at the same time, this is t=0 in the release study.
4. Move disks to new, labeled tubes containing fresh PBS at set time intervals: t= 0.5, 1, 1.5, 2, 3, 4, 6 etc. (extend intervals after burst is complete)

6. UV treatments

To be completed after 2 hours (between $t=2$ and $t=3$) on specific sets of cells
365nm

1. Warm up Curezone II UV lamp at least 5 minutes prior to use.
2. Place gels into 1mL PBS in wells of a 48-well microplate.
3. Remove lid and cover with thin layer of parafilm.
4. Place on ziplock of ice-water sitting on a Petri dish.
5. Leave in curezone for allotted time **note that ice bag must be replaced after 30 min.

248 nm excimer laser

1. Using tweezers, transfer each gel to a slide, bab slightly with kimwipe and place in laser projection area.
2. Treat with appropriate laser exposure.
3. Put gel back into 1mL PBS in a 48 well plate.

APPENDIX 5

Retinal Pigment Epithelial (RPE) and Corneal Epithelial (CE) Cell Culture Methods

Materials

- Dulbecco's modified Eagle's medium F12 (DMEM-F12) and Keratinocyte-serum free medium (SFM) plus supplements.
- Fetal Bovine Serum
- 0.05% trypsin-EDTA
- Sterile PBS (Ca^{2+} and Mg^{2+} free)
- DMSO
- Cell culture equipment (petri dishes, tubes, cryovials etc)

Methods

1. Medium Preparation

RPE cells: Dulbecco's modified Eagle's medium F12 (DMEM-F12) media containing 5% fetal bovine serum, 1% L-glutamine and 0.8% sodium bicarbonate with 1% penicillin/streptomycin.

CE cells: Keratinocyte-serum free medium (SFM) containing human recombinant epidermal growth factor 1-53 and bovine pituitary extract with 1% penicillin/streptomycin.

2. Growth Conditions

Incubate at 37°C with 5% carbon dioxide and 95% air under humidity.

3. Cell thawing

1. Prepare media, pre-heat in a 37°C water bath.
2. Heat up cryovial in 37°C water bath, dip it in approximately $\frac{3}{4}$ and gently swirl it until thawed.
3. Transfer cryovial to bio-cabinet be sure to disinfect it with 70% ethanol.
4. Transfer the cryovial contents to a flacon tube, dropwise (while swirling) add 8mL of medium.
5. Transfer cell suspension to a 100mm culture dish
6. Incubate at 37°C with CO_2 .
7. Change the culture flask medium every 2-3 days.
8. Split the culture when the culture flask is approximately 70% confluent.

4. Cell Splitting

Split cells when the culture flask is 60-70% confluent.

1. Aspirate the medium from the culture dish.
2. Rinse the attached cells with sterile PBS (Ca^{2+} and Mg^{2+} free) and remove afterwards.
3. Add 1 ml of 0.05% trypsin-EDTA and incubate the cells at 37°C for 1-4 min shaking periodically to help the cells detached from the surface.

4. Suspend the cells/trypsin mixture in 5-10mL of medium to deactivate the trypsin-EDTA.
 5. Centrifuge at 1000 rpm for 5 minutes, remove medium from pellet and resuspend cells with fresh medium.
 6. Split as required (1:4 is recommended), 10mL per 100mm culture dish.
 7. Culture until 60-70% confluent changing the medium every 2-3 days.
5. Cell Freezing for long term storage
1. Aspirate the medium from the culture dish.
 2. Rinse the attached cells with sterile PBS (Ca^{2+} and Mg^{2+} free) and remove afterwards.
 3. Add 1 ml of 0.05% trypsin-EDTA and incubate the cells at 37°C for 1-4 min shaking periodically to help the cells detached from the surface.
 4. Suspend the cells/trypsin mixture in 5-10mL of medium to deactivate the trypsin-EDTA.
 5. Transfer cell suspension to a 15mL falcon tube.
 6. Using a centrifuge, spin the cells down into a pellet (1000 rpm for 5 min at room temperature).
 7. Remove the supernatant with a pipette and replace with 2mL (per dish of cells) of fresh medium containing 10% DMSO (premix the DMSO medium before adding). Pipette up and down to resuspend.
 8. Transfer the suspension into cryovials (2mL per vial). Place cryovials in “Mr Freeze” or a styrofoam container.
 9. Place container in a -70°C freezer for several days then transfer to liquid nitrogen storage.

APPENDIX 6**MTT Assay*****Materials***

- MTT solution
- PBS
- Cell medium

Methods**1. Solution Preparation**

Make a 4 mg/mL stock solution of MTT in PBS, sterile filter and store frozen.
For cell assay dilute to 0.4 mg/mL with cell media.

2. 24 well plate procedure

1. Carefully remove medium from wells.
2. Rinse cells with PBS (~0.2 mL) to remove residual test medium
3. Add 337.5 μ L of MTT solution and incubate wrapped in aluminum foil for 4 hours
4. Observe cells under microscope for formazan precipitates (purple) then dissolve with 1125 μ L DMSO
5. Shake by rotation for 10 minutes or until precipitate has fully dissolved.
6. Transfer 200 μ L to a 96 well plate and read at 595 nm and 700 nm (background)

3. 48 well plate procedure

1. Carefully remove medium from wells.
2. Rinse cells with PBS (~0.1 mL) to remove residual test medium
3. Add 150 μ L of MTT solution and incubate wrapped in aluminum foil for 4 hours
4. Observe cells under microscope for formazan precipitates (purple) then dissolve with 500 μ L DMSO
5. Shake by rotation for 10 minutes or until precipitate has fully dissolved.
6. Transfer 200 μ L to a 96 well plate and read at 595nm and 700nm (background)

APPENDIX 7

Cytocompatibility Tests

Materials

- Medium
- MTT solution
- Photogels
- RPE and HCE cells

Methods

1. Gel Disinfection
 1. Add 2 mL of 70% ethanol in vials containing pre-massed gels (1 gel per vial)
 2. Let sit for to 2 hours
 3. Remove EtOH, air dry over night (closed cabinet, half speed, tinfoil the front)
 4. Soak in 1 mL of medium for 1 hour prior to adding to well dishes for cell tests.
2. Cells Grown in Indirect Contact with Gels (3 days and 7 days)

Day 1: Seed a 24 well plate with 300 000 cells/well with a total volume of 1.8 mL of medium.

Day 2: Put gels + inserts into well plates

 1. Remove medium
 2. Add 0.85mL of fresh medium
 3. Put in inserts and 0.85mL medium
 4. Add gels

Day 5: Test 3 Day growth with MTT assay or change the medium for 7 Day growth study

Day 9: Test 7 Day Growth with MTT assay
3. Long Term Degradation Product Test

Day 1: Begin gel and medium soaks to obtain degradation products.

 - In 24 well plate add 2mL of medium to 8 wells (4 control, 4 for gels)
 - Add gels to 4 wells
 - Wrap in tinfoil and incubate

Day 42: Seed a 48 well plate with 120 000 cells

Day 43: Add soaking solution

 - 4 wells for degradation products: Remove medium and replace with 0.2 soaking solution and 0.4 new medium or 0.6 mL of soaking solution if testing high concentrations.
 - 4 wells for medium soak: Remove medium and replace with 0.2 soaking medium solution and 0.4 new medium or 0.6 mL of soaking medium if testing high concentrations.
 - 4 wells control of fresh medium: Remove medium and replace with 0.6 mL of new medium

Day 46: Perform MTT assay

4. Testing PEG-anthracene Solutions

1. Seed a 48 wellplate with varying densities of cells and incubate for 24 hours.
2. Dissolve crosslinker in sterile PBS (2mL)- calculate concentration
3. Filter into 15 mL Falcon tube using a syringe filter (0.2 μm)
4. Add variety of concentrations to cells.
5. Freeze leftovers and wrap in tinfoil (markdown concentration)
6. Grow cells for 3 days then run MTT assay.

5. Testing HA solution

Day 1: Seed 48 well plate with 120 000 cells and add a total of 0.7 mL medium.

Day 2: Add HA solution to wells.

1. Remove medium
2. Make HA concentrations
Stock = 6mg/mL
0.1 mg/mL: 0.2 mL of stock HA solution + 11.8 mL of medium
0.01 mg/mL: 0.05 mL of stock HA solution + 29.95 mL of medium
*Stock solution is very viscous, use 1mL syringe to take out solution
3. Add 0.7 mL of HA concentration to well
4. Fill control wells with 0.7 mL of medium

Day 3: Test cells with MTT assay.